

REMARKS

Claims 233-247 and 466-479 are all the claims pending in this application.

The pending claims are rejected based on 35 U.S.C. § 112, second paragraph, as being indefinite.

Claims 234-235, 246-247, 466-467, and 478-479 are rejected under 35 U.S.C. §103(a) as being unpatentable over ILIADIS et al. (IDS ref: Computers and Biomed. Res. (2000), vol. 33, pages 211-226).

Claims 234-242, 244-247, 466-474, and 476-479 are rejected under 35 U.S.C. §103(a) as being unpatentable over ILIADIS et al. (IDS ref: Computers and Biomed. Res. (2000), vol. 33, pages 211-226) in view of PERIERA et al. (IDS ref: Frontiers Med. Biol. Eng. (1995), vol. 6 (4), pages 257-268).

Claims 243 and 475 are rejected under 35 U.S.C. §103(a) as being unpatentable over ILIADIS et al. (IDS ref: Computers and Biomed. Res. (2000), vol. 33, pages 211-226) in view of PERIERA et al. (IDS ref: Frontiers Med Biol. Eng. (1995), vol 6 (4) pages 257-268) as applied to claims 234-242, 244-247, 466-474, and 476-479, above, and further in view of LEMELSON (US 5,919,135).

The Applicants traverse the rejections and request reconsideration.

The Applicants have amended the claims to overcome each of the section 112 rejections.

All the pending rejections are based on ILLIADAS, either standing alone or in combination with other references. As evidenced by the attached database report (Appendix A) from PubMed, the ILLIADAS reference, though having a "received" date of January 2000, has a publication date of June 2000.

The Applicants respectfully attach a declaration under 37 C.F.R. § 1.131, executed by Dr. Zvia Agur, swearing behind the ILLIADAS reference. The declaration and the attached Exhibits demonstrate a conception date of at least prior to June 2000 and continued diligence until October 19, 2000, the filing date of the present application.

Therefore, the Applicants respectfully submit that ILLIADAS does not qualify as prior art under any sections of 35 U.S.C. § 102.

Since there are no other pending grounds for the rejection of the pending claims, they should be allowed.

The Applicants respectfully note that the pending claims were first rejected in an Office Action dated May 8, 2001, based on the combined teachings of Barry (6,081,786), Fink (5,808,918) and Thalhammer-Reyero (5,930,154). After a response was filed by the Applicants on August 8, 2001, the Examiner maintained the rejections of these claims based on the same references in an Office Action dated October 25, 2001. The Applicants provided a further response on January 25, 2002. Based on this response, the Examiner appears to have withdrawn the rejections and issued the present rejection based on a new combination of references.

In an unpublished, non precedential opinion, Administrative Judge Bahr asserted that "The application is remanded to the examiner for compliance with section 706.02 of the MPEP, which directs that prior art rejections should ordinarily be confined strictly to the best available art...Accordingly upon remand, the examiner should select the best prior art rejection for each claim and withdraw all cumulative rejections" (see generally, Appeal No. 2002-0965).

It is assumed that the Examiner has followed the requirements of MPEP §706 .02 and issued rejections based on the best possible references on both the occasions noted above; first, when the claims were rejected based on Barry/Fink/Thalhammer-Royero as well as, second, when they were rejected based on Illiadas in combination with other references. In this connection, the Applicants respectfully note that during the course of the prosecution while these claims were amended to overcome minor informalities, the subject matter of the claims has not been changed. Therefore, it is clear that the Examiner **has already searched the subject matter recited in these claims twice and has found the best possible references to cite as prior art.**

Considering the above, it is respectfully requested that the pending claims be passed into allowance and the Applicants be awarded what is believed to be their rightful due.

CONCLUSION

In view of the above, reconsideration and allowance of this application are now believed to be in order, and such actions are hereby solicited. If any points remain in issue which the Examiner feels may be best resolved through a personal or telephone interview, the Examiner is kindly requested to contact the undersigned at the telephone number listed below.

Serial No. 09/691,053

Docket No. Q60688

The USPTO is directed and authorized to charge all required fees, except for the Issue Fee and the Publication Fee, to Deposit Account No. 19-4880. Please also credit any overpayments to said Deposit Account.

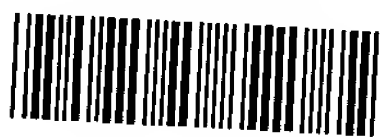
Respectfully submitted,

Chidambaram Subramanian

Chidambaram Subramanian
Registration No. 43,355

SUGHRUE MION, PLLC
Telephone: (202) 293-7060
Facsimile: (202) 293-7860

WASHINGTON OFFICE



23373

PATENT TRADEMARK OFFICE

Date: March 18, 2003

APPENDIX
VERSION WITH MARKINGS TO SHOW CHANGES MADE

IN THE CLAIMS:

The claims are amended as follows:

234. (Amended) A computer system for recommending an optimal treatment protocol for treating cancer using drugs, for an individual, said system interfacing with the computer and said system further comprising:

a cancer system model;

a treatment protocol generator for generating a plurality of treatment protocols for treating cancer using [chemotherapy] drugs;

a system model modifier, wherein said the system model modifier is adapted to modify said cancer system model based on parameters specific to the individual; and

a selector adapted to select an optimal treatment protocol from said plurality of treatment protocols based on the modified system model.

240. (Amended) The system of claim 238 where the system includes a set of control functions that are adapted to uniquely determine an outcome of every single step, wherein said control functions comprise age of cells, state of a current population and associated environment.

244. (Amended) The system of claim 243, wherein the system is adapted to incorporate [pharmacokinetic] pharmacokinetics and [pharmacodynamic] pharmacodynamics, cytostatic effects, cytotoxic effects, and other effects on cell disintegration of anticancer drugs.

246. (Twice Amended) The system of claim 234 wherein, said parameters specific to the individual comprise parameters related to tumor dynamics, patient specific drug [pharmacokinetic, pharmacodynamic] pharmacokinetics, pharmacodynamics and dynamics of dose-limiting host tissues.

466. (Amended) A computer-implemented method for recommending an optimal treatment protocol for treating cancer using drugs [, including chemotherapy,] for an individual, said method comprising:

- creating a cancer system model;
- enumerating a plurality of treatment protocols for treating cancer using drugs;
- modifying the system model based on parameters specific to the individual;
- selecting an optimal treatment protocol from said plurality of treatment protocols based on the modified system model; and
- recommending said optimal treatment.

472. (Amended) The method of claim 470 where a set of control functions uniquely determine an outcome of every single step, wherein said control functions comprise age of cells, state of a current population and associated environment.

476. (Amended) The method of claim 475, wherein [pharmacokinetic and pharmacodynamic,] pharmacokinetics, pharmacodynamics, cytotoxic effects, cytostatic effects and other effects on cell disintegration of anticancer drugs are incorporated into the model.

478. (Amended) The method of claim 466 wherein, said parameters specific to the individual comprise parameters related to tumor dynamics, patient specific drug [pharmacokinetic, pharmacodynamic,] pharmacokinetics, pharmacodynamics and dynamics of dose-limiting host tissues.



PATENT APPLICATION
IN THE UNITED STATES PATENT AND TRADEMARK OFFICE

In re application of

Zvia AGUR, et al.

Appln. No.: 09/691,053

Confirmation No.: 5359

Filed: October 19, 2000

Docket No: Q60688

Group Art Unit: 1631

Examiner: Marjorie A. MORAN

#19
Plunkett
3/26/03

For: SYSTEM AND METHOD FOR OPTIMIZED DRUG DELIVERY AND
PROGRESSION OF DISEASED AND NORMAL CELLS

DECLARATION UNDER 37 C.F.R. § 1.131

Honorable Commissioner of
Patents and Trademarks
Washington, D.C. 20231

Sir:

I, Zvia Agur, hereby declare as follows:

I am an inventor and an applicant of the invention entitled "System and Method for Optimized Drug Delivery and Progression of Diseased and Normal Cells", disclosed and claimed in U.S. Application No. 09/691,053 filed October 19, 2000.

I graduated from the Hebrew University of Jerusalem and Université Libré, Brussels, Belgium in 1983, and obtained a Ph.D. Degree in Biomathematics.

Presently I am the Chairperson and CSO at OPTIMATA, the owner of the above application.

Prior to June 2000, I, along with the other named inventors, had invented the invention as described and claimed in the above-identified application, and pursued the present invention in

the ordinary course of business, including preparing the above-identified patent application, until the filing of the above-identified application, as evidenced by the following:

Prior to August 1, 1999, having earlier invented the claimed invention, I contacted the law firm of Eitan, Perl, Latzner and Cohen-Zedek in Herzlia, Israel, [hereinafter "MC"] to assist the applicants in preparing a patent application.

On August 7, 1999, a meeting was held at MC's office where technical discussions were held to convey the inventive subject matter to MC. Several related technical documents were handed to MC, including the overall concept diagram as shown in Exhibit 1.

Subsequent to the meeting on August 7, 1999, several discussions were held over a period of several months while MC and the applicants together prepared four manuscripts (Exhibits 11-14) disclosing the invention. Exhibits 2-8 include transcripts of emails evidencing continued work on the four manuscripts until June-July 2000.

In July, 2000, we contacted the law firm of SUGHRUE MION, PLLC [hereinafter SUGHRUE] to provide further assistance and prepare patent applications based on the four manuscripts (Exhibits 11-14).

Exhibit 8-9 shows email correspondence evidencing our discussions with SUGHRUE during July-August 2000.

Prior to August 18, 2003, technical materials including the four manuscripts (Exhibits 11-14) were provided to SUGHRUE.

We held a meeting on August 28, 2000, at the offices of SUGHRUE in Washington DC, with Messrs. Bill Mandir and Chid Subramanian to hold technical discussions on the subject matter of the invention.

From the time of our meeting with SUGHRUE until the filing of the application on October 19, 2000, several drafts were exchanged between SUGHRUE and Optimata.

The above-identified application was then filed on October 19, 2000.

In view of the discussion above, and the attached exhibits, we had invented the claimed invention disclosed in the subject application prior to June 2000, and pursued the present invention in the ordinary course of business, including preparing the above-identified patent application, until the application was filed on October 19, 2000.

I declare further that all statements made herein are of my own knowledge and are true and that all statements made on information and belief are believed to be true; and further that these statements were made with the knowledge that willful false statements and the like so made are punishable by fine or imprisonment, or both, under Section 1001 of Title 18 of the United States Code, and that such willful false statements may jeopardize the validity of the application or any patent issuing thereon.

Date: 13.3.03

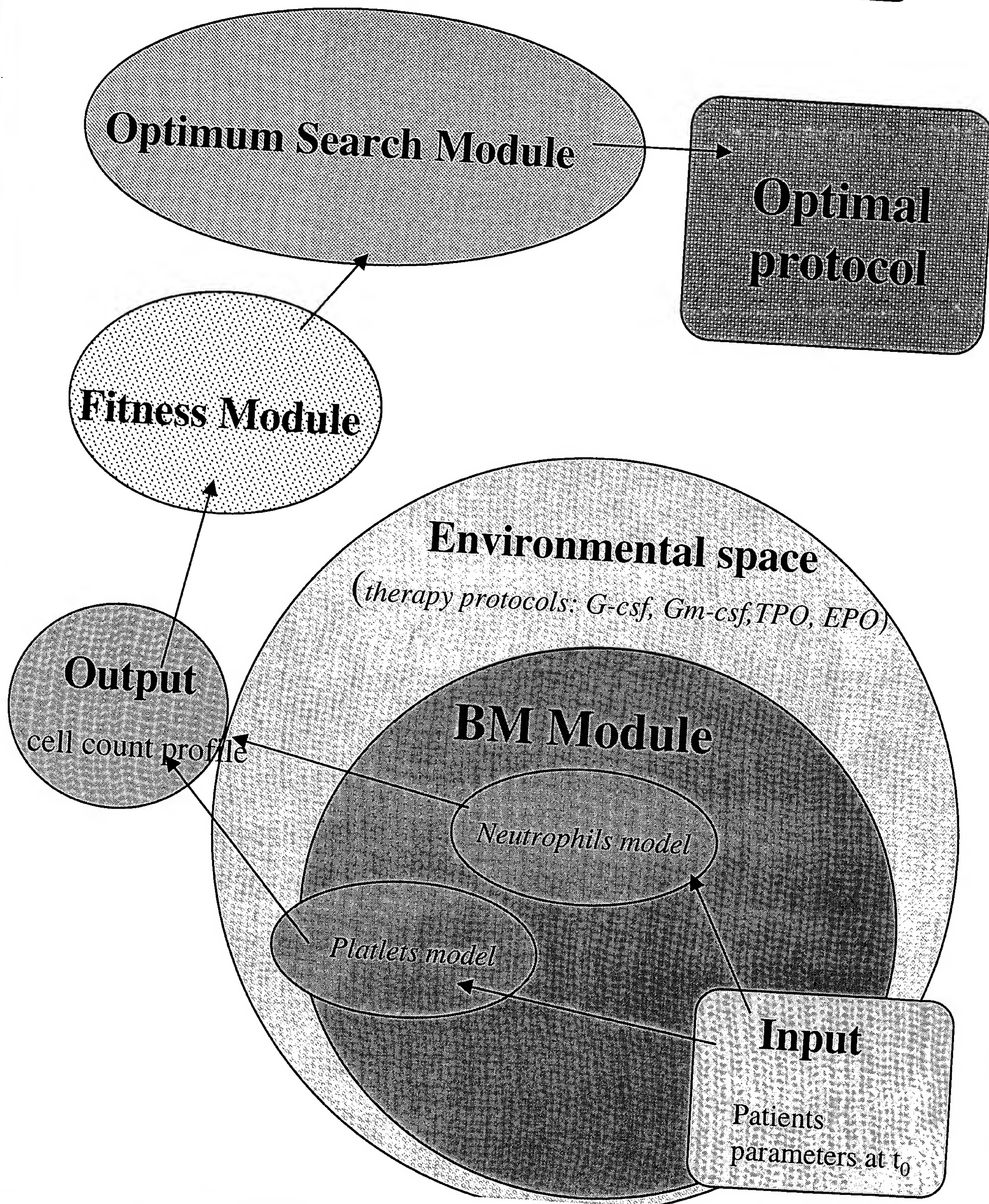
By: 3 Via Agor

LIST OF EXHIBITS

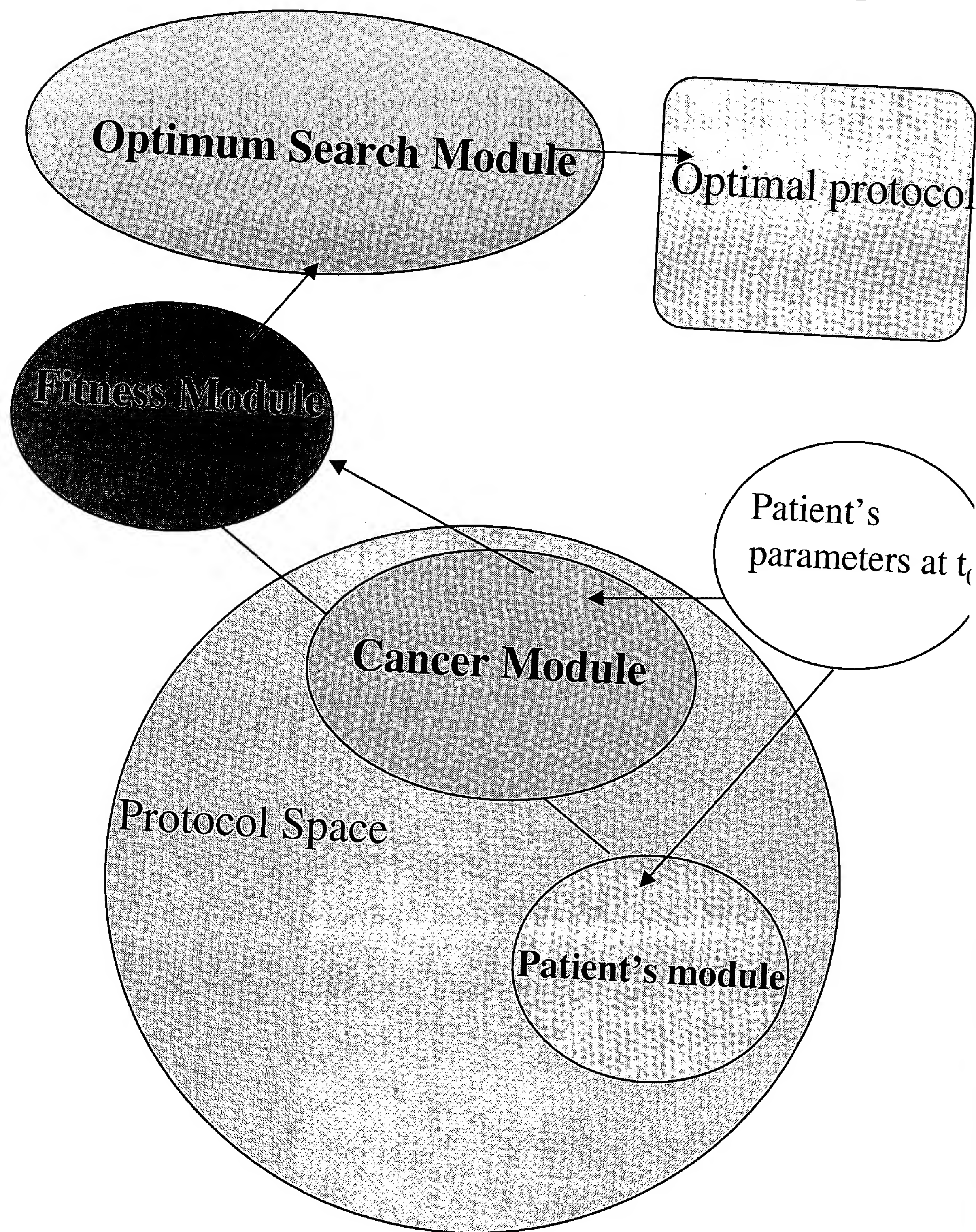
1. Figure showing an overview of the invention provided to MC at a meeting on Aug 7, 1999.
2. E-mail from Dr. Agur to MC dated August 1999 confirming earlier meeting with MC.
3. E-mail from Dr. Agur to MC dated March 16, 2000.
4. Patent search report generated March 21, 2000.
5. Memo of a meeting dated June 11, 2000.
6. Letter in Hebrew dated July 21, 2000 from Dr. Agur to MC, evidencing communications between Dr. Agur and MC regarding patent registration in June-September 1999.
7. E-mail dated July 31, 2000 from Dr. Agur to MC.
8. E-mail dated July 31, 2000 from Mr. Rick Abboudi of MC to Dr. Agur.
9. E-mail to Bill Mandir with SUGHRUE dated August 1, 2000.
10. E-mails in August 2000 between SUGHRUE and OPTIMATA.
11. Technical Disclosure prepared by MC and Applicants.
12. Document titled APPENDIX A: Computer Simulator of Human Thrombopoiesis.
13. Document titled APPENDIX B: A Model of the Neutrophil Bone Marrow and Peripheral Blood Compartment under the Effects of Growth-Factors and its Use as a Tool for Optimizing Treatment with Granulocyte Colony Stimulating Factor (G-CSF).
14. Document titled APPENDIX C: Optimizing cytotoxic drug delivery (administration/efficacy) for cancer patients.

09/691,053 #18

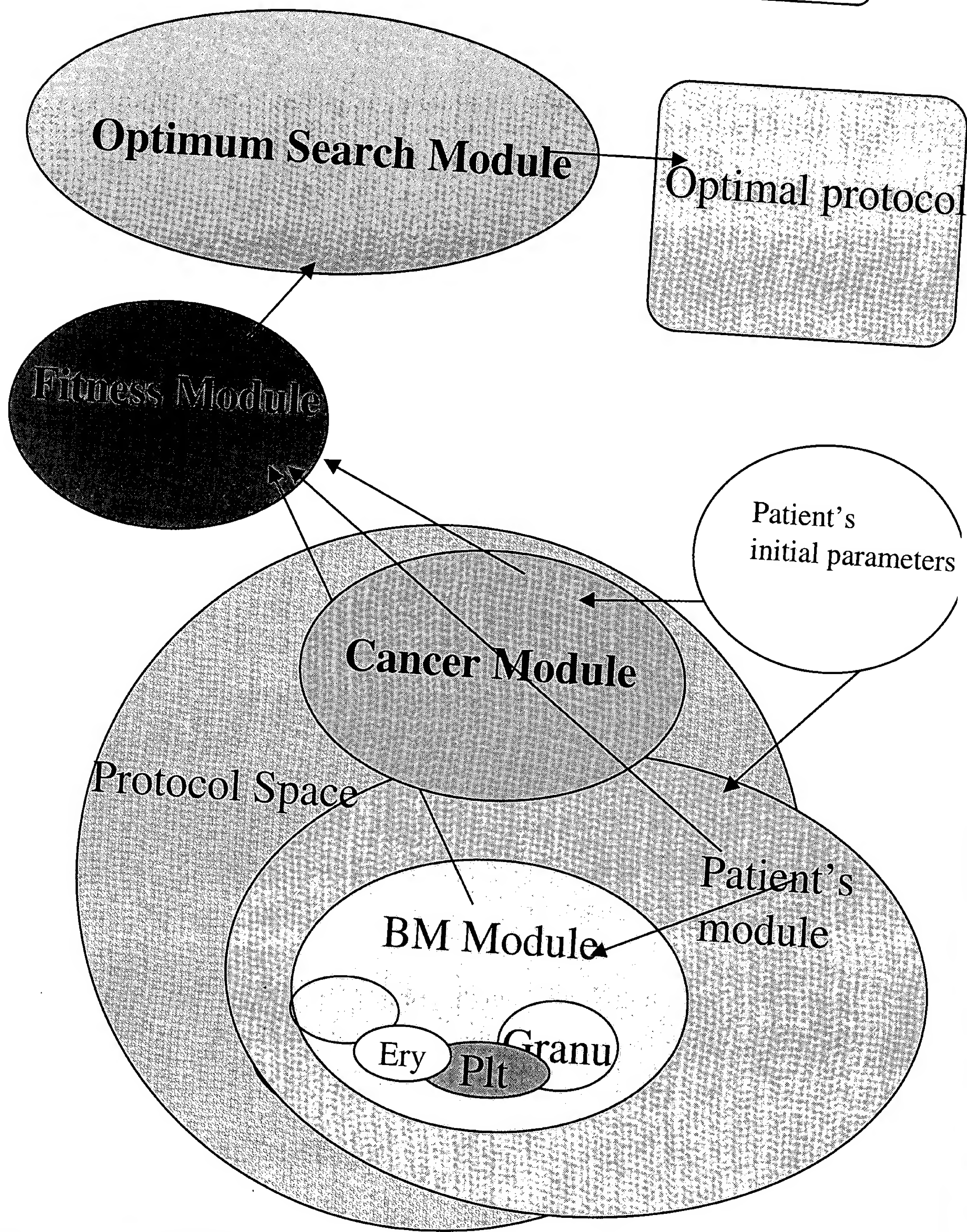
Bone Marrow Project-VBM



OPTIMA project



VBM+OPTIMA project



To: cohenm
From: agur@ccsg.tau.ac.il (Zvia Agur)
Subject: advice (Ely Lilly)
Cc:
Bcc:
X-Attachments:

Dear Mark,

I enjoyed very much our discussion last week and am looking forward to our next meeting and to our prospective cooperation in building an IP portfolio for the institute for medical biomaths (IMBM). There is a matter that may be of high relevance, a potential collaboration with Eli Lilly which is described in the email I enclose below. I have to give the guy some initial answer this week and I wonder whether you have any suggestions about how to say to him that (1) we can do what he needs if he gives us enough information; (2) unlike what he imagines the basis for answering his questions reliably is a series of models that involve maths, biology, biomaths, operation research and computer science. we have these models and it is our IP. In case I do not hear from you, I will answer him more or less the above, adding that any commitment on my part will have to be approved by my attorneys. All the best,
Zvia Agur

Date: Tue, 20 Jul 1999 13:16:51 -0500
From: "Craig M. Zwickl" <zwickl_craig_m@Lilly.com> Subject: Mathematical
Modelling of Cancer/Hematopoiesis To: agur@ccsg.tau.ac.il
Organization: Eli Lilly and Company
MIME-version: 1.0

Dear Professor Agur,

I recently came across your internet home page as I was searching for information about mathematical modeling of biological systems. I am a Senior Toxicologist at Eli Lilly and Company in Indianapolis, IN (USA) and I give lectures in pharmacology and toxicology at the Indiana University School of Medicine. At Lilly, I am the principle investigator in a hematotoxicology laboratory which characterizes the effects of drug candidates on the hematopoietic system, generally using in vitro colony-forming assays. Since the bone marrow is often a target organ of toxicity for oncolytic agents, I work fairly closely with the Cancer Discovery area.

As I'm sure you are already well aware, the majority of biologists (myself included) don't make optimal use of the mathematical tools available to us (probably attributable to mathematics angst when we were in school). However, I am convinced that mathematical modeling of dose-response data would be very beneficial for gaining an understanding of how changes in dose scheduling, etc. could affect a compound's therapeutic index, thereby potentially altering the effectiveness of treatment. For this reason, I have developed an interest in learning how to apply principles of mathematical modeling to these types of problems but don't really know where to begin, as I have not been able to locate any good resources for self-teaching. Your experience and interest in modeling hematopoiesis, cell cycle control, cancer growth, and cancer therapy, suggests to me that you might be able to help me become acquainted with the mathematical tools required to model these systems. I am seeking

a mentor/collaborator arrangement with someone else who is interested in this area of modeling and would welcome the opportunity to discuss this further with you.

If this is something which also might interest you, please send me an e-mail (cmz@lilly.com). Thank you for your time, I look forward to hearing from you.

Regards,

Dr. Craig M. Zwickl
Senior Toxicologist
Eli Lilly and Company
PO Box 708
Greenfield, IN 46140

Date: Thu, 05 Aug 1999 10:08:55 -0500
From: Craig M Zwickl <ZWICKL_CRAIG_M@Lilly.com> Subject: Mathematical models of cancer therapies
To: agur@post.tau.ac.il (Zvia Agur)
MIME-version: 1.0
X-Lotus-FromDomain: LILLY
Status: RO

Dear Professor Agur,

Thanks for your willingness to discuss mathematical modelling of cancer chemotherapy and hematopoiesis. As I said in my original e-mail, I am very eager to learn more about how one approaches these types of modelling problems and would welcome any advice and instruction you could offer. There are a number of problems that I work on that I feel could benefit from modelling, but let me start with one which requires immediate attention due to time-constraints which have been placed on the project.

At the moment, I can only discuss the problem in general terms unless and until you sign a Confidentiality Agreement with Eli Lilly and Company and we can find a way to encrypt our e-mail messages. Signing the agreement does not necessarily mean that any work cannot be published, but that the Project Team for the compound would have the right to determine the timing of any disclosure. Would you be willing to sign such an agreement? If so, I would list you as a consultant to my laboratory. Initially, this would not involve monetary compensation, but if we are able to make some progress in this area of modelling, eventually I might be able to make a case for such compensation.

Background: We have been studying a series of microtubule inhibitors as potential chemotherapeutic agents. My laboratory conducted a series of in vitro experiments using rat, dog, and human bone marrow cells to determine IC50 and IC90 concentrations for inhibition of CFU-GM colony growth. The intention of these experiments was to compare the animal data to verify a correlation between the in vitro IC90 and severity of neutropenia at plasma levels obtained in vivo, then to use the in vitro data for the human CFU-GM to predict plasma concentrations that would

be expected to cause severe neutropenia in patients (I'll send you a copy of the poster that was presented at the Society of Toxicology meeting this past March). Such an approach assumes that, like in animals, the clinical dose-limiting toxicity will be hematotoxicity, which is not always the case (e.g. vincristine).

In oncology, the conventional wisdom has been to hit the patient hard with the maximum tolerated dose over several cycles. However, I am skeptical that this approach is the best for all forms of chemotherapy. For example, with the compound tested, the in vitro inhibition curves for CFU-GM are bi-phasic. Approximately 20 to 25% inhibition occurs at very low doses; this is followed by a plateau as concentration is increased, then a rapid drop to 100% inhibition at the higher concentrations. Inhibition at low concentrations appears to be an AUC-driven process (dependent on both concentration and time of exposure), whereas inhibition at the higher concentrations appears to be solely dependent on concentration. In addition, there is experimental evidence that at low concentrations, microtubules associated with the spindle apparatus are inhibited and that at higher concentrations, the microtubules associated with cytoskeletal structure also become involved.

Hypothesis: In my opinion, it is likely that inhibition of CFU-GM at the low concentrations represents killing of actively proliferating cells and that the more pronounced inhibition obtained at the higher concentrations are due to non-selective cytotoxicity which occurs as a result of cytoskeletal disruption (which will kill cells without regard to their cell cycle status). If this is true, I would think that the better schedule could be one in which the compound is given at very low concentrations over a prolonged period of time. This would presumably target proliferating cells, thereby giving a better therapeutic index. However, the chemical properties of the present compound may preclude prolonged administration (days instead of hours) and there would undoubtedly be reluctance to develop a backup compound without clear evidence that such a schedule would be equally efficacious.

Status: I am designing in vitro experiments using human tumor cell lines that have different cycle times in which we will look very carefully at AUC vs concentration-dependent colony inhibition.

Opportunities for Modelling: If we assume that the 25% inhibition of CFU-GM colonies at low exposure concentrations represents the proliferation cell population 1) what is the best schedule/dose combination for targeting proliferating tumor cells? 2) would it be expected that this optimum schedule would maintain the therapeutic index? 3) would the schedule be expected to eradicate the cancer, and if so, how many treatment cycles would be required? and 4) how would the tumor cycle time be expected to influence estimates obtained from modelling?

I think these are very interesting questions and appreciate your thinking about them. As I indicated, this is only one of a number of opportunities where I think mathematical modelling could be very useful to our laboratory. I am looking forward to your thoughts on how we might collaborate and how I might learn from you. I have Mathematica 3.0 installed on my computer and am (re)teaching myself some of the calculus that I'm guessing might be useful. In terms of sharing ideas and data, I use Microsoft Office '97 (Word, Excel, Powerpoint, Access, Project) and SigmaPlot 4.0. TableCurve is available, and my e-mail system is LotusNotes 4.6.2a. Are these

compatible with your system?

Regards,
Craig

P.S. I will be on vacation (much needed) next week.

Zvia,

patentmeeting1603001.txt

He was out last week and Monday. I hope to speak with him this week.
Mark

> -----Original Message-----

> From: Zvia Agur [SMTP:agur@imbm.org]

> Sent: Wed, March 22, 2000 9:14 AM

> To: Mark Cohen

> Subject:

>

> Dear Mark,

> I enjoyed very much our meeting last Thursday and the patent procedure is
> much clearer to me now.
> I wonder if you had a chance to talk to Malcolm A.S. Moore about clinical
> trials for G-CSF. In essence, we have developed a sophisticated software
> tool for optimizing granulopoiesis. It is based on our detailed
> mathematical model for the Granulocytic line, which is based on the
> available biological information, and on a special-purpose optimization
> algorithm. The outcome is a patient-specific optimal G-CSF protocol.
> Collaboration: The model and its predictions need to be tested on 2
> independent sets of clinical data. Subsequently, we will provide the
> optimal use for G-CSF with or without chemotherapy.
>
> Collaboration with Prof Moore can be of much value to us.
> Thanks very much for your help, Mark. Looking forward to hearing from you.
> Zvia

1. Searching in the following databases

=> file hcaplus wpindex japio

=> s mathemat? (5a) model? or comput? simulat? or dynamic simulat? or comput? or software# or simulat?

L1 653372 FILE HCAPLUS
L2 314784 FILE WPINDEX
L3 158516 FILE JAPIO

TOTAL FOR ALL FILES

L4 1126672 MATHEMAT? (5A) MODEL? OR COMPUT? SIMULAT? OR DYNAMIC SIMULAT?
OR COMPUT? OR SOFTWARE# OR SIMULAT?

=> s l4 and (hemopiesis or hematopoiesis or bone marrow or stem cell#)

L5 579 FILE HCAPLUS
L6 26 FILE WPINDEX
L7 1 FILE JAPIO

TOTAL FOR ALL FILES

L8 606 L4 AND (HEMOPIESIS OR HEMATOPOIESIS OR BONE MARROW OR STEM CELL#
)

=> s l5 and p/dt

L13 16 FILE HCAPLUS
L14 25 FILE WPINDEX
L15 1 FILE JAPIO

TOTAL FOR ALL FILES

L16 42 L5 AND P/DT

=> s l16 and (cancer or tumour# or tumor# or carcinogen? or neoplasm#)

L17 5 FILE HCAPLUS
L18 13 FILE WPINDEX
L19 0 FILE JAPIO

TOTAL FOR ALL FILES

L20 18 L16 AND (CANCER OR TUMOUR# OR TUMOR# OR CARCINOGEN? OR NEOPLASM#
)

=> dup rem **(duplicate removal between the databases)**

ENTER L# LIST OR (END):120

PROCESSING COMPLETED FOR L20

L21 18 DUP REM L20 (0 DUPLICATES REMOVED)
ANSWERS '1-5' FROM FILE HCAPLUS
ANSWERS '6-18' FROM FILE WPINDEX

Please read the titles and choose which ones are most relevant to you :

=> d l21 1-18 ti

L21 ANSWER 1 OF 18 HCAPLUS COPYRIGHT 2000 ACS
TI Cloning and cDNA sequence of a human multidrug resistance-associated polypeptide and its use in improving the effectiveness of **cancer** chemotherapy

- L21 ANSWER 2 OF 18 HCAPLUS COPYRIGHT 2000 ACS
TI Broad specificity affinity arrays: a qualitative approach to complex sample discrimination
- L21 ANSWER 3 OF 18 HCAPLUS COPYRIGHT 2000 ACS
TI Tissue-derived **tumor** growth inhibitors for preventing cytotoxic poisoning
- L21 ANSWER 4 OF 18 HCAPLUS COPYRIGHT 2000 ACS
TI **Computerized** electrophoresis device for fractionating serum globulins, detg. monoclonal proteins, and diagnosing diseases
- L21 ANSWER 5 OF 18 HCAPLUS COPYRIGHT 2000 ACS
TI Methods for diagnosis and monitoring of **tumors** employing analysis of silver staining in interphasenuclei
- L21 ANSWER 6 OF 18 WPINDEX COPYRIGHT 2000 DERWENT INFORMATION LTD
TI Detecting **tumors** including malignant melanoma by administration of radio-labeled diamine.
- L21 ANSWER 7 OF 18 WPINDEX COPYRIGHT 2000 DERWENT INFORMATION LTD
TI **Computer** implemented patient accounting data processing method for use in insurance company, hospitals.
- L21 ANSWER 8 OF 18 WPINDEX COPYRIGHT 2000 DERWENT INFORMATION LTD
TI Complex for stimulation bone growth, particularly in the mastoid cavity, is isolated from ground bone.
- L21 ANSWER 9 OF 18 WPINDEX COPYRIGHT 2000 DERWENT INFORMATION LTD
TI Assay of human Wilm's **tumor** gene expression for diagnosis of leukemia, sarcoma, **bone marrow** transplantation - involves multiplying the expression ratio of amounts of mRNA expressed by Wilm's **tumor** gene to that of the standard b actin gene, with mean value of gene expressed in healthy person.
- L21 ANSWER 10 OF 18 WPINDEX COPYRIGHT 2000 DERWENT INFORMATION LTD
TI Stable crystalline bromide or chloride salts of swainsonine - useful for stimulating immune system, treating proliferative disorders or microbial or parasitic infections.
- L21 ANSWER 11 OF 18 WPINDEX COPYRIGHT 2000 DERWENT INFORMATION LTD
TI Immune deficient mouse having implanted prostate **cancer** - useful as models for, e.g. studying stagewise progression of **cancer** and for designing specific therapeutic regimen(s).
- L21 ANSWER 12 OF 18 WPINDEX COPYRIGHT 2000 DERWENT INFORMATION LTD
TI Granulocyte colony stimulating factor analogues - with altered, biological activity, identified by analysis of three-dimensional structure of native protein.
- L21 ANSWER 13 OF 18 WPINDEX COPYRIGHT 2000 DERWENT INFORMATION LTD
TI New DNA sequences as DNA probes - for use in paternity and maternity testing, analysis of **tumour** cells, animal or plant breeding, etc..
- L21 ANSWER 14 OF 18 WPINDEX COPYRIGHT 2000 DERWENT INFORMATION LTD
TI Cryogenic storage of specimen in ampoule in liq. nitrogen - with **computer** control to bring required ampoule to discharge opening.
- L21 ANSWER 15 OF 18 WPINDEX COPYRIGHT 2000 DERWENT INFORMATION LTD

- TI New prostate-associated serum protease and polynucleotides which identify and encode PRASP, useful for treating reproductive disorders and **cancer**.
- L21 ANSWER 16 OF 18 WPINDEX COPYRIGHT 2000 DERWENT INFORMATION LTD
 TI Isolated and purified polynucleotide for modulating the expression of human RNA binding proteins which play a role in **cancer**, immune disorders and developmental disorders.
- L21 ANSWER 17 OF 18 WPINDEX COPYRIGHT 2000 DERWENT INFORMATION LTD
 TI New human mitochondrial processing peptidase subunit, useful in the diagnosis, prevention and treatment of smooth muscle disorders, neurological disorders and **cancer**.
- L21 ANSWER 18 OF 18 WPINDEX COPYRIGHT 2000 DERWENT INFORMATION LTD
 TI New human growth associated methyltransferases and the DNA encoding them, useful in the diagnosis, treatment or prevention of neoplastic disorders, immunological disorders, reproductive disorders and vesicle trafficking disorders.

We refined the search with the following terms :

```
=> s l21 and (rehabilit? or regenerat?)
L22      5 S L21
L23      0 FILE HCAPLUS
L24      13 S L21
L25      0 FILE WPINDEX
L26      0 S L21
L27      0 FILE JAPIO
```

Please notice that we received zero answers to that.

```
TOTAL FOR ALL FILES
L28      0 L21 AND (REHABILIT? OR REGENERAT?)
```

2.

```
=> file uspatfull europatfull
```

```
=> s l4
L29      421282 FILE USPATFULL
L30      70452 FILE EUROPATFULL
```

```
TOTAL FOR ALL FILES
L31      491734 L4
```

```
=> s l31 (p) (hemopiesis or hematopoiesis or bone marrow or stem cell#)
L32      122 FILE USPATFULL
L33      384 FILE EUROPATFULL
```

```
TOTAL FOR ALL FILES
L34      506 L31 (P) (HEMOPIESIS OR HEMATOPOIESIS OR BONE MARROW OR STEM
          CELL#)
```

```
=> s l34 (p) (cancer or tumour# or tumor# or carcinogen? or neoplasm#)
L35      23 FILE USPATFULL
L36      303 FILE EUROPATFULL
```

TOTAL FOR ALL FILES
L37 326 L34 (P) (CANCER OR TUMOUR# OR TUMOR# OR CARCINOGEN? OR NEOPLASM#
)

=> s 137 (p) (rehabilit? or regenerat?)
L38 0 FILE USPATFULL
L39 88 FILE EUROPATFULL

TOTAL FOR ALL FILES
L40 88 L37 (P) (REHABILIT? OR REGENERAT?)

2. Searching 2 fulltext files :

=> file uspatfull europatfull

=> s 140 and (chemotherapy or drug treatment# or drug protocol# or drug regime#)
L41 0 FILE USPATFULL
L42 16 FILE EUROPATFULL

TOTAL FOR ALL FILES
L43 16 L40 AND (CHEMOTHERAPY OR DRUG TREATMENT# OR DRUG PROTOCOL# OR
DRUG REGIME#)

**There were 16 records in the Europatfull database. You can
receive the patents in full-text.**

=> d 143 1-16 bib ab

L43 ANSWER 1 OF 16 EUROPATFULL COPYRIGHT 2000 WILA

PATENT APPLICATION - PATENTANMELDUNG - DEMANDE DE BREVET

AN 965346 EUROPATFULL ED 20000112 EW 199951 FS OS
TIEN Use of acetylated mannan derivatives for treating chronic respiratory
diseases.
TIDE Verwendung von acetylierte mannanderivate zur behandlung von chronischen
atemwegserkrankungen.
TIFR Utilisation des derives acetyles du mannane pour le traitement des
maladies respiratoires chroniques.
IN McAnalley, Bill H., 4921 Corn Valley, Grand Prairie, Texas 75052, US;
Carpenter, Robert H., 1303 Pecan Street, Bastrop, Texas 78602, US;
McDaniel, Harley R., 5450 Fairfield, Dallas, Texas 75205, US
PA CARRINGTON LABORATORIES, INC., 2001 Walnut Hill Lane, Irving, TX 75038,
US
PAN 833042
AG Fisher, Adrian John, CARPMAELS & RANSFORD 43 Bloomsbury Square, London
AGN WC1A 2RA, GB
OS 52611
SO ESP1999094 EP 0965346 A2 991222
DT Wila-EPZ-1999-H51-T1b
LA Patent
DS Anmeldung in Englisch; Veroeffentlichung in Englisch
PIT R DE; R FR; R GB; R IT
PI EPA2 EUROPAEISCHE PATENTANMELDUNG
OD EP----965346 A2 19991222
AI 1999EP-0200519 19991222
19911105

RLI EP 611304 DIV
ABEN Acetylated mannan derivatives, such as acemannan, has been shown to be effective in treating a number of conditions where the principal mechanism of resolution or cure requires intervention by the patient's immune system. Acemannan has direct stimulatory affects on the immune system. Methods for treating respiratory diseases are described.

L43 ANSWER 2 OF 16 EUROPATFULL COPYRIGHT 2000 WILA
PATENT APPLICATION - PATENTANMELDUNG - DEMANDE DE BREVET

AN 965345 EUROPATFULL ED 20000112 EW 199951 FS OS
TIEN Use of acemannan.
TIDE Verwendung von Acemannan.
TIFR Utilisation d'acemannan.
IN McAnalley, Hill H., 4602 Chalk Court, Grant Prairie, TX 75952, US;
Carpenter, Robert H., 1303 N. Pecan St., Bastrop, TX 78602, US;
McDaniel, Harley R., 5450 Fairfield, Dallas, TX 75205, US
PA CARRINGTON LABORATORIES, INC., 1300 E. Rochelle Blvd, Irving, TX 75062, US
PAN 833041
AG Manitz, Finsterwald & Partner, Postfach 22 16 11, 80506 Muenchen, DE
AGN 100614
OS ESP1999094 EP 0965345 A2 991222
SO Wila-EPZ-1999-H51-T1b
DT Patent
LA Anmeldung in Englisch; Veroeffentlichung in Englisch
DS R AT; R BE; R CH; R DE; R FR; R GB; R IT; R LI; R LU; R NL; R SE
PIT EPA2 EUROPAEISCHE PATENTANMELDUNG
PI EP----965345 A2 19991222
OD 19991222
AI 1999EP-0115500 19890803
PRAI 1988US-0229164 19880805
RLI EP 619117 DIV
ABEN The use of acemannan for the manufacture of a medicament for the production of a defective virus and a method of producing a defective virus in master seed cultures for vaccine production comprising the addition of a pharmaceutically effective amount of acemannan to a master seed culture to produce altered viral replication are described.

L43 ANSWER 3 OF 16 EUROPATFULL COPYRIGHT 2000 WILA
PATENT APPLICATION - PATENTANMELDUNG - DEMANDE DE BREVET

AN 861667 EUROPATFULL ED 19980913 EW 199836 FS OS
TIEN Particulate agents.
TIDE Partikelfoermige Mittel.
TIFR Agents particuliers.
IN Filler, Aaron Gershon, UCLA Medical Center, Div. Neurosurgery, Rm. 74-140 CHS, 10833 Le Conte, Los Angeles, CA 90095-6901, US
PA SYNGENIX LIMITED, Mount Pleasant House 2 Mount Pleasant Huntingdon Road, Cambridge CB3 0BL, GB
PAN 1765141
AG Perry, Robert Edward, GILL JENNINGS & EVERY Broadgate House 7 Eldon Street, London EC2M 7LH, GB
AGN 41331
OS ESP1998059 EP 0861667 A2 980902
SO Wila-EPZ-1998-H36-T1b
DT Patent

LA Anmeldung in Englisch; Veroeffentlichung in Englisch
DS R DE; R FR; R GB
PIT EPA2 EUROPAEISCHE PATENTANMELDUNG
PI EP----861667 A2 19980902
OD 19980902

AI 1997EP-0119199 19910913
PRAI 1990GB-0020075 19900914
1990GB-0023580 19901030
1990GB-0027293 19901217
1991GB-0000233 19910107
1991GB-0000981 19910116
1991GB-0002146 19910131
1991GB-0010876 19910520
1991GB-0016373 19910730
1991GB-0017851 19910819
1991GB-0018676 19910830

RLI EP 548157 DIV
ABEN

A novel means of pharmaceutical delivery for therapy or prophylaxis or to assist surgical or diagnostic operations on the living body is provided by neuronal endocytosis and axonal transport following pharmaceutical administration into vascularised, peripherally innervated tissue, e.g. intramuscular injections of a nerve adhesion molecule in coupled particle comprising a physiologically active substance or a diagnostic marker.

L43 ANSWER 4 OF 16 EUROPATFULL COPYRIGHT 2000 WILA
PATENT APPLICATION - PATENTANMELDUNG - DEMANDE DE BREVET

AN 837073 EUROPATFULL ED 19980503 EW 199817 FS OS
TIEN Human mad proteins and uses thereof.
TIDE MAD Proteine vom Menschen und deren Verwendung.
TIFR MAD proteines humaines et leur utilisation.
IN Laping, Nicholas J., SmithKline Beecham Pharma., 709 Swedeland Road,
PA King of Prussia, Pennsylvania 19406, US
SMITHKLINE BEECHAM CORPORATION, One Franklin Plaza P.O. Box 7929,
PAN Philadelphia Pennsylvania 19103, US
AG 201244
Connell, Anthony Christopher et al, SmithKline Beecham plc Corporate
Intellectual Property, Two New Horizons Court, Brentford, Middlesex TW8
AGN 9EP, GB
69941
OS ESP1998026 EP 0837073 A1 980422
SO Wila-EPZ-1998-H17-T1a
DT Patent
LA Anmeldung in Englisch; Veroeffentlichung in Englisch
DS R AT; R BE; R CH; R DE; R DK; R ES; R FI; R FR; R GB; R GR; R IE; R IT;
PIT R LI; R LU; R MC; R NL; R PT; R SE
EPA1 EUROPAEISCHE PATENTANMELDUNG
PI EP----837073 A1 19980422
OD 19980422
AI 1997EP-0308160 19971015
PRAI 1996US-0732028 19961016
ABEN Human MADr3 or MADr4 polypeptides and DNA (RNA) encoding such MADr3 or
MADr4 and a procedure for producing such polypeptides by recombinant
techniques is disclosed. Also disclosed are methods for utilizing such
MADr3 or MADr4, or compounds which inhibit or stimulate MADr3 or MADr4
for stimulating wound healing, and treating cancers, among others, are
also disclosed. Agonist and antagonists of these MAD proteins and
methods of their use are also disclosed. Also disclosed are diagnostic

assays for detecting diseases related to mutations in the nucleic acid sequences and altered concentrations of the polypeptides. Also disclosed are diagnostic assays for detecting mutations in the polynucleotides encoding the MADr3 or MADr4 and for detecting altered levels of the polypeptide in a host.

L43 ANSWER 5 OF 16 EUROPATFULL COPYRIGHT 2000 WILA

GRANTED PATENT - ERTEILTES PATENT - BREVET DELIVRE

AN 824545 EUROPATFULL ED 19991219 EW 199949 FS PS
TIEN PEPTIDE COMPOSITIONS WITH GROWTH FACTOR-LIKE ACTIVITY.
TIDE PEPTIDVERBINDUNGEN MIT WACHSTUMSFAKTORAEHNLICHER AKTIVITAET.
TIFR COMPOSITIONS PEPTIDIQUES PRESENTANT UNE ACTIVITE DU TYPE FACTEUR DE
CROISSANCE.
IN BHATNAGAR, Rajendra, S., 173 Los Robles, Burlingame, CA 94010, US;
QIAN, Jing, Jing, 3761 Elston Drive, San Bruno, CA 94066, US
PA The Regents of the University of California, 1111 Franklin Street, 12th
Floor, Oakland, CA 94607-5200, US
PAN 2137868
AG Goldin, Douglas Michael, J.A. KEMP & CO. 14 South Square Gray's Inn,
London WC1R 5LX, GB
AGN 31061
OS EPB1999066 EP 0824545 B1 991208
SO Wila-EPS-1999-H49-T1
DT Patent
LA Anmeldung in Englisch; Veroeffentlichung in Englisch
DS R AT; R BE; R CH; R DE; R DK; R ES; R FI; R FR; R GB; R GR; R IE; R IT;
R LI; R LU; R MC; R NL; R PT; R SE
PIT EPB1 EUROPAEISCHE PATENTSCHRIFT (Internationale Anmeldung)
PI EP----824545 B1 19991208
OD 19980225
AI 1996EP-0913807 19960418
PRAI 1995US-0431954 19950501
RLI WO 96-US5374 960418 INTAKZ
WO 9634881 961107 INTPNR
REP EP-530804 A WO91-19510 A
WO94-17099 A WO96-40771 A
US5002583 A US5171574 A
US5258029 A US5270300 A
US5324519 A US5364839 A
REN JOURNAL OF PHARMACEUTICAL SCIENCES, January 1977, Vol. 66, No. 1, BERGE
et al., pages 1-19

L43 ANSWER 6 OF 16 EUROPATFULL COPYRIGHT 2000 WILA

GRANTED PATENT - ERTEILTES PATENT - BREVET DELIVRE

AN 765478 EUROPATFULL ED 19980816 EW 199832 FS PS
TIEN POSITIVE AND POSITIVE/NEGATIVE CELL SELECTION MEDIATED BY PEPTIDE
RELEASE.
TIDE POSITIVE UND POSITIVE/NEGATIVE ZELLSELEKTION VERMITTELT DURCH
PEPTIOFREISETZUNG.
TIFR SELECTION CELLULAIRE POSITIVE ET POSITIVE/NEGATIVE, OBTENUE PAR L'ACTION
LIBERATRICE DE PEPTIDES.
IN TSENG-LAW, Janet, 4512 Workman Mill Road 320, Whitter, CA 90601, US;
KOBORI, Joan, A., 3600 Fairmeade Road, Pasadena, CA 91107, US;
AL-ABDALY, Fahad, A., 3014 Sonoma Street, Torrance, CA 90503, US;
GUILLERMO, Roy, 21810 Water Street, Carson, CA 90745, US;
HELGERSON, Sam, L., 820 S. Rosemead 219, Pasadena, CA 91107, US;

PA DEANS, Robert, J., 415 Furman Drive, Claremont, CA 91711, US
 BAXTER INTERNATIONAL INC., One Baxter Parkway, Deerfield, IL 60015-4633,
 US
 PAN 318507
 AG Bassett, Richard Simon, Eric Potter Clarkson, Park View House, 58 The
 Ropewalk, Nottingham NG1 5DD, GB
 AGN 52833
 OS EPB1998041 EP 0765478 B1 980805
 SO Wila-EPS-1998-H32-T2
 DT Patent
 LA Anmeldung in Englisch; Veroeffentlichung in Englisch
 DS R AT; R BE; R DE; R DK; R ES; R FR; R GB; R GR; R IE; R IT; R NL; R PT;
 R SE
 PIT EPB1 EUROPAEISCHE PATENTSCHRIFT (Internationale Anmeldung)
 PI EP----765478 B1 19980805
 OD 19970402
 AI 1995EP-0923835 19950613
 PRAI 1994US-0259427 19940614
 RLI WO 95-US7491 950613 INTAKZ
 WO 9534817 951221 INTPNR
 REP EP-344006 A WO93-14781 A
 WO94-02016 A WO94-03487 A
 WO95-07466 A WO95-09230 A
 REN PROC. NATL. ACAD. SCI. USA, vol. 90, August 1993 pages 7573-7577, J. F.
 ZAGURY ET AL. 'Identification of CD4 and major histocompatibility
 complex functional peptide sites and their homology with olidopeptides
 from human immunodeficiency virus type 1 glycoprotein gp 120: role in
 AIDS pathogenesis.'

L43 ANSWER 7 OF 16 EUROPATFULL COPYRIGHT 2000 WILA
 PATENT APPLICATION - PATENTANMELDUNG - DEMANDE DE BREVET

AN 676470 EUROPATFULL ED 19991121 EW 199541 FS OS STA B
 TIEN Stem cell factor.
 TIDE Stammzellenfaktor.
 TIFR Facteur de stimulation des cellules souches.
 IN Zsebo, Krisztina M., 411 Larch Crest Court, Thousand Oaks, California
 91320, US;
 Suggs, Sidney Vaughn, 509 Sierra Heights Court, Newbury Park, California
 91320, US;
 Bosselman, Robert A., 3301 Baccarat, Thousand Oaks, California 91362,
 US;
 Martin, Francis Hall, 337 North Greenmeadow Avenue, Thousand Oaks,
 California 91320, US
 PA AMGEN INC., 1840 Dehavilland Drive, Thousand Oaks California 91320
 -1789, US
 PAN 923231
 AG Brown, John David, FORRESTER & BOEHMERT Franz-Joseph-Strasse 38, D-80801
 Muenchen, DE
 AGN 28811
 OS ESP1995063 EP 0676470 A1 951011
 SO Wila-EPZ-1995-H41-T1a
 DT Patent
 LA Anmeldung in Englisch; Veroeffentlichung in Englisch
 DS R AT; R BE; R CH; R DE; R DK; R ES; R FR; R GB; R GR; R IT; R LI; R LU;
 R NL; R SE
 PIT EPA1 EUROPAEISCHE PATENTANMELDUNG
 PI EP----676470 A1 19951011
 OD 19951011
 AI 1995EP-0105391 19901004

PRAI 1989US-0422383 19891016
 1990US-0537198 19900611
 1990US-0573616 19900824
 1990WO-US05548 19900928
 1990US-0589701 19901001
 RLI EP 423980 DIV
 ABEN Novel stem cell factors, oligonucleotides encoding the same, and
 methods of production, are disclosed. Pharmaceutical compositions and
 methods of treating disorders involving blood cells are also
 disclosed.

L43 ANSWER 8 OF 16 EUROPATFULL COPYRIGHT 2000 WILA

GRANTED PATENT - ERTEILTES PATENT - BREVET DELIVRE

AN 661993 EUROPATFULL ED 19970604 EW 199719 FS PS
 TIEN PROTECTION AGAINST LIVER DAMAGE BY HGF.
 TIDE SCHUTZ GEGEN LEBERSCHADEN MIT HGF.
 TIFR PROTECTION CONTRE DES LESIONS HEPATIQUES AU MOYEN DU FACTEUR DE
 CROISSANCE D'HEPATOCYTES (HGF).
 IN ROOS, Filip, 71 Thomas Avenue, 12, Brisbane, CA 94055, US;
 PA SCHWALL, Ralph, 400 Griffin Avenue, Pacifica, CA 94044, US
 GENENTECH, INC., Legal Department 460 Point San Bruno Boulevard, South
 San Francisco, CA 94080, US
 PAN 210484
 AG Armitage, Ian Michael et al, MEWBURN ELLIS York House 23 Kingsway,
 London WC2B 6HP, GB
 AGN 27761
 OS EPB1997031 EP 0661993 B1 970507
 SO Wila-EPS-1997-H19-T1
 DT Patent
 LA Anmeldung in Englisch; Veroeffentlichung in Englisch
 DS R DE; R FR; R GB
 PIT EPB1 EUROPAEISCHE PATENTSCHRIFT (Internationale Anmeldung)
 PI EP----661993 B1 19970507
 OD 19950712
 AI 1993EP-0922207 19930915
 PRAI 1992US-0946263 19920916
 1992US-0968711 19921030
 RLI WO 93-US8718 930915 INTAKZ
 WO 9406456 940331 INTPNR
 REP EP-456188 A WO92-22321 A
 WO93-08821 A
 REN DATABASE WPI Week 9103, Derwent Publications Ltd., London, GB; AN
 91-017990 &
 JP-A-2288899 (TOYOBO KK) 28 November 1990 DATABASE WPI Week 9142,
 Derwent Publications Ltd., London, GB; AN 91-306734 &
 JP-A-3204899 (OTSUKA PHARM KK) 6 September 1991 DATABASE WPI Week 9211,
 Derwent Publications Ltd., London, GB; AN 92-085905 &
 JP-A-4030000 (TOYOBO KK) 31 January 1992 DATABASE WPI Week 9103, Derwent
 Publications Ltd., London, GB; AN 91-017990; &
 JP-A-2288899 DATABASE WPI Week 9142, Derwent Publications Ltd., London,
 GB; AN 91-306734; &
 JP-A-3204899 DATABASE WPI Week 9211, Derwent Publications Ltd., London,
 GB; AN 92-085905; &
 JP-A-4030000

L43 ANSWER 9 OF 16 EUROPATFULL COPYRIGHT 2000 WILA

GRANTED PATENT - ERTEILTES PATENT - BREVET DELIVRE

AN 640131 EUROPATFULL ED 19990502 EW 199916 FS PS
 TIEN GENETICALLY ENGINEERED ANTIBODIES.
 TIDE GENTECHNOLOGISCH HERGESTELLTE ANTIKOERPER.
 TIFR ANTICORPS PRODUITS PAR GENIE GENETIQUE.
 IN HARDMAN, Norman, Gstatenrainweg 67/3, CH-4125 Riehen, CH;
 PLUSCHKE, Gerd, Am Schoenberg 6, D-7802 Merzhausen, DE;
 MURRAY, Brendan, Matthaeusstrasse 14, CH-4057 Basle, CH
 PA Novartis AG, Schwarzwaldallee 215, 4058 Basel, CH, in BE, CH, DE, DK,
 ES, FR, GB, GR, IE, IT, LI, LU, MC, NL, PT, SE;
 Novartis-Erfindungen Verwaltungsgesellschaft m.b.H., Brunner Strasse 59,
 1235 Wien, AT, in AT
 PAN 2240421; 2317280
 OS EPB1999024 EP 0640131 B1 990421
 SO Wila-EPS-1999-H16-T1
 DT Patent
 LA Anmeldung in Englisch; Veroeffentlichung in Englisch
 DS R AT; R BE; R CH; R DE; R DK; R ES; R FR; R GB; R GR; R IE; R IT; R LI;
 R LU; R MC; R NL; R PT; R SE
 PIT EPB1 EUROPAEISCHE PATENTSCHRIFT (Internationale Anmeldung)
 PI EP----640131 B1 19990421
 OD 19950301
 AI 1993EP-0905306 19930305
 PRAI 1992EP-0810188 19920317
 RLI WO 93-EP505 930305 INTAKZ
 WO 9319180 930930 INTPNR
 REP EP-428485 A WO91-04055 A
 REN NATURE vol. 332, 24 March 1988, LONDON, GB pages 323 - 327 L. RIECHMANN
 ET AL. 'Reshaping human antibodies for therapy.' PROCEEDINGS OF THE
 NATIONAL ACADEMY OF SCIENCES OF THE USA vol. 89, no. 2, January 1992,
 WASHINGTON DC, US pages 466 - 470 A. MITTELMAN ET AL. 'Human high
 molecular weight melanoma-associated antigen (HMW-MAA) mimicry by mouse
 anti-idiotypic monoclonal antibody MK2-23: Induction of humoral
 anti-HMW-MAA immunity and prolongation of survival in patients with
 stage IV melanoma.' EUROPEAN JOURNAL OF IMMUNOLOGY vol. 19, no. 10,
 October 1989, WEINHEIM, GERMANY pages 1961 - 1963 A. ALANEN ET AL.
 'Sequence and linkage of the V κ 21A and G germ-line gene segments in
 the mouse.'

L43 ANSWER 10 OF 16 EUROPATFULL COPYRIGHT 2000 WILA
 GRANTED PATENT - ERTEILTES PATENT - BREVET DELIVRE

AN 621880 EUROPATFULL ED 19990919 EW 199936 FS PS
 TIEN DRUG DELIVERY SYSTEM FOR THE SIMULTANEOUS DELIVERY OF DRUGS ACTIVATABLE
 BY ENZYMES AND LIGHT.
 TIDE DURCH ENZYME UND LICHT AKTIVIERBARES ARZNEIMITTELABGABESYSTEM ZUR
 GLEICHZEITIGEN ABGABE VON ARZNEIMITTELN.
 TIFR SYSTEME D'APPORT DE MEDICAMENTS POUR L'APPORT SIMULTANE DE MEDICAMENTS
 IN ACTIVABLES PAR LES ENZYMES ET LA LUMIERE.
 KOPECEK, Jindrich, 1103 South Alton Way, Salt Lake City, UT 84108, US;
 KRINICK, Nancy, 1201 West Swallow Road 7, Fort Collins, CO 80526, US
 PA UNIVERSITY OF UTAH, Technology Transfer Office 421 Wakara Way, Suite
 170, Salt Lake City, Utah 84108, US
 PAN 243414
 AG Thomson, Paul Anthony, Potts, Kerr & Co. 15, Hamilton Square, Birkenhead
 Merseyside L41 6BR, GB
 AGN 36701
 OS EPB1999051 EP 0621880 B1 990908
 SO Wila-EPS-1999-H36-T1
 DT Patent

LA Anmeldung in Englisch; Veroeffentlichung in Englisch
DS R AT; R BE; R CH; R DE; R DK; R ES; R FR; R GB; R GR; R IE; R IT; R LI;
R NL; R PT; R SE
PIT EPB1 EUROPÄISCHE PATENTSCHRIFT (Internationale Anmeldung)
PI EP----621880 B1 19990908
OD 19941102
AI 1993EP-0904633 19930121
PRAI 1992US-0822924 19920121
RLI WO 93-US683 930121 INTAKZ
WO 9314142 930722 INTPNR
REP EP-103184 A EP-213811 A
US5037883 A
REN BRITISH JOURNAL OF CANCER, vol.55, no.2, February 1987 pages 165 - 174
R. DUNCAN ET AL. 'ANTICANCER AGENTS COUPLED TO N-(2-
HYDROXYPROPYL)METHACRYLAMIDE COPOLYMERS. I. EVALUATION OF DAUNOMYCIN AND
PUROMYCIN CONJUGATES IN VITRO.' Makromol. Chem., 191, "Synthesis of
N-(2-hydroxypropyl)methacrylamide copolymer-anti-Thy 1.2
antibody-chlorin e6 conjugates and a preliminary study of their
photodynamic effect on mouse splenocytes in vitro", (KRINICK), 1990,
pages 839-856. The Journal of Investigative Dermatology, Vol. 77, No. 1,
"Photoradiation Therapy for Cutaneous and Subcutaneous Malignancies",
(DOUGHERTY), 1981, pages 122-124. Journal of Controlled Release, Vol.
16, "Targetable photoactivatable polymeric drugs", (KOPECEK), 1991,
pages 137-144

L43 ANSWER 11 OF 16 EUROPATFULL COPYRIGHT 2000 WILA

GRANTED PATENT - ERTEILTES PATENT - BREVET DELIVRE

AN 601043 EUROPATFULL ED 19981206 EW 199848 FS PS
TIEN HYBRID CYTOKINES.
TIDE HYBRIDE CYTOKINE.
TIFR CYTOKINES HYBRIDES.
IN TODARO, George, J., 1940-15th Avenue, Seattle, WA 98112, US;
ROSE, Timothy, M., 5045 N.E. 70th Street, Seattle, WA 98115, US
PA Fred Hutchinson Cancer Research Center, 1124 Columbia Street, Seattle
Washington 98104, US
PAN 699390
AG Vossius, Volker, Dr. et al, Dr. Volker Vossius, Patentanwaltskanzlei -
Rechtsanwaltskanzlei, Holbeinstrasse 5, 81679 Muenchen, DE
AGN 12524
OS EPB1998062 EP 0601043 B1 981125
SO Wila-EPS-1998-H48-T1
DT Patent
LA Anmeldung in Englisch; Veroeffentlichung in Englisch
DS R AT; R BE; R CH; R DE; R DK; R ES; R FR; R GB; R GR; R IE; R IT; R LI;
R LU; R MC; R NL; R SE
PIT EPB1 EUROPÄISCHE PATENTSCHRIFT (Internationale Anmeldung)
PI EP----601043 B1 19981125
OD 19940615
AI 1992EP-0918688 19920824
PRAI 1991US-0753178 19910830
RLI WO 92-US7112 920824 INTAKZ
WO 9305169 930318 INTPNR
REP WO90-12877 A WO91-02754 A
US4935233 A
REN International Journal of Cell Cloning, Vol. 9, issued 1991, D.E.
WILLIAMS et al., "Hybrid cytokines as hematopoietic growth factors",
pages 542-547, see entire document. Cancer, Vol. 67, issued 1991, D.E.
WILLIAMS and L.S. PARK, "Hematopoietic effects of granulocyte macrophage
colony-stimulating factor/interleukin-3 fusion protein", pages

2705-2707, see entire document. Eur. J. Biochem., Vol. 175, issued 1988, R.J. SIMPSON et al., "Structural characterization of murine myeloid leukemia inhibitory factor", pages 541-547, see entire document. EMBO J., Vol. 6, No. 10, issued October 1987, K. YASUKAWA et al., "Structure and expression of human B cell stimulatory factor-2 (BSF-2/IL-6) gene", pages 2939-2945, see entire document. Mol. Cell. Biol., Vol. 9, No. 7, issued July 1989, N. MALIK et al., "Molecular cloning, sequence analysis, and functional expression of a novel growth regulatory, oncostatin M", pages 2847-2853, see entire document. FEBS LETTERS., vol.306, no.2 3, 20 July 1992, AMSTERDAM NL pages 262 - 264 FRANK W.G. LEEBEEK ET AL. 'Construction and functional analysis of hybrid interleukin-6 variants. Characterization of the role of the C-terminus for species specificity'

L43 ANSWER 12 OF 16 EUROPATFULL COPYRIGHT 2000 WILA

PATENT APPLICATION - PATENTANMELDUNG - DEMANDE DE BREVET

AN 597503 EUROPATFULL UP 20000216 EW 199420 FS OS STA B
 TIEN ECK receptor ligands.
 TIDE ECK-Rezeptor-Liganden.
 TIFR Ligands de recepteurs ECK.
 IN Bartley, Timothy D., 2431 McCrea Road, Thousand Oaks, CA 91362, US;
 Fox, Gary M., 35 West Kelly Road, Newbury Park, CA 91320, US;
 Boyle, William J., 13024 Williams Ranch Road, Moorpark, CA 93021, US;
 Welcher, Andrew A., 707 Danvers Circle, Newbury Park, CA 91320, US;
 Parker, Vann P., 1086 Antelope Place, Newbury Park, CA 91320, US
 PA AMGEN INC., Amgen Center, 1840 Dehavilland Drive, Thousand Oaks, CA
 91320-1789, US
 PAN 923233
 AG Vossius, Volker, Dr. et al, Dr. Volker Vossius, Patentanwaltskanzlei-
 Rechtsanwaltskanzlei Holbeinstrasse 5, D-81679 Muenchen, DE
 AGN 12524
 OS ESP1994035 EP 0597503 A2 940518
 SO Wila-EPZ-1994-H20-T1a
 DT Patent
 LA Anmeldung in Englisch; Veroeffentlichung in Englisch
 DS R AT; R BE; R CH; R DE; R DK; R ES; R FR; R GB; R GR; R IE; R IT; R LI;
 R LU; R MC; R NL; R PT; R SE
 PIT EPA2 EUROPAEISCHE PATENTANMELDUNG
 PI EP----597503 A2 19940518
 OD 19940518
 AI 1993EP-0118469 19931115
 PRAI 1992US-0977708 19921113
 1993US-0145616 19931109

GRANTED PATENT - ERTEILTES PATENT - BREVET DELIVRE

AN 597503 EUROPATFULL ED 19981025 EW 199842 FS PS
 TIEN ECK receptor ligands.
 TIDE ECK-Rezeptor-Liganden.
 TIFR Ligands de recepteurs ECK.
 IN Bartley, Timothy D., 2431 McCrea Road, Thousand Oaks, CA 91362, US;
 Fox, Gary M., 35 West Kelly Road, Newbury Park, CA 91320, US;
 Boyle, William J., 13024 Williams Ranch Road, Moorpark, CA 93021, US;
 Welcher, Andrew A., 707 Danvers Circle, Newbury Park, CA 91320, US;
 Parker, Vann P., 1086 Antelope Place, Newbury Park, CA 91320, US
 PA AMGEN INC., Amgen Center, 1840 Dehavilland Drive, Thousand Oaks, CA
 91320-1789, US
 PAN 923233
 AG Vossius, Volker, Dr. et al, Dr. Volker Vossius, Patentanwaltskanzlei -

Rechtsanwaltskanzlei, Holbeinstrasse 5, 81679 Muenchen, DE
 12524
 AGN EPB1998056 EP 0597503 B1 981014
 OS Wila-EPS-1998-H42-T1
 SO Patent
 DT Anmeldung in Englisch; Veroeffentlichung in Englisch
 LA R AT; R BE; R CH; R DE; R DK; R ES; R FR; R GB; R GR; R IE; R IT; R LI;
 DS R LU; R MC; R NL; R PT; R SE
 PIT EPB1 EUROPAEISCHE PATENTSCHRIFT
 PI EP----597503 B1 19981014
 OD 19940518
 AI 1993EP-0118469 19931115
 PRAI 1992US-0977708 19921113
 1993US-0145616 19931109
 REP WO91-17427 A WO92-07094 A
 REN MOLECULAR & CELLULAR BIOLOGY, vol. 10, no. 11, Washington, DC (US); L.B. HOLZMAN et al., pp. 5830-5838 MOLECULAR & CELLULAR BIOLOGY, vol. 10, no. 12, Washington, DC (US); R.A. LINDBERG et al., pp. 6316-6324 SCIENCE, vol. 254, 1991, Lancaster, PA (US); S.A. AARONSON pp. 1146-1153 MOLECULAR & CELLULAR BIOLOGY, vol. 12, no. 4, Washington, DC (US); J. PARTANEN et al., pp. 1698-1707 NATURE, vol. 368, no. 6471, 1994, London (GB); T.D. BARTLEY et al., pp. 558-560
 ABEN Ligands which bind to the eck receptor are disclosed. More particularly, polypeptides which bind specifically to the eck receptor (eck receptor binding proteins or EBPs) and DNA sequences encoding said polypeptides are disclosed. Methods of treatment using eck receptor ligands and soluble eck receptor and disclosed, as are pharmaceutical compositions containing same. A rapid and sensitive method for the detection of receptor binding activity in crude samples is provided.

L43 ANSWER 13 OF 16 EUROPATFULL COPYRIGHT 2000 WILA

GRANTED PATENT - ERTEILTES PATENT - BREVET DELIVRE

AN 576625 EUROPATFULL ED 19970108 EW 199634 FS PS
 TIEN METHOD FOR ANALYZING THE GLYCATION OF HEMOGLOBIN.
 TIDE VERFAHREN ZUR ANALYSE DER GLYKIERUNG VON HAEMOGLOBIN.
 TIFR PROCEDE POUR ANALYSER LA GLYCERATION DE L'HEMOGLOBINE.
 IN SAUNDERS, Alexander, 8 Trillum Lane, San Carlos, CA 94070, US
 PA CHRONOMED, INC., 1755 E. Bayshore Road, Ste. 22, Redwood City, CA 94063, US
 PAN 1567100
 AG Plougmann, Vingtoft & Partners A/S, Sankt Annae Plads 11, P.O. Box 3007, 1021 Copenhagen K, DK
 AGN 101171
 OS EPB1996051 EP 0576625 B1 960821
 SO Wila-EPS-1996-H34-T2
 DT Patent
 LA Anmeldung in Englisch; Veroeffentlichung in Englisch
 DS R AT; R BE; R CH; R DE; R DK; R ES; R FR; R GB; R GR; R IT; R LI; R LU;
 R MC; R NL; R SE
 PIT EPB1 EUROPAEISCHE PATENTSCHRIFT (Internationale Anmeldung)
 PI EP----576625 B1 19960821
 OD 19940105
 AI 1992EP-0912238 19920316
 PRAI 1991US-0681693 19910408
 RLI WO 92-US2096 920316 INTAKZ
 WO 9217107 921015 INTPNR
 REP US4835097 A
 REN THE JOURNAL OF THEORETICAL BIOLOGY vol. 81, no. 3, 1979, LONDON GB pages

547 - 561; KIRK W. BEACH: 'A Theoretical Model to Predict the Behavior of Glycosylated Hemoglobin Levels' THE JOURNAL OF LABORATORY AND CLINICAL MEDICINE vol. 102, no. 1, July 1983, ST. LOUIS MO. US pages 628 - 636; M. M. ELSEWEIDY, M. STALLINGS, AND E.C. ABRAHAM: 'Changes in glycosylated hemoglobine with red cell aging in normal and diabetic subjects and in newborn infants of normal and diabetic mothers' DANISH MEDICAL BULLETIN vol. 32, no. 6, December 1985, COPENHAGEN DK pages 309 - 328; HENRIK BINDESBOL MORTENSEN: 'Glycated hemoglobin: Reaction and Biokinetic Studies; Clinical Application of Hemoglobin Alc in the Assessment of Metabolic Control in Children with Diabetes Mellitus' cited in the application

L43 ANSWER 14 OF 16 EUROPATFULL COPYRIGHT 2000 WILA
GRANTED PATENT - ERTEILTES PATENT - BREVET DELIVRE

AN 506773 EUROPATFULL ED 19970108 EW 199615 FS PS
TIEN A STIMULATOR OF VASCULAR ENDOTHELIAL CELLS AND USE THEREOF.
TIDE STIMULATOR VON VASKULAEREN ENDOTHELZELLEN UND SEINE VERWENDUNG.
TIFR STIMULATEUR DES CELLULES VASCULAIRES ENDOTHELIALES ET SON UTILISATION.
IN XIU, Rui-Jean, Magnus Ladulasgatan 31, S-116 27 Stockholm, SE
PA XIU, Rui-Jean, Magnus Ladulasgatan 31, S-116 27 Stockholm, SE
PAN 1391830
AG Halldin, Bo et al, Dr. Ludwig Brann Patentbyra AB P.O. Box 17192, S-104 62 Stockholm, SE
AGN 23041
OS EPB1996024 EP 0506773 B1 960410
SO Wila-EPS-1996-H15-T1
DT Patent
LA Anmeldung in Englisch; Veroeffentlichung in Englisch
DS R AT; R BE; R CH; R DE; R DK; R ES; R FR; R GB; R GR; R IT; R LI; R LU;
PIT EPB1 EUROPAEISCHE PATENTSCHRIFT (Internationale Anmeldung)
PI EP----506773 B1 19960410
OD 19921007
AI 1991EP-0901497 19901221
PRAI 1989SE-0004353 19891222
RLI WO 90-SE868 901221 INTAKZ
REN WO 9109607 910711 INTPNR
Dialog Information Services, File 351, World
Patent Index 81-90, Dialogaccession No. 88-253386/36, YG NONOGAWA SHOJI:
"Antiinflammatory prepn. -contains active substance extracted from
fruiting body or mycelium ofheterobasidiae", JP 63183537, A, 880728,
8836 (Basic) CHEMICAL ABSTRACTS, Volume 104, No. 23, 9 June 1986,
(Columbus, Ohio, US), LIUSHUHUA et al: "Regeneration of hemopoietic
tissue in grafted murine femur anddemonstration of the effect of some
radioprotectants", see page 380, Abstract203144p, & Zhonghua Fangshe
Yixue Yu Fanghu Zazhi 1985, 5 (4), 262-265a CHEMICAL ABSTRACTS, Vol. 104
(1986), Abstract No. 122768t, Zhongcaoyao 1984, 15(9), 23-6, 22 (Ch)

L43 ANSWER 15 OF 16 EUROPATFULL COPYRIGHT 2000 WILA
GRANTED PATENT - ERTEILTES PATENT - BREVET DELIVRE

AN 474691 EUROPATFULL ED 19970307 EW 199646 FS PS
TIEN MONOCLONAL ANTIBODIES FOR INDUCING TOLERANCE.
TIDE MONOKLONALE ANTIKOERPER ZUR INDUZIERUNG VON TOLERANZ.
TIFR ANTICORPS MONOCLONAUX POUR SUSCITER UNE TOLERANCE.
IN Cobbold, Stephen Paul, University of Oxford, South Parks Road, Oxford
OX1 3RE, GB;
Waldmann, Herman, University of Oxford, South Parks Road, Oxford OX1

3RE, GB
 PA THE WELLCOME FOUNDATION LIMITED, Glaxo Wellcome House, Berkeley Avenue,
 Greenford, Middlesex UB6 0NN, GB
 PAN 201576
 AG Marchant, James Ian et al, Elkington and Fife, Prospect House, 8
 Pembroke Road, Sevenoaks, Kent TN13 1XR, GB
 AGN 33511
 OS EPB1996071 EP 0474691 B1 961113
 SO Wila-EPS-1996-H46-T1
 DT Patent
 LA Anmeldung in Englisch; Veroeffentlichung in Englisch
 DS R AT; R BE; R CH; R DE; R DK; R ES; R FR; R GB; R IT; R LI; R LU; R NL;
 R SE
 PIT EPB1 EUROPÄISCHE PATENTSCHRIFT (Internationale Anmeldung)
 PI EP----474691 B1 19961113
 OD 19920318
 AI 1990EP-0908270 19900531
 PRAI 1989GB-0012497 19890531
 RLI WO 90-GB840 900531 INTAKZ
 WO 9015152 901213 INTPNR
 REN TRANSPLANTATION PROCEEDINGS, vol. XIX, no. 5, October 1987, Grune &
 Stratton Inc., New York, NY (US); M. JONKER et al., pp. 4308-4314
 IMMUNOLOGICAL & CELLULAR BIOLOGY, vol. 67, no. 1, January 1989, Adelaide
 (AU); B. CHARLTON et al., pp. 1-7 JOURNAL OF IMMUNOLOGY, vol. 142, no.
 5, 01 March 1989, American Association of Immunologists, Baltimore, MD
 (US); N.L. CARTERON et al., pp. 1470-1475 EUROPEAN JOURNAL OF
 IMMUNOLOGY, vol. 17, 1987, VCH VerlagsgesmbH., Weinheim (DE); S. QIN et
 al., pp. 1159-1165

L43 ANSWER 16 OF 16 EUROPATFULL COPYRIGHT 2000 WILA

GRANTED PATENT - ERTEILTES PATENT - BREVET DELIVRE

AN 316440 EUROPATFULL ED 19970108 EW 199601 FS PS
 TIEN SYSTEM AND METHOD FOR PROVIDING LOCALIZED MOESSBAUER ABSORPTION IN AN
 ORGANIC MEDIUM.
 TIDE VERFAHREN UND SYSTEM ZUR ERZIELUNG EINER LOKALEN MOESSBAUER-ABSORPTION
 IN EINEM ORGANISCHEN MEDIUM.
 TIFR SYSTEME ET METHODE POUR OBTENIR UNE ABSORPTION MOESSBAUER LOCALISEE DANS
 UN MILIEU ORGANIQUE.
 IN Mills, Randell L., R.D. 2, Cochranville Pennsylvania 19330, US
 PA Mills, Randell L., R.D. 2, Cochranville Pennsylvania 19330, US
 PAN 745290
 AG Patentanwaelte Beetz - Timpe - Siegfried Schmitt-Fumian - Mayr,
 Steinsdorfstrasse 10, D-80538 Muenchen, DE
 AGN 100712
 OS EPB1996001 EP 0316440 B1 960103
 SO Wila-EPS-1996-H01-T2
 DT Patent
 LA Anmeldung in Englisch; Veroeffentlichung in Englisch
 DS R AT; R BE; R CH; R DE; R FR; R GB; R IT; R LI; R LU; R NL; R SE
 PIT EPB1 EUROPÄISCHE PATENTSCHRIFT (Internationale Anmeldung)
 PI EP----316440 B1 19960103
 OD 19890524
 AI 1988EP-0906289 19880527
 PRAI 1987US-0055591 19870528
 RLI WO 88-US1796 880527 INTAKZ
 WO 8809152 881201 INTPNR
 REP EP-198257 A EP-240990 A
 US3631247 A US4059769 A
 US4363965 A

Aim: To determine what the actual specifics for filing patents are in view of progress in both the thrombocyte and the neutrophil models.

Minutes:

1. The patent should be formulated with two intentions: The first is that it should be stated in a way that would allow a colleague versed in optimization and the hemapoietic system to recreate our results. This means that the model should be presented much as a scientific article is presented, i.e. very detailed. Secondly, the patent request should include every other conceivable way to achieve the same or similar results. This is obviously the essence of the protection we would need. This doesn't however mean that we should actually implement every possible idea, but rather to state in words that this and that optimization scheme could also do the trick, that this or that change in the mathematical model would also work etc. We could in this respect simply reference a large review on optimization schemes and state that they all could apply.
2. We could file for a general patent on optimization of growth factor administration to assist chemotherapy. In this filing we should state any possible growth factor that we know exists today and its effects on any lineage. However, this would obviously not work in the case of new growth factors. Our current thrombocyte and neutrophil models would then serve as examples of this capacity of ours.
3. Concretely, we could first file a patent for general optimization of growth factor administration, and then file additional patents as we go along and extend our capabilities. If we intend to sell our rights later to other firms then we should think of actually formulating different patents since one patent cannot be carved up.
4. Within one year of filing a patent we could still make substantial changes in it, but after that any change must be considered as a completely different patent that has to prove its novelty with respect to the previous patent. Within 18 months of filing for a patent, it is published. Then there is a period of time when any person may contest our patent before it is finally endorsed. This is an important point: It is essential that our patent request 'hold water' against attacks by other biologists and modelers. It is therefore important that we have substantial data and that our model (especially the mathematical core) would not be challenged easily.
5. Mr. Cohen suggested that we only turn to external optimization experts with a view to improving our model after we file the initial patent so that there is no breach in our knowledge.

Suggested course of action for the neutrophil model:

Since filing a patent should be considered one of the two major tasks for the neutrophil project (the other being simulating chemotherapy) we should follow Mr. Cohen's advice on writing quickly (and well) our patent request. Mr. Cohen emphasized that the mathematical model is the core of the project and that this will probably be the target of any challenges on the patent. I therefore think that a critical look into the model is warranted. This means the formulation very specifically of every possible way that the model may be considered flawed, a determination of what could be formulated otherwise, why it isn't formulated that way, and how we can state that that formulation as a possibility etc. I therefore suggest that Yuval or Nathan (preferably both) undertake this effort.

After this is achieved the patent should be filed as soon as possible.

Sarel.

Zvia,

Markmail310700.txt

I am concerned by the tone and request of your previous e-mails to Ricki. She is working on the drafts and is aware of her commitment as to the time to provide you with a draft of the application.

As I have explained previously, the process in my Group is for the associates/scientific members of my Group to draft the applications and I review them and then the applications go to the client.

In two previous meetings we have reviewed the patent strategy and it has not changed. It seems that we have to review the patent strategy for commercial questions, Ricki is not in a position to answer them, otherwise she would have. Members of my Group do not guess. Ricki's time is most efficiently spent on drafting applications.

In the future, please direct scientific/patent questions to Ricki and other commercial/license questions to me.

Mark

> -----Original Message-----

> From: Zvia Agur [SMTP:agur@imbm.org]

> Sent: Mon, July 31, 2000 2:45 PM

> To: Ricki Abboudi

> Cc: Mark Cohen; Pearl Zeev

> Subject: Re: Patent Application

> Ricki hi,

> Following our phone conversation yesterday, please let me know whether I am to expect the draft of the patent in this week (your commitment was July 30).

> In a separate mail I enclose the file you were asking for.

> In general, I am ready to help in any way I can, but this does not include the internal arrangements and communication in your own office. Therefore I reiterate my previous request. i.e., that I will be much obliged to you for

> taking care to explain to us our patent, its exact wording and their significance.

> Best regards,

> Zvia Agur

> ----- Original Message -----

> From: Ricki Abboudi <Abboudir@TechnologyLaw.co.il>

> To: Zvia Agur (E-mail) <agur@imbm.org>

> Cc: Mark Cohen <CohenM@TechnologyLaw.co.il>

> Sent: Monday, July 31, 2000 1:32 PM

> Subject: Patent Application

>

>

> > Dear Zvia,

> >

> > I am still working on the draft, and I will let you know when it is ready.

> > I was wondering whether you could send me by e-mail the text of your appendix B (G-CSF model), the way you sent me appendix A (thrombocytopenia)

> > and C (cancer).

> >

> > Regarding your wish to discuss legal aspects concerning the ability to protect your patents, their commercial significance, etc., please direct all legal/commercial questions to Mark Cohen as I am strictly the

Markmail310700.txt
> > science/technology contact person at the present time.
> >
> > Sincerely,
> >
> >
> > Ricki Abboudi
> >
> >
> >
> >
> > _____
> > Ricki Abboudi
> > EITAN, PEARL, LATZER & COHEN-ZEDEK
> > Main Office
> > 2 Gav Yam Center
> > 7 Shenkar St.
> > Herzelia
> > Tel: 972-9-970-9401
> > Fax: 972-9-970-9001
> >
> >

Dear Zvia,

patentmeeting310700.txt

I am still working on the draft, and I will let you know when it is ready. I was wondering whether you could send me by e-mail the text of your appendix B (G-CSF model), the way you sent me appendix A (thrombocytopenia) and C (cancer).

Regarding your wish to discuss legal aspects concerning the ability to protect your patents, their commercial significance, etc., please direct all legal/commercial questions to Mark Cohen as I am strictly the science/technology contact person at the present time.

Sincerely,

Ricki Abboudi

Ricki Abboudi
EITAN, PEARL, LATZER & COHEN-ZEDEK
Main Office
2 Gav Yam Center
7 Shenkar St.
Herzeliya
Tel: 972-9-970-9401
Fax: 972-9-970-9001


```

mailbill1010800.txt
<x-htm!><!DOCTYPE HTML PUBLIC "-//W3C//DTD HTML 4.0 Transitional//EN">
<HTML><HEAD>
<META content="text/html; charset=windows-1255" http-equiv=Content-Type>
<META content="MSHTML 5.00.2314.1000" name=GENERATOR>
<STYLE></STYLE>
</HEAD>
<BODY bgColor=#ffffff>
<DIV><FONT face=Arial size=2><FONT face=Arial size=2>
<P align=left dir=ltr><FONT color=#ff0000 face=Arial>zvia- I wrote in a familiar
way in hope that his friendship with nitzan will yield a discount. yhis is the
reason that the mail is from me and not from you. please send it back to me and
I will move it forward to him.</FONT>
<P align=left dir=ltr>Dear Mr. Mandir
<DIV></DIV>
<P></P>
<P align=left dir=ltr>The Institute for Medical BioMathematics (IMBM) is an
academic institute that is devoted to Bio-Mathematical research in the cancer
area. The institute's chief scientist and president is Prof. Zvia Agur, a
well-known biomathematician and respected scientist. The institute has a
commercial company on its side, Optimata, which is devoted to commercializing
its innovations. We have come to the stage that sufficient scientific
break-through have been achieved, and there is need for patent registration.
<DIV></DIV>
<P></P>
<P align=left dir=ltr>I am the head of the cancer project in the institute, and
therefor responsible for these matters. I received warm recommendations about
your office from our mutual friend Nitzan Hirsch-Falk from Kleinhendler &
Halevy office in Israel.
<DIV></DIV></FONT><FONT size=2>
<P></P></FONT><FONT face=Arial size=2>
<P align=left dir=ltr>I will explain in a very general way our claim, and
proceed with a few questions. We have developed a <STRONG>method for optimizing
drug delivery: optimal administration/treatment/efficacy of (specific) drugs to
(specific) disease by a (specific) user (physician, drug developer, or
scientist) using mathematical and computational methods and biological and
clinical knowledge.
<DIV></DIV></FONT></STRONG><FONT size=2>
<P></P></FONT><FONT face=Arial size=2>
<P align=left dir=ltr>Of course this is only a very general description, and
more material will be delivered upon agreement. We have full detailed scientific
description of our methods.
<DIV></DIV></FONT><FONT size=2>
<P></P></FONT><FONT face=Arial size=2>
<P align=left dir=ltr>Now- what do we need to know:
<DIV></DIV></FONT><FONT size=2>
<P></P></FONT><FONT face=Arial size=2>
<P align=left dir=ltr>1) Can your office take charge of our patent strategy?
<DIV></DIV></FONT><FONT size=2>
<P></P></FONT><FONT face=Arial size=2>
<P align=left dir=ltr>2) What is the time scale for this process, and when
should we put our milestones? Time is crucial!
<DIV></DIV></FONT><FONT size=2>
<P></P></FONT><FONT face=Arial size=2>
<P align=left dir=ltr>3) How will the work be done? ways of communications,
meetings, etc. Your office must have a wide experience with overseas clients?
<DIV></DIV></FONT><FONT size=2>
<P></P></FONT><FONT face=Arial size=2>
<P align=left dir=ltr>4) Can your office guarantee worldwide IP coverage
(Europe, Japan)?
<DIV></DIV></FONT><FONT size=2>
<P></P></FONT><FONT face=Arial size=2>
<P align=left dir=ltr>5) What are the costs?
<DIV></DIV></FONT><FONT size=2>

```

mailbill1010800.txt

<P></P>
<P align=left dir=ltr>I thank you very much for your reply and am looking
forward for it. Please take into consideration that our time scale at the moment
is measured in days.
<DIV></DIV>
<P></P>
<P align=left dir=ltr>Thank You,
<DIV></DIV>
<P></P>
<P align=left dir=ltr>Moshe Vardi: <FONT
face=Arial size=2>moshv@imbm.org
<DIV></DIV>
<P></P></DIV></BODY></HTML>
</x-html>

Subramanian, Chid

From: Moshe Vardi [moshv@imbm.org]
Sent: Sunday, August 20, 2000 8:58 AM
To: Mandir, William H.
Cc: CSubramanian@sughrue.com
Subject: Re: Optimata meeting

Dear Bill,

Thank you for your comments on some of the issues we have talked about, and for the helpful tips. As we see it, you are now our patent attorney, and therefor you can feel free to move on with the job. We shall discuss everything on the 28th (9:30 will be convenient), and perhaps 29th. I would say that you have a green light to progress with our job, and I expect this to bring us to a point where next week's meeting/s would be more than a "getting to know each other", but real work. This in my opinion is mostly a question of how you and Mr. Subramanian are coping with the material. I am here this week to answer on any preliminary technical issues. Last but not least, it will be a pleasure to have dinner with you, and I would like very much to thank you for the kind invitation. Monday the 29th is less dangerous in terms of us making it in time (I'll be landing on Sunday, but I cannot guarantee for Israeli airline scheduling). As to dietary restrictions, none exist, therefor we are in your arms. I'm looking forward to meeting you and Mr. Subramanian ,

Regards,
Moshe

p.s. I'll bring the tex file on hard-copy. If you would like to open it- try downloading ghost-viewer from the net.

----- Original Message -----

From: Mandir, William H. <wmandir@sughrue.com>
To: 'Moshe Vardi' <moshv@imbm.org>
Cc: Subramanian, Chid <CSubramanian@sughrue.com>
Sent: Friday, August 18, 2000 9:39 PM
Subject: RE: Optimata meeting

> Shalom Moshe:
>
> Sorry I missed your call. We have left open Monday, August 28 for a
> meeting with you and Professor Agur--we understand that you have a meeting
> on Monday afternoon at 4:00. Please come to our offices around 9:30 am at
> 2100 Pennsylvania Avenue, N.W., which is on the corner of 21st street and
> Pennsylvania Ave--we are about 6 blocks from the White House. Also, we
are
> very close to the Foggy Bottom Metro stop. There will be a directory in
the
> lobby, but I am on the 7th floor. By the way, our dress code is business
> casual--no coats or ties. At this point, I am unable to gauge the amount
of
> time we will need. Perhaps we should see how much progress we make on
> Monday, and then you can determine what additional days you would like to
> meet. I am available all day Monday, and Chid Subramanian will be
available
> to also meet on Tuesday, and even Wednesday if need be. Chid Subramanian
> will be the primary attorney responsible for drafting the application.
Chid
> is the attorney I mentioned who graduated from the Indian Institute of
> Technology, and has degrees in both Chemical engineering and Computer
> Science. Chid also has a great source for asking any biochemistry
> questions--his wife has a Ph.D. in BioChemistry. Chid has already started

> to review the materials you sent, and he sees no problems in handling the
 > technology. However, we are having some problems opening the .tek and .ps
 > files, and even if we are able to open these files, we do not have the
 > necessary conversion software. Therefore, please send these files again
 in
 > a WORD format directly to Chid at CSubramanian@Sughrue.com.
 >
 > As mentioned, I plan on being at the meeting all day on Monday,
 > August 28. So, Monday would be the best time to discuss such topics as
 > strategy, costs and procedures, as well as technical topics relating to
 the
 > invention. Tuesday (and Wednesday) will be left open for further
 technical
 > meetings with Chid. Below are some general preparatory comments for our
 > meeting on Monday, August 28:
 >
 > Patent Strategy
 >
 > Our firm has vast experience in advising clients concerning patent
 > strategy. However, that advice will depend on several factors, such as
 > costs, development stage of the invention, and timing. For example,
 > recently an Israeli start-up company came to us wanting to patent their
 > invention. At this point, the start-up is just obtaining their first
 round
 > of VC money and was still refining the invention, so the option of filing
 a
 > provisional application, which is somewhat less expensive in comparison to
 a
 > regular application, especially if new subject matter will be added, is
 very
 > appealing and made sense. On the other hand, if that same company was a
 > Fortune 500 company, and the invention was at a late stage of development,
 > perhaps a provisional application would not make much sense. Your e-mail
 > mentioned that time is critical. At this point I am not sure what time
 > constraints you face, but in general a provisional application can be
 > prepared and filed much quicker than can a regular application. So, by
 > learning more about your company, the invention and your goals, both
 short-
 > and long-term, I am confident we will develop the best strategy for your
 > company.
 >
 > Communication
 >
 > You also asked about ways of communicating. I can tell you how I
 > have been communicating with existing Israeli clients. First, I view an
 > Israeli client no different than say a client we have in California. Just
 > like our Californian clients there are time-differences and distance
 issues
 > we must deal with. We communicate both with our Israeli and California
 > clients using the telephone, e-mail and fax. The only difference, really,
 is
 > that we adjust our schedule knowing that Israel's work week is
 > Sunday-Thursday, not Monday-Friday. Also, we have found that the
 > opportunities for patent work in Israel is tremendous. As a result, we
 have
 > scheduled to send 1 or 2 attorneys to Israel every quarter to meet with
 > clients. I last visited Israel in June, and another attorney from my
 office
 > will visit Israel next month.
 > We can discuss this issue more during our meeting, but we have had no
 > problems communicating with our Israeli clients. We have a lot of
 Japanese
 > clients--in comparison, communicating with Israeli clients is a breeze!
 >

> World-Wide IP Coverage

>

> We can advise you as to how to protect your invention in the U.S.

> and around the world. We have long-term relationships with foreign

> associates all over the world, and we have our own office in Tokyo, Japan.

> We cannot guarantee coverage in the U.S. or anywhere else in the world--I

> wish we could, but none can. What we can do is put you in the best

position

> to obtain the maximum possible patent coverage. Every patent in the U.S.

> and abroad requires examination by a patent examiner. For that reason, no

> one can possibly guarantee coverage. However, we have vast experience in

> dealing with the U.S. Patent Office, as well as patent offices throughout

> the world, and based on that experience we can advise you so your

invention

> is in the best possible condition for allowance.

>

> Costs

>

> Based on our preliminary examination, it appears your disclosure

> material contains several inventions (perhaps 3 or 4). Assuming we

prepare

> one application containing all inventions, we would estimate the cost to

> file a regular application in the U.S. to be approximately \$8,000 to

> \$11,000, including all government filing and other fees. A provisional

> application would be significantly less, about \$2,000-\$2,500.

>

> We look forward to meeting you and Prof. Agur on August 28.

> Finally, we would like to invite you and Prof. Agur to dinner either on

> Sunday, August 27 or Monday, August 28. Please let me know if you are

free,

> and if so, of any dietary restrictions. I know of a terrific Kosher

French

> restaurant, but it is difficult to get reservations, so let me know if you

> are available. I will be out of the office until August 25, but will be

> checking my e-mails. Regards, Bill

>

> William H. Mandir, Esq.

> Sughrue, Mion, Zinn, Macpeak & Seas, PLLC

> Tel: 202-293-7060

> Fax: 202-293-7860

>

> > -----Original Message-----

> > From: Moshe Vardi [SMTP:moshv@imbm.org]

> > Sent: Friday, August 18, 2000 1:26 AM

> > To: William H. Mandir

> > Subject: Optimata meeting

> >

> > Dear Bill,

> > Myself and Prof. Agur are in Washington on Aug. 28, 29th. We have

> > scheduled a meeting for the afternoon of the 28th in the city, and would

> > very much like to meet with you and your team prior to that. I would

also

> > consider staying in Washington any needed additional time, to enhance

our

> > patent filing procedure. I urge you to consider the opportunity to move

> > forward the patent drafting, taking full advantage of my stay in

> > Washington, and the option to delay my flight back. I would very much

like

> > if some work would be done by that time, and through a day or two of

mind

> > storming we could bypass all possible obstacles. Nevertheless, I cannot

do

> > so without your advise.

> > Please reply ASAP. Note that Prof. Agur is leaving Israel on the 22nd,



FIELD OF THE INVENTION

The present invention relates to a system and method for predicting and optimization of treatment of disease and of certain stages in drug development and trials.

5

BACKGROUND OF THE INVENTION

Drugs that are administered to combat disease are often toxic to healthy cells as well. In prescribing a treatment protocol, it is necessary to consider the effect of the protocol on both abnormal and normal cells.

Mathematical models of biological systems are well known in the art.

10 As a broad category, these models are...

More specifically, can have models of cell lines, tumor growth, etc.

Use of these models for prediction of treatment results is also known in the art.

However, predictive models generally employ an analytical approach, in which generalizations about the use of the treatment on a disease must be made.

15 This approach, while providing useful general information, cannot be used to predict results of treatment in realistic circumstances. Thus, a method which is inclusive of more complex and detailed scenarios is needed.

SUMMARY OF THE INVENTION

To be completed when claims are finalized.

BRIEF DESCRIPTION OF THE DRAWINGS

The present invention will be understood and appreciated more fully from the following detailed description taken in conjunction with the appended drawings in which:

5 Fig. 1 is a schematic illustration of the basis of the present invention;

Fig. 2 is a flow chart illustration of steps of the invention, useful in understanding Fig. 1;

Fig. 3 is a schematic illustration of a biological model, in accordance with one embodiment of the present invention;

10 Fig. 4 is a chart illustration of the biological model of Fig. 3;

Fig. 5 is a graphical illustration of the chart of Fig. 4;

Fig. 6 is a chart illustration of the biological model of Fig. 3 in a different format;

Fig. 7 is a graphical illustration of the chart of Fig. 6;

15 Figs. 8A and 8B are graphical illustrations of the output of the model of Fig. 3;

Figs. 9A and 9B are graphical illustrations of experimental data as compared to the output shown in Figs. 8A and 8B;

20 Fig. 10 is a schematic illustration of a biological model, in accordance with a further embodiment of the present invention;

Fig. 11 is a graphical illustration of results of the simulation of the model shown in Fig. 10;

Figs. 12A and 12B are graphical illustrations of the effects of two doses of G-CSF on the neutrophil line, according to the model of Fig. 10;

Fig. 13 is a schematic illustration of a biological model, in accordance with a further embodiment of the present invention;

DETAILED DESCRIPTION OF THE PRESENT INVENTION

A system and method have been developed for identifying optimal treatment protocols for selected parameters. Unlike prior art optimization schemes, the present invention uses heuristic determinations. The use of
5 heuristics enables to find near optimal solutions even for complex (hence, realistic) mathematical descriptions of the relevant biological/clinical/pharmacological scenarios; this holds both for the general case ("optimal generic treatment"), as well as at the level of an individual patient. Reference is now made to Fig. 2, which is a flow chart illustration
10 generally showing the optimization method. The Figure generally depicts the basic concept. The present invention optimizes a drug delivery protocol after consideration of possible protocols, referred to as a protocol space. Determination of optimal protocol is based on specific parameters input by a user. The user may be a physician, a drug developer, a scientist, or anyone
15 else who may need to determine a treatment protocol for a drug. The specific parameters may include several categories, such as individual patient characteristics and/or medical history, needs of a specific user (research, efficacy, treatment, etc.), and other particulars (such as maximum length of treatment, confidence level, etc.).

20 The first steps include generation of several types of models. A set of models for all the relevant biological processes, is created. In addition, a model of treatment effects on each of these processes is created. The combination of these models provides a detailed mathematical model of the overall bio-clinical scenario in a general or specific sense together with the
25 specific effects of a particular treatment. Once the comprehensive model is

constructed the characteristic parameters (either population averaged or patient specific e.g., – age, gender, weight or clinical indications) are implemented in it. In this way a “virtual” patient is generated. The next step is definition of a protocol space. To do this, possible permutations of certain parameters such as drug doses, dosing intervals, drug quantity, etc. are considered. Thus, a number (can be very large) of possible treatment protocols is generated. The amount of possibilities depends on the number and ranges of parameters considered. At this point, the fitness function is constructed by mathematically considering different possible factors which may be influenced by the treatment. These may include survival, tumor or pathogen load, cytotoxicity, side effects, pain etc. The user can put certain specific parameters in the fitness function so as to adjust this function to his/her specific goals. Based on the selected parameters, the fitness function is applied, and calculates a fitness score for each and every possibility in the protocol space. Finally, the optimization step is carried out, either by search heuristics or by **analytical methods**, in order to select the optimal treatment protocol from all the scored possibilities.

In this way, a disease specific, patient specific, situation specific, drug specific, objective specific treatment protocol may be obtained. The actual time it takes once the parameters are entered may be negligibly short or up to hours, depending on the length of the simulated treatment period and the power of the specific search heuristics and the computational tools, making this a very feasible tool.

Construction of detailed mathematical models for biological processes and treatments will be shown by way of example. A model of platelets

production and thrombocytopenia with treatment by TPO, a model of neutrophil production and neutropenia and treatment by G-CSF, and a model of cancer growth and chemotherapy are described. An example for specific optimization (by linear programming) is implemented in the neutrophil model. A general
5 heuristic optimization method is described as well.

EXAMPLE 1: Thrombocytopenia and Treatment by Thrombopoietin (TPO)

Thrombocytopenia is a common hazardous blood condition, which may appear in different clinical situations, including cancer chemotherapy. Recently, a thrombopoiesis-controlling cytokine, thrombopoietin (TPO), was
10 isolated and its human recombinant analog became available. A mathematical model has been developed to imitate dynamics of a thrombopoietic lineage in the bone marrow, of platelet counts in the periphery, and effects of TPO administration on them [on what? Platelets?].

TPO is a cytokine, glycoprotein of about 350 amino acids, that
15 resembles erythropoiesis-stimulating hormone, erythropoietin. Its synthetic analogs, recombinant human thrombopoietin (rHuTPO) and recombinant human megakaryocyte growth and development factor (rHuMGDF), are available as well and are undergoing clinical trials. These compounds have been shown to have the same biological activity as TPO has, so the term
20 TPO will be used without distinguishing between its different forms and analogs.

TPO is a primary growth factor of the thrombopoietic cell line both *in vivo* and *in vitro*. Aside from this, TPO may be potent in stimulation and co-

stimulation of other hemopoietic lineages (e.g., granulopoietic or erythropoietic).

I. MODEL OF BIOLOGICAL SYSTEM

A. Background of Thrombopoiesis

5 Like all other hemopoietic lines, the thrombopoietic line originates from poorly differentiated, multipotential cells, capable of some division and self-reconstitution. Other bone marrow cell lines, such as pluripotential hemopoietic stem cells and common myeloid progenitor cells (CFU-GEMM) have these characteristics as well.

10 Starting out as undifferentiated stem cells, the cells gradually become more and more differentiated and committed to a specific line. Once they commit to the thrombopoiesis line, they proliferate extensively within certain compartments. One such compartment is that of colony-forming units – megakaryocytes (CFU-Meg). Other examples of compartments burst-forming
15 units – megakaryocyte (BFU-Meg) and megakaryoblast compartments, which have similar properties as one another.

20 The committed thrombopoietic cells, which are megakaryocyte precursors, go through several stages of maturation when proliferation is no longer possible. However, megakaryocyte maturation is somewhat different from maturation within other hemopoietic lines. In megakaryocytes, cell nuclei undergo mitosis in parallel with cytoplasmic maturation. However, although the DNA material of these cells doubles, cell division does not happen. Such incomplete mitosis is called endomitosis. Consequently, the cell becomes

polyploid with 2N, 4N, 8N, etc., amounts of DNA. The cells with 2N to 4N chromosomes are called either megakaryoblasts or megakaryocytes.

Usually, megakaryocytes do not start to release platelets until the 16N state. Then they begin to create demarcation membranes that envelop cytoplasm fragments **generating platelets** [what does this refer to?]. The platelets are then released into the blood stream. The amount of cytoplasm, cell volume and an ability to release platelets all increase proportionally to the cell ploidy.

B. Mathematical Model

Reference is now made to Fig. 3, which is a detailed illustration of a model predicting thrombopoiesis. As shown in Fig. 3, the thrombopoietic lineage is divided into eight compartments. The first compartment, called Stem Cells (SC) and labeled 30, refers to all bone marrow hemopoietic progenitors that have an ability to differentiate into more than one line (e.g., pluripotential stem cells, CFU-GEMM, and others). Cells of SC compartment 30 proliferate, mature, and subsequently differentiate into megakaryocytes or other precursors, or they may give rise to new stem cells. Although the term "new" is not biologically accurate, it serves as an acceptable assumption for the purposes of the model.

Cell death through apoptosis may have a significant effect on cell number within proliferating compartments. However, the effect of apoptosis is combined with the effect of cell proliferation into a total amplification of cell number in a given compartment. Thus, for example, the amplification rate of cells in SC compartment 30 is normally 1.029 new cells per hour. An

assumption is made that no apoptosis occurs in non-proliferating megakaryocytic compartments, due to lack of evidence to the contrary.

Biologically, rates of proliferation and maturation, the ability to reconstitute, and other characteristics differ between particular cell types within a primitive progenitor population. However, in this model there is no distinction between them; all progenitor cells are considered to be one population with common properties.

Based on some works [which ones?] that have shown that probabilities of stem cell differentiation into one or another hemopoietic lineage are constant, it is assumed that a flow of stem cells into the megakaryocyte lineage depends only on the number of mature stem cells. The same was assumed about the stem cell self-renewal. Thus, after the cells spend a defined transit time, for example 24 hours, in SC compartment 30² a certain constant fraction of the cells (0.5181) return to their "young state", i.e. start their passage through SC compartment 30 again, as shown in line 31.² Another constant fraction (0.342, for example) of cells pass into the next compartment called Colony-Forming Units (CFU-Meg), labeled 40. It is presumed that remaining stem cells differentiate into other hematopoietic lineages.

CFU-Meg refers to all cells that are already committed to the megakaryocyte line but are still capable of proliferation. Cells of CFU-Meg compartment 40, like those of SC compartment 30, spend some time (normally 60 hours) multiplying at an amplification rate of about 1.0255 [per

what?] and maturing before losing their proliferative abilities and passing on to the next compartment 50, called megakaryoblasts (MKB).

MKB compartment 50 includes all the cells that have lost the ability to proliferate, but are not yet sufficiently mature to release platelets. For the purposes of the model, the assumption is made that megakaryocytes do not start to release platelets until they reach the 16N-ploidy phase. Hence, MKB refers to 2N, 4N and 8N cells of megakaryocyte lineage that cannot divide, at all stages of cytoplasmic maturity. After these cells spend the designated transit time (normally 132 hours) in MKB compartment 50, they move to the next compartment 60, which is an MK16 bone marrow compartment.

The cells of MK16 compartment 60 are megakaryocytes of 16N-ploidy class that release platelets until they exhaust their capacity, and then are disintegrated. Cell volume has a linear relationship with megakaryocyte ploidy. Hence, we assume that all 16N-megakaryocytes have the same volume and, thus, the same platelet-releasing capacity. Therefore all platelet-releasing 16N-megakaryocytes are in transit for the same amount of time (120 hours) until they are exhausted and disintegrated.

However, some 16N-megakaryocytes do not participate in platelet release, but rather continue with another endomitosis over a 48-hour time period, and become 32N-megakaryocytes. These constitute a new and distinct MK32 compartment 70. Thus, after 48 hours in MK16 compartment 60, a certain fraction of the cells (normally 0.26) leave MK16 compartment 60 and go on to MK32 compartment 70.

32N-megakaryocytes release platelets as well. The rate of platelet release is constant for every compartment and proportional to the ploidy state of megakaryocytes in it. Thus, every 16N-megakaryocyte releases 10.2 platelets per hour and every 32N-megakaryocyte releases 20.4 platelets per hour. However, 32N-megakaryocytes are not exhausted more quickly than 16N-megakaryocytes, since they have 2 times greater volume and platelet-releasing capacity. Consequently, all platelet-releasing megakaryocyte compartments have the same transit time.

Once again, some fraction of cells (normally 0.016) are not engaged in platelet formation, and continue to the 64N-stage. Additional endomitosis in MK32 compartment 70 takes the same amount of time (48 hours) as in MK16 compartment 60. The 64N-megakaryocytes continue the process in a new MK64 compartment 80, and 0.4 of them become 128N-cells in yet another MK128 compartment 90. Additional endomitosis in MK64 compartment 80 takes the same amount of time (48 hours) as before.

Normally, 64N- and 128N-megakaryocytes are not found in humans. However, these cells were detected in human bone marrow in some abnormal conditions. Therefore, we included these compartments in our model, but in the normal state their number is negligible. As far as we know, megakaryocytes of greater ploidy classes have not been encountered in humans.

Finally, there is a platelet compartment 100. This is not a bone marrow compartment, but rather the platelet pool in the peripheral blood [(spleen sequestration???)]. Platelets released from megakaryocytes of 16N-, 32N-,

64N-, and 128N-ploidy classes enter platelet compartment 100. Platelet elimination from the blood is presumed to occur after a defined transit time in circulation by a mechanism of death from senescent [what is this?]. To simplify the model we ignore the destruction of platelets by their use [?].
5 Transit time through platelet compartment 100 is 240 hours but can vary, as will be discussed below.

II. MODEL OF TREATMENT EFFECTS

A. Background of TPO

The major sites of TPO production are the liver and kidney. TPO is also
10 produced in the spleen and bone marrow, but the production rate in these organs is 5 times lower than in the liver and kidney. Some low TPO production has also been found in many other sites in the body. Rates of liver and kidney TPO production are constant under thrombocytopenia and thrombocytosis of varying degrees of severity. TPO production in the spleen
15 and bone marrow is inversely related to the megakaryocyte mass, but the actual contribution is negligible with regard to total TPO production.

Another mechanism of TPO concentration regulation is receptor-mediated TPO uptake, since TPO-receptors on the platelet and megakaryocyte surfaces are the main TPO-clearance mechanism. Thus,
20 TPO concentration is inversely related to the total platelet and megakaryocyte mass.

The effects of TPO on the thrombopoietic line may be divided into three types: (i) stimulation of proliferation of megakaryocyte progenitors that have

an ability to proliferate; (ii) stimulation of maturation of all megakaryocyte progenitors; (iii) induction of additional endomitosis of already mature megakaryocytes, which leads to an increase in the modal megakaryocyte ploidy.

5 ***B. Mathematical Model of TPO Effects***

TPO concentration effects on the thrombopoiesis line is now considered. As discussed above, three things depend on TPO concentration: (i) amplification rate (amp), (ii) the rate of cell maturation or, alternatively, transit time through a given compartment (transit), and (iii) the fraction of
10 megakaryocytes of given ploidy that undergo additional endomitosis and pass on to the next ploidy class.

1. TPO Concentration

Recombinant human full-length TPO and its truncated form rHuMGDF
15 are fully active biologically. Therefore, in our model we add exogenously administered recombinant protein to endogenously produced TPO in order to calculate actual TPO concentration.

As mentioned above, the rate of TPO production in the main TPO production sites, i.e. liver and kidney, is constant under thrombocytopenia or
20 thrombocytosis. The level of TPO mRNA in sites like the bone marrow and spleen, where it is produced in a 5-fold lower rate than in the liver and kidney, is not significantly different from the TPO level in peripheral blood. Therefore, the assumption is made that the bone marrow and spleen contributions to the total TPO concentration are insignificant. Endogenously produced TPO is

assumed to have a constant rate of production of 7 pg/ml/hour. However, this number can change.

The main mechanism that controls TPO concentration in the blood is
5 receptor-mediated TPO uptake. Both megakaryocyte and platelet mass
contribute to the total receptor number (normally 8.375×10^9) and,
consequently, to the rate of TPO clearance. We assume that every platelet
bears 220 TPO receptors **[based on what?]**. Each megakaryocyte at any
given moment bears an amount of receptors equal to the number of platelets
10 that can be released during the remaining life-span, times 220 receptors per
potential platelet. We assume also that every receptor molecule removes
 4.776×10^{-10} pg/ml/hour of TPO from circulation. However, this number can
change.

Another mechanism of TPO removal from the blood is non-specific
15 TPO-receptor-independent clearance. This mechanism is rather insignificant
in the normal state, when receptor-mediated TPO binding, endocytosis, and
degradation remove most of the TPO. However, when the amount of TPO
rises significantly above the ability of the receptor pool to remove it, non-
specific clearance becomes important. In our model this type of TPO
20 clearance is exponential, i.e. every hour some fraction (0.03) of a current
amount of TPO is removed from circulation.

Exogenous TPO is included in the model as a linear relation of the
initial maximum TPO blood concentration to the administered intravenous (IV)
dose (the relation coefficient is 0.0167) based on literature data.

The state when TPO completely disappears from the blood is very unlikely, the lower limit of possible TPO concentration is restricted to a certain minimum, in this case 0.01 pg/ml.

Thus, the formula that calculates TPO concentration hourly is given in
5 Equation 1 as follows:

$$C_{i+1} = \max((C_i + Endo + 0.0167 \cdot Exo - Nc \cdot C_i - Rc \cdot Rp), 0.01) \quad (1)$$

where C_i is TPO concentration at the current hour (i), C_{i+1} is TPO
10 concentration at the next hour, $Endo$ is endogenously produced TPO per hour, Exo is the total amount of TPO administered intravenously during the current hour, Nc is the coefficient of non-specific TPO clearance, Rc is the coefficient of receptor-mediated TPO clearance, i.e. amount of TPO that each receptor removes per hour, and Rp is the total TPO-receptor pool.

15 In steady-state TPO concentration is constant and equals 100 pg/ml.

2. TPO effects on amplification rate

In our model, there are only two compartments, SC compartment 30 and CFU-Meg compartment 40, whose cells are capable of dividing. These compartments differ significantly from each other, so they will be discussed
20 separately. Cells of other compartments do not proliferate, so their amplification rate equals 1 under all circumstances.

a. SC compartment 30:

Cells of SC compartment 30 are relatively insensitive to TPO as compared to committed megakaryocytic cells. In our model this is considered

as a threshold of 2500 pg/ml of TPO concentration, but this number can be changed. TPO affects stem cells only above this concentration. As long as TPO remains below the threshold, stem cells are regulated by an intrinsic TPO-independent mechanism that keeps the size of their population almost
 5 constant.

Thus, below the threshold, SC amplification rate (amp_{sc}) is determined hourly depending on the current number of cells in SC compartment 30. The dependence equation gives a sigmoidal function: amp_{sc} changes from 1 (i.e., no amplification, the cell number remains the same) up to the maximal value
 10 when the cell number approaches infinity or 0, respectively [??]. When the cell number is normal [define normal] amp_{sc} equals one fourth of its maximal possible value. Stem cell amplification rate is defined by Equation 2 as follows:

$$15 \quad amp_{sc}(quant_{sc}) = (amp_{sc\max} - 1) \cdot \frac{quantnorm_{sc}^S}{3 \cdot quant_{sc}^S + quantnorm_{sc}^S} + 1 \quad (2)$$

where $amp_{sc\max}$ is the maximal possible rate of cell amplification in SC compartment 30, $quantnorm_{sc}$ is the normal quantity of cells in SC
 20 compartment 30, $quant_{sc}$ is an actual quantity of cells there, and S is a value that determines the sensitivity of the mechanism that links the amplification rate to the number of cells. A high value for S means that amp_{sc} changes significantly due to silent changes of $quant_{sc}$, and a low value for S means that amp_{sc} remains relatively constant whatever the changes of $quant_{sc}$ may
 25 be. S generally equals 0.2, but this number can be changed.

In a range of very low cell numbers (100 times lower than normal or less), the model must define the stem cell parameters for the quickest recovery of SC compartment 30. Thus, amp_{sc} in these conditions achieves the maximal value (amp_{scmax}).

5 On the other hand, the rise of TPO concentration above the threshold should occur in severe platelet and/or megakaryocyte deficiency, or when TPO has been administered exogenously. In these situations the hemopoietic system mobilizes additional resources for recovery of platelets and platelet-releasing compartments. Hence, we assume that in an effective
10 concentration, TPO increases the rate of cell amplification in SC compartment 30. This is shown in Equation 3, as follows:

$$amp_{sc}(quant_{sc}, C_i) = \left((amp_{scmax} - 1) \cdot \frac{quantnorm_{sc}^s}{3 \cdot quant_{sc}^s + quantnorm_{sc}^s} + 1 \right) + (amp_{scmax} - 1) \cdot F^*(G^*(C_i - thres), St) \quad (3)$$

15 where the first of two operands is the amplification calculated based on a TPO-independent mechanism, and the second is the TPO-related addition to the amplification rate.

G^* is a function that transforms concentration (C) into a form that is
20 easy to use in the calculation of both amp_{sc} and $transit_{sc}$ as will be discussed further [where?]. G^* is defined by Equation 4 as follows:

$$G^*(C) = \ln(C + 1) \cdot 0.23 + 0.03949 \quad (4)$$

25 F^* in Equation 3 is a function that determines the steepness, denoted St , of the amp_{sc} -versus- C_i curve. F^* , as shown in Equation 5, is a recurrent function

that adds 1 to its first argument and applies a logarithm to this sum. Thereafter, 1 is added another time and a logarithm is applied to the sum again. This operation is repeated St times.

$$F^*(x) = \dots \log(\log(\log(\log(x+1)+1)+1)+1) \dots \quad (5)$$

Although St appears in several equations, its value is specific for every case. In Equation 3, $thres$ is the threshold above which TPO has an effect on the cells. In order to avoid an abrupt change of amp_{sc} when TPO concentration transcends the threshold, the TPO-related addition is calculated relative to the difference between an actual TPO concentration and the threshold.

b. CFU-Meg Compartment 40:

In contrast to the cells of SC compartment 30, cells of CFU-Meg compartment 40 are very sensitive to TPO and respond to the absolute TPO concentration, rather than its level above a certain threshold. Biologically, these cells have no TPO-independent proliferation mechanism, and thus cease to proliferate when deprived of TPO. However, in our model, CFU-Meg cells continue to proliferate without TPO at almost the same rate as with TPO. With normal TPO concentrations, amp_{CFU} equals one eighth of its maximal possible value ($amp_{CFU_{max}}$). The equation that describes the relation of amplification rate of CFU-Meg cells (amp_{CFU}) to TPO concentration (C_i) is:

$$amp_{CFU}(C_i) = (amp_{CFU_{max}} - 1) \cdot F(G(C_i), St) + 1 \quad (6)$$

Function **G** resembles function **G*** (Equation 4) qualitatively but differs quantitatively, having the following form:

5
$$G(C) = 2.56 \times 10^{-6} \cdot (\ln(C + 1) + 0.3949)^7 + 0.3 \quad (7)$$

Function **G** is changed from function **G*** by adding 0.3949, raising to a power of 7, multiplying by 2.56×10^{-6} , and adding 0.3. These changes provide the
10 following features:

- (a) in the region near the normal TPO concentrations the function rises with an increasing rate from about 0.3 up to about 0.8;
- (b) in the normal TPO concentration (100 pg/ml) it equals 0.5;
- (c) in high TPO concentrations, which occur in cases of exogenous
15 TPO administration, the function rises with a decreasing rate;
- (d) despite (iii), in high TPO concentrations that may arise in a logical situation (i.e. severe thrombocytopenia or TPO administration in logical doses), the rate of function growth does not drop down to zero and the function does not reach a
20 maximum, but rather the rate gradually stabilizes at a nearly constant value and the function continues to rise almost linearly.

Function **F** in Equation 6 is almost the same function as function **F*** in Equation 5. The difference is that while **F*** returns the number solely on the basis of Equation 3, **F** is required to return to 0.5 when its first argument is
25 0.5, no matter what *St* is. This is achieved by multiplying the returned number by a certain coefficient, which is specific for every value of *St*. Thus, **F** is defined by Equation 8 as follows:

$$F(x) = k \cdot (... \log(\log(\log(\log(x+1)+1)+1)+1)...) \quad (8)$$

where k is the St -specific coefficient.

5

3. TPO effects on transit time

As noted earlier, all platelet-releasing megakaryocyte compartments have the same transit time. Since neither the relationship of megakaryocyte volume (and thus, its platelet releasing capacity) to megakaryocyte ploidy, nor its rate of platelet release, are affected by TPO, the transit time through the compartments are constant, for example 120 hours. Platelets in circulation also spend constant period of time (eg. 120 hours) which is not affected by TPO concentration.

15 In contrast, SC, CFU-Meg, and MKB compartments have changeable transit times. If the transit time were continuously strictly related to the TPO concentration, then during an abrupt concentration change (in exogenous administration, for example) there could be either massive cell exit from the given compartment or absolute absence of cell exit for the period of time that equals the difference between current and previous transit time. Since this situation seems biologically unlikely, in the present model transit time changes gradually, approaching the value that it should be equal to based on TPO concentration step by step.

20 Regarding the amplification rate, transit time in SC compartment 30 differs from the other compartments.

25

a. SC compartment 30:

Cells of this compartment respond to TPO only when its concentration rises above the threshold. Below the threshold stem cell transit time is regulated by an intrinsic mechanism dependent on the current cell number only. The value that the transit time should approach is determined based on the cell number, according to the following equation [=?]:

$$\boxed{\text{[redacted]}} \quad (9)$$

where transit_{SCmin} is the minimal possible transit time through SC compartment 30 (12 hours). It is two-fold lower than the normal transit time.

Unless the value that transit time should approach does not differ from the current transit time by more than 1.0, transit time does not changes. When it does differ, the transit time begins to change every hour by 1 hour in the direction of the value. [explain??]

When TPO concentration rises above the threshold, it sets the value which stem cell transit time approaches, to the following number [=?]:

$$\boxed{\text{[redacted]}} \quad (10)$$

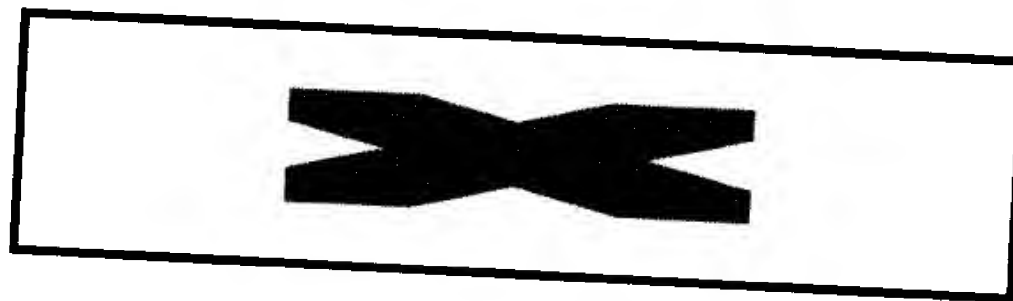
where G^* is the function given in Equation 4, C_i is the actual TPO concentration and thres is the same threshold as for stem cell amplification rate. Thus, TPO shortens stem cell transit time, which allows for the quickest recovery of committed megakaryocyte compartments when those [what?] are diminished. [?]

We assume maximal possible transit time (300 hours), above which transit time does not rise.

As in amplification rate, in a range of very low cell numbers (100 times lower than normal or less), the model must define the stem cell parameters for the quickest recovery of SC compartment 30. Thus, $transit_{sc}$ in these conditions achieves the maximal value, which is 300.

b. CFU-Meg and MKB compartments:

Transit times of these CFU-Meg and MKB compartments 40 and 50 are completely dependent on TPO concentration. The value, which the transit time approaches, is $[= ?]$:



(11)

where $transit_{(CFU-Meg/MKB) min}$ is the minimal possible transit time through CFU-Meg compartment 40 (eg. 30 hours) or MKB compartment 50 (66 hours), respectively. G is given in Equation 7, and F is the same function as in Equation (7 or 8??), but the value of St is different in each equation. Maximal possible transit time is 100 hours for CFU-Meg compartment 40 and 350 hours for MKB compartment 50.

4. TPO effects on cell flow from one compartment to another

Cell flow between compartments refers not to the rate of cell passage from one compartment to the next, and not to the number of cells that pass

during a time unit, but rather to the proportion of "mature" cells that pass to the next compartment at any given moment, designated "*flowon*". "Mature" cells are ones that are potentially ready to pass to the next compartment but do not necessarily pass.

5 As was noted earlier, it is assumed that the fraction of SC compartment
30 that commits to the megakaryocytic lineage is constant (0.342) and TPO-
independent. From the two following compartments, CFU-Meg compartment
40 and MKB compartment 50, every mature cell emerges to the next
compartment regardless of external circumstances **[is this correct? Or just**
10 **TPO circumstances?]**. Thus, TPO does not affect the *flowon* in the first
three compartments.

In contrast, the fraction of MK16-, MK32-, and MK64- megakaryocytes
that continue with additional endomitosis and flow to the next compartment
may change from almost 0 up to 1 depending on TPO concentration.
15 Because there is no compartment with ploidy greater than 128N, the
megakaryocytes of MK128 compartment 90 do not flow to any other
compartment, so there is no *flowon* value for MK128 compartment 90.

The dependence of MK16, MK32, and MK64 *flowon* parameters on TPO
concentration is expressed by the following bi-phasic function:

20

$$\boxed{\text{[Redacted Equation]}}$$

(12)

25 where *flowonnorm* is the value of *flowon* under normal TPO concentration
(100 pg/ml). This value for MK16 is 0.26, for MK32 it is 0.016, and for MK64
it is 0.4.

G° is a function that resembles the function G in Equation 7. The difference is that G° relates to the TPO concentration before a certain period of time rather than to the current TPO concentration. The reason for this is that it is assumed that a cell that enters a given megakaryocyte compartment first "decides" whether to undergo additional endomitosis and not participate in platelet release in this compartment, or whether to begin with platelet release and remain in this compartment until complete exhaustion. TPO-dependent determination of what fraction of cells will "choose" each possibility occurs at the start of the cells' path through the given compartment. However, the result of this determination can be seen when the cells that "decide" to leave the compartment actually leave it, i.e. after they complete one endomitosis. Thus, the fraction of cells that pass to the next compartment, *flowon*, is calculated based on the TPO concentration that existed before the period of one endomitosis (48 hours):



(13)

The time needed for additional endomitosis is the same in all three compartments, MK16, MK32, and MK64.

III. COMPLETE DETAILED MODEL

The complete model was built as an imitation of what happens in real bone marrow. Each compartment is subdivided into small sections that contain the cells of a specific age with a resolution of one hour. For example, the fifth age-section of MKB compartment 50 contains cells within MKB

compartment 50 that have been within that compartment for 5 hours. Every hour, all the cells in the "bone marrow" pass to the next age-section in the same compartment.

When the cell has spent all the transit time predetermined for it in a given compartment, it passes to the next compartment to the zero age-section. Thus, every hour the cells that leave one compartment fill the zero age-section of the next one. The cells that leave MK128 compartment 90 have nowhere to go and therefore disappear. The zero age-section of SC compartment 30 is filled by a certain fraction (0.5181) of the cells that leave SC compartment 30.

The cells that release platelets add a certain platelet number to the zero age-section of PL compartment 100 every hour.

Reference is now made to Fig. 4, which is an illustration of the implementation of the model. The model is implemented as a chart of 8 rows and 360 columns. The 8 rows relate to 8 cell compartments, and the columns relate to the age sections, with the assumption that transit time does not exceed 360 hours. This chart is updated hourly according to the rules described above.

Reference is now made to Fig. 5, which shows a graphical representation of the chart of Fig. 4. Within the compartments that proliferation occurs (SC and CFU-Meg), the number of proliferating cells increases from the first to the last age-section. In contrast, the cell number in the compartments that have no proliferating ability remains constant (MKB, MK128, PL), or decreases when cells that have undergone additional endomitosis leave the compartment for the next one (MK16, MK32, MK64).

Reference is now made to Fig. 6, which is an illustration of another representation of the model, based on the time courses of different compartments. The rows in the chart represent cell compartments and the columns represent time of simulation course. At every time-step of the simulation (one hour of "patient's life"), the number of cells in all age-sections is summarized for each compartment and the next column in time-course chart (Fig. 6) is filled. Thus, every cell in the chart represents the total number of cells in a given compartment at a given time point.

There is an additional row in the time-course chart that relates to the TPO concentration in the blood. TPO concentration is written down every time-step concurrently with the cell numbers.

Reference is now made to Fig. 7, which is a graphical representation of the chart of Fig. 6, and is the most useful model output [why? Describe graph and how it is used].

The implementation of the described model results in a computer simulator that describes the changes that occur in the human thrombopoietic system (platelet counts, bone marrow precursor numbers, and TPO concentration) over several years. The resolution of the simulator output is one hour.

Time units and periods that we will speak about relate to the simulated patient's life, not to the running time of the program.

IV. PARAMETER-SPECIFIC ADAPTATION OF MODEL

This model may be fit to patients with diverse blood and bone marrow parameters. People differ in their baseline platelet counts and numbers of bone marrow precursors, in the cells' transit times and amplification rates,

rates of platelet release by megakaryocytes, fractions that each megakaryocyte ploidy class donate for additional endocytosis, and in the time needed for endomitosis. Furthermore, the rate of TPO production, receptor- and non-receptor-mediated TPO clearance, the threshold of TPO effect on SC compartment 30, and the sensitivity of different cell parameters to TPO also differ from one person to the next.

To obtain an ideal fitness of the model to each patient, the patient-related parameters should be given individually for each patient. However, practically, it would be extremely difficult to predetermine many of these parameters for every patient. Therefore, certain average parameters have been calculated based on published data, and are shown in Table 1 below. These averaged parameters are used as a framework into which known individual characteristics are included. Thus, before a particular simulation is begun, relevant known information about the individual may be included, sometimes replacing certain parameters of the model.

TABLE

Feature Compartment	Baseline number (x 10 ³ /kg)	Normal amplification rate (increase per hour)	Normal transit time (hrs)	Normal cell flow* (hour ⁻¹)	Rate of platelet release (hour ⁻¹ x megakaryocyte ⁻¹)	Time needed for additional endomitosis (hrs)	
SC	478	1.029	24	0.342	----	----	
CFU-Meg	1250	1.0255	60	1	----	----	
MKB	5105	----	132	1	----	----	
MK16	4080	----	120	0.26	10.2	48	
MK32	1250	----	120	0.016	20.4	48	
MK64	15	----	120	0.4	40.8	48	
MK128	7.5	----	120	----	81.6	----	
PL	15 050 000	----	240	----	----	----	
TPO-related parameters	Rate of production	Non-receptor- mediated clearance	Receptor- Mediated clearance	Threshold for the effect on SC			
	7 pg/ml/hr	3 % /hr	4.776 x 10 ⁻¹⁰ pg/ml/receptor/hour	2500 pg/ml			
Steepness of the TPO sensitivity curve of	SC amplifica tion rate	CFU-Meg amplification rate	CFU-Meg transit time	MKB transit time	Fraction of MK16 undergoing additional	Fraction of MK32 undergoing additional	Fraction of MK64 undergoing additional

different parameters (S_i)					endomitosis	endomitosis	endomitosis
	4***	30	100	7	3	3	3

* - fraction of mature cells of a given compartment that goes to the next compartment

** - Sensitivity of the intrinsic TPO-independent mechanism that determines SC amplification rate (S) is 0.2.

*** - the logarithm base is 10, not e , like in others

5

Usually, the known patient-related data are not parameters in the form defined by our model, but rather measurements obtained in the clinic (e.g., day and value of post-chemotherapy thrombocytopenia nadir, day and value of platelet peak after TPO administration, change in megakaryocyte modal ploidy following some perturbation, etc.). In these cases, the available data is converted into a model-compatible format.

Sometimes, the only available patient-related data is the graphic representation of the patient's platelet course following some perturbation (e.g., cell-suppressive therapy or TPO administration). The data may also be a picture of the platelet course without any external disturbance (e.g., cyclic thrombocytopenia). In these cases the model parameters are changed by trial-and-error until a good compliance of the model graphic output and the patient's graphs is achieved. It should be noted, however, that even in the case of trial and error, the choices of parameter sets are not random but rather are also based on some analysis [for example?].

Specifically, the following tools are available for providing maximum flexibility:

- 1) The user can set the baseline values and all other known patient-specific thrombopoietic parameters before starting the simulation.
- 2) The user (e.g., physician) can determine how long of a time period to simulate, from 12 hours up to several years.

- 3) The user can determine the frequency of showing the course of a patient counts up to the moment. The frequency can change from as much as every 12 hours to once during the overall period of simulation.
- 5 4) The user can determine the resolution of the output graph, from the hourly representation of the patient's state down to any other resolution. **[What does this mean? Can it be resolved at units of less than an hour? If so, how?]**
- 10 5) The user can choose to view the graphical representation of the age distribution through the compartments at any moment of the simulation.
- 6) The user can imitate a cell-suppressive therapy at any moment while running the simulation by reducing one or several of the compartments by any value.
- 15 7) The user can simulate exogenous TPO administration at any moment while running the simulation by controlling dose height, number of dosings or frequency of dosings.

The simulation tool has been carefully tested with respect to the published experimental results, and has proved to be well calibrated for average human data. Parameters may be modified relatively quickly for efficient use of the system. The following model parameters are important for individualized adjustment of the model:

- baseline number of: SC, CFU-Meg, MKB, MK16, MK32, platelets.
- amplification rate of: SC, CFU-Meg.
- transit time of: MKB, MK16, MK32, MK64.

- fraction undergoing additional endomitosis in: MK16, MK32, MK64.
- rate of platelet release of: MK16, MK32, MK64, MK128.
- Time needed for additional endomitosis.
- Rate of endogenous TPO production.
- 5 • Ratio of receptor- and non-receptor-mediated TPO clearance.
- Steepness of the sensitivity curve of: CFU-Meg amplification rate; MKB transit time; MK16, MK32, and MK64 fraction undergoing additional endomitosis.

10 [Question: which of these parameters can actually be measured and input into the program? All? Are there other parameters too such as age, weight, medical history, etc.? I think we need to distinguish between types of parameters.]

Reference is now made to Figs. 8A, 8B, 9A and 9B, which show a comparison between experimentally obtained data and the simulated model.

15 Experimentally obtained *in vivo* platelet counts following TPO administration are shown in Fig. 8A [is this with chemotherapy too?], and chemotherapy without TPO is shown in Fig. 9A. Figs. 8B and 9B show simulations of the same. By using a TPO schedule designed by the described model, one can obtain platelet profiles that are similar to those obtained clinically (Fig. 8B) or

20 even more effective (Fig. 9B). In this case, these results are achieved by administering a pre-calculated TPO protocol whose total dose amounts to 25% of the original total dose. **explain the point of this better**

The complete model simulates cell and platelet counts in the steady state, as well as after perturbations to the hematopoietic system, e.g., cell-

25 suppressive therapy, recombinant thrombopoietin administration, etc. It is

possible to simulate any protocol of drug administration and any hematological state of a patient, regarding his/her platelet count and number of bone marrow megakaryocytes and their precursors. The model can be adapted to many categories of patients, or healthy platelet donors. It can also
5 be modified to fit species other than human. By providing specific parameters one can adjust the model so as to yield particular predictions about the thrombopoietic profile of an individual patient. Platelet disorders, such as cyclic thrombocytopenia, may also be simulated.

**EXAMPLE 2: Neutrophil Bone Marrow and Peripheral Blood Compartment
under the Effects of Growth-Factors and Treatment with Granulocyte
5 Colony Stimulating Factor (G-CSF)**

The neutrophil lineage originates in pluripotent stem cells that proliferate and become committed to the neutrophil lineage. These cells then undergo gradual maturation accompanied with proliferation through the three
10 morphologically distinguishable mitotic compartments: Myeloblasts, promyelocytes and myelocytes. The myelocytes then mature and lose their capacity to proliferate, and thus enter the post mitotic compartment. In the post-mitotic compartment the cells continue their gradual maturation, which is not accompanied with proliferation through the three morphologically
15 distinguishable sub-compartments: Metamyelocyte, band and segmented-neutrophils. Cells exit the various sub-compartments in the post-mitotic compartment and enter the blood as neutrophils. They then migrate from the blood to the tissues.

The Granulocyte-Colony Stimulating Factor (G-CSF) effects an
20 increase in blood neutrophil levels primarily by increasing production in the mitotic compartment and shortening the transit time of the post-mitotic compartment.

Thus, the first compartment of the mitotic pool (myeloblast) receives an inflow of cells from stem-cell precursors. Inflow for each of the other
25 compartments is from outflow of the previous one, subject to multiplication factors due to cell replication in the mitotic stages.

Models regarding granulopoiesis in normal humans and in humans with pathologies of the bone marrow were suggested previously in order to give a coherent description of the kinetics of granulocytes from experimental data (Cartwright – 1964, Mary – 1978, Rubinow – 1974). In recent years
5 Schmitz et al. developed a kinetic simulation model for the effects of G-CSF on granulopoiesis (Schmitz – 1993), and used it for the analysis of administration of G-CSF to patients suffering from cyclic neutropenia (Schmitz – 1995). However, the data Schmitz rests upon for his model has been more accurately assessed in recent years by Price et al. (1998) and Chatta et al.
10 (1996). Actual empirical data regarding compartment sizes and their transit times was not incorporated into their model despite the importance of these data (Dancey et al. 1976).

I. MODEL OF NEUTROPHIL LINEAGE AND EFFECTS OF G-CSF

A. G-CSF

The effects of G-CSF on the neutrophil lineage are relayed in the model in three stages. The first is the administered amount of cytokine given
5 at time t , which is marked: G_{adm}^t

The G_{adm} vector serves as the control variable for optimization of G-CSF administration.

The second stage represents the pharmacokinetic behavior of G-CSF in circulation. It incorporates, for instance, the half-life of G-CSF, and could in
10 the future be modified to express more of the effects of time on G-CSF activity. This level is marked G_{blood}^t .

G-CSF is eliminated from the blood in a Poissonic manner according to the following equation, as stated by Stute N, Furman WL, Schell M and Evans WE in "Pharmacokinetics of recombinant human granulocyte-macrophage
15 colony stimulating factor in children after intravenous and subcutaneous administration" Journal of Pharmaceutical Science, 84(7): 824-828, 1995:

$$G_{blood}^{t+1} = G_{blood}^t \left(1 - \frac{\ln 2}{\tilde{t}_{1/2}}\right) + G_{adm}^{t+1} \quad (14)$$

where $\tilde{t}_{1/2}$ is the half-life of G-CSF in the blood, and $G_{blood}^1 = G_{adm}^1$

Recent data by Terashi K, Oka M, Ohdo S, Furudubo T, Ideda C,
20 Fukuda M, Soda H, Higuchi S and Kohno S, in "Close association between clearance of recombinant human granulocyte colony stimulating factor (G-CSF) and G-CSF receptor on neutrophils in cancer patients", Antimicrobial

Agents and Chemotherapy, 43(1): 21-24, 1999, points to the dependence of the half-life of G-CSF on neutrophil counts. In the absence of exact kinetics of G-CSF effects on the neutrophil lineage, the half-life is considered as a constant, though this could be modified should more exact information
5 emerge.

Only exogenously produced G-CSF is considered to affect the kinetic parameters, and endogenously produced G-CSF levels and effects are set to zero. If more empirical data regarding the production of endogenous G-CSF is made available, it could be incorporated into the equation as well.

10 The third and final stage models the pharmacodynamic effects of G-CSF on the kinetic parameters. As will be elaborated subsequently, the dependence of the various kinetic parameters of the neutrophil lineage on the level of G-CSF in the blood is assumed to be through either non-decreasing concave or non-increasing convex functions. This reproduces the effects of
15 saturation that are seen in clinical studies on the effects of G-CSF, such as the study by Duhrsen U, Villeval JL, Boyd J Kannourakis G, Morstyn G and Metcalf D in "Effects of recombinant human granulocyte colony-stimulating factor on hematopoietic progenitor cells in cancer patients", Blood, 72(6): 2074-2081, 1988. That is, addition of G-CSF carries a lesser effect when its
20 level in circulation is already high.

B. Biological Model

Mitotic Compartment

Long-term effects of G-CSF administration take place in the mitotic compartment. Although the major contributor to heightened blood

neutrophil counts in the short term is the post mitotic compartment's shortening of transit time due to G-CSF administration, this high level cannot be maintained over the long term without increased production in the mitotic compartment.

5 The mitotic compartment is divided into subcompartments. The k th subcompartment contains all cells of chronological age between $k-1$ and k hours, relative to the time of entry into the mitotic compartment. The number of cells in subcompartment k at time t is marked as m_k^t .

$$k \in \{1..^{10}\tau\}$$

$$m_1^t = \ell_1^t(G_{blood}^t)$$

(15)

where τ is the transit time of the entire mitotic compartment, and is assumed to be the same and constant for all cells entering the mitotic compartment, and ℓ_1 is a vector reflecting the flow of newly committed cells into the mitotic compartment. The biological grounds for this definition is the existence of a myeloid stem cell reservoir, which is known to supply new committed cells to the mitotic compartment. However, the reservoir's actual kinetics are not very well explored empirically. We therefore fix ℓ_1 to levels such that the overall size of the mitotic compartment as well as the kinetics of the neutrophils in circulation would match those obtained empirically.

Any new biological data that emerges may help define the kinetics more accurately within the framework of this model, although results of this model indicate that the assumption of a constant rate of stem cells flowing

into the mitotic compartment in the absence of G-CSF is plausible. For every $n \in \{1.. \tau\}$, and for every t , amplification occurs at the exit from m_n^t , according to Equation 15 as follows:

$$m_{n+1}^{t+1} = m_n^t \cdot \alpha_n(G_{blood}^t) \quad (16)$$

where:

α_n is a non-decreasing concave function of G-CSF levels in the blood, which determines the factor of amplification in the hourly subcompartment n . If, for instance, no amplification occurs at subcompartment n_0 at time X ? then

$$\alpha_{n_0} = 1$$

$$\forall n, G_{blood}^t \quad 1 \leq \alpha_n(G_{blood}^t) \leq 2$$

(17) The size of the morphological sub-compartments in the mitotic compartment at time t is determined as:

(18) Where n_0 is the first hourly sub-compartment of a morphological sub-compartment and n_1 is its last hourly sub-compartment. The division into the morphological sub-compartments is used only for fine-tuning of the kinetic parameters with the use of experimental data.

The mitotic compartment was modeled with an intention to facilitate the specific cell-cycle cytotoxic effects of chemotherapy. Therefore, cohorts of one hour are modeled as undergoing a process of maturation and amplification culminating in their entry into the post-mitotic as described below. Effects of chemotherapy may be incorporated into the model by mapping the various cell-cycle phases (G1, S, G2, M) to the hourly cohorts

modeled and formulating a function of the cytotoxic effects of chemotherapy on these phases.

The experimental literature shows wide agreement regarding the steady state normal amounts of circulating neutrophils, size of the post-mitotic compartment and the three morphologically distinct sub-compartments of the mitotic compartment, and post-mitotic transit time and amplification rates in the mitotic sub-compartments (see, for example, Dancey JT, Deubelbeiss KA, Harker LA and Finch CA, in "Neutrophil kinetics" in *Man. Journal of Clinical Investigation*, 58(3): 705-715, 1976; Price TH, Chatta GS and Dale DC, "Effect of recombinant granulocyte colony-stimulating factor on neutrophil kinetics in normal young and elderly humans", *Blood* 88(1): 335-340, 1996; and Dresch Mary in "Growth fraction of myelocytes in normal human granulopoiesis", *Cell Tissue Kinetics* 19: 11-22, 1986). To determine other relevant kinetic parameters, which were either not available in the literature or were given a wide range by experimentalists, steady state kinetics was assumed and an iterative process was employed. These parameters include the inflow of stem cells to the myeloblast compartment and the transit times of the mitotic sub-compartments.

The half life of blood neutrophils and the steady state number of neutrophils were taken as 7.6h and 0.4×10^9 cells/kg body weight, respectively (Dancey et al., 1976). Similarly, the same calculation may be made for each patient that is to be modeled. This would allow the dynamics of every patient to be described by the simulation. The average size of the post-mitotic compartment (5.84×10^9 cells/kg body weight – Dancey, 1976) and the transit time of the compartment (160h – Dancey, 1976; Mary, 1986; Price, 1996) are

compatible with the size and half-life of the circulating neutrophil compartment reported by Dancey, thus supporting the steady state analysis.

In order to determine the amount of cells in the hourly sub-compartments in the mitotic compartment, all compartments in the lineage were modeled using a steady state assumption. The number of cells exiting the circulating neutrophil pool equals the number of cells exiting the post mitotic compartment, which in turn equals the hourly production of cells in the mitotic compartment. Thus, the number of cells in the last hourly cohort of the mitotic compartment can be determined from the neutrophil decay rate, which is available in the literature. However, this calculation is based on assumptions that there is no apoptosis in the post-mitotic compartment. Direct experimental data by Thiele J, Zirbes TK, Lorenzen J, Kvasnicka HM, Scholz S, Erdmann A, Flucke U, Diehl V and Fischer R, in "Hematopoietic turnover index in reactive and neoplastic bone marrow lesions: Quantification by apoptosis and PCNA labeling," *Annals of Hematology* 75(1-2): 33-39, 1997, suggests that apoptosis is not a significant phenomenon in normal human bone marrow. The size calculated for the mitotic compartment is close to that experimentally obtained by Dancey and Price, thus supporting the notion that apoptosis is not a significant kinetic factor in the lineage. Values for the production of cells in the mitotic compartment can later be modified in light of new evidence.

Regarding the transit time of the mitotic compartment there is little agreement in the literature, with a range of 90-160 hours given by most experimentalists (see Dresch Mary in "Growth fraction of myelocytes in normal hman granulopoiesis," *Cell Tissue Kinetics* 19: 11-22, 1986). In order

to determine the transit times of the mitotic morphological sub-compartments, as in Equation 18, the following constraints were considered:

1. The sizes of the theoretically obtained morphological sub-compartments must fit those reported experimentally in normal human hematopoiesis (Dancey, 1976) and under the effects of G-CSF (Price, 1996);
2. At least 24 hours, the typical cell cycle, must separate amplification points;
3. The size of the last hourly sub-compartment must equal the hourly production of the mitotic compartment (calculated with the aforementioned iterative process assuming steady state kinetics);
4. Amplification inside the compartment is set at the levels determined by Mary 1984; and
5. The total transit time of the mitotic compartment must be within the 90-160 hour range.

By using the values shown in Table x, an excellent fit was obtained within the above-mentioned constraints.

It should be noted that when other alternatives with shorter transit times were attempted, results could not be obtained that agreed with the literature regarding the size of the mitotic pool or its production. Furthermore, a fit between our simulation model's results regarding PMN counts in peripheral blood with empirical data could not be achieved without speculating extensively on the nature of G-CSF effects

on non-committed stem cells (data not provided). It should be noted, that little empirical quantitative data is available regarding stem cells.

The effects of G-CSF on this compartment are modeled as an increase in the rate of cells entering the myeloblasts from the uncommitted stem cell pool, increases in the rates of mitosis, and introduction of new points of amplification as shown in Equation 15, 16. Since little data is available regarding the increases in amplification due to G-CSF, an initial assumption was made that amplification reaches full potential at points that under normal conditions undergo an amplification of below a factor of 2. Additionally, it was assumed that the transit time in all mitotic sub-compartments and the typical cell cycle duration are not affected by G-CSF, based on lack of evidence to the contrary.

Reference is now made to Figs. X and y, which show a comparison of neutrophil production according to the described model and experimental data in the literature. Increased neutrophil production is in accordance with the neutrophil counts reported by Price et al. In addition, these increases are in accordance with Price's data about neutrophil bone marrow pool sizes.

Reproduction of the effect of G-CSF on neutrophil counts and the mitotic compartment sizes beyond day 5 of administration was accomplished by assuming an increase (15% with the highest dose of G-CSF) in the rate of cells entering the myeloblast compartment. Alternatively, G-CSF may change the behavior of the myeloblast compartment such that some of the cells there undergo self-renewal instead of moving on to the promyelocyte compartment. However, no empirical data to support this is available. The model can be modified in light of new experimental data in the future.

Post-mitotic compartment

The post mitotic compartment is relatively insensitive to cytotoxic chemotherapy. Therefore, it is biologically acceptable and computationally
5 sensible to model this compartment as a single pool of cells, such that the last hourly cohort of the mitotic compartment enters the compartment, and a proportion of the cells within the compartment enter the neutrophil pool every hour.

The post mitotic compartment at time t is a single quantity of cells p^t ,
10 such that:

$$p^{t+1} = l_3(G_{blood}^t) \cdot p^t + m_\tau^t \quad (19)$$

where l_3 is a convex, non-increasing function of G-CSF levels in the blood, which takes values in the range of [0-1]. This definition entails $p^t > 0$.

15 G-CSF affects the post-mitotic compartment by shortening its transit time (i. e. decreasing l_3). Price notes that the number of cells in the post mitotic compartment is not significantly changed following administration of G-CSF. This determination is based on counts made on day 5 after G-CSF administration. Thus, it can be safely assumed that any increased production
20 of the mitotic compartment flowing into the post mitotic compartment is translated over the long-term to an increase in the flow of cells from the post mitotic compartment to the neutrophil pool. This increased flow is compensated by increased production in the mitotic compartment only at a

later stage. Therefore, an upper limit to the number of cells in the post mitotic compartment was set, which is at the values given as steady state counts (Π).

In brief, the effects of G-CSF on the neutrophil lineage are modeled during the first few days primarily as a decrease in the counts of the post-mitotic compartment, which is then compensated by an increased production in the mitotic pool. This compensation sustains the increase in neutrophil counts in peripheral blood.

Reference is now made to Fig. 11, which is a graphical illustration of a simulation of the model. Though no empirical data is available on this point, simulations of the model predict that the number of cells in the post-mitotic compartment decreases substantially during the first two days of G-CSF administration, and then replenishes, so that on the sixth day the counts return almost to their normal levels. This replenishment lags behind that of Price et al report by a few hours. We can thus formulate a **testable hypothesis**, i.e., whether using the same G-CSF protocol Price et al used, there is indeed a nadir on day 3 of the treatment.

Compartment	Day 0 (no G-CSF) ($\times 10^9$ cells/ kg. Body weight)	Day 15 of G-CSF treatment ($\times 10^9$ cells/ kg. body weight)	Relative increase in compartment size due to G-CSF
Myeloblasts	0.140	0.153	1.09
Promyelocytes	0.582	0.898	1.54
Myelocytes	1.373	3.564	2.60
Mitotic Total =	2.10	4.615	2.20
Circulating neutrophils	0.4	2.35	5.88

Table 1. Simulated kinetics after 15 days of subcutaneous administration of 300 μ g G-CSF/kg weight. Day 0 values are the mean values Dancey et al (1976) use.

We shall mark as o^t the outflow from the post mitotic compartment:

$$o^t = m^t + p^t - p^{t+1}$$

(20)

The number of neutrophils in the circulating blood compartment at time t is marked n^t and is modeled as a single quantity of cells, such that:

$$n^{t+1} = o^t + n^t \left(1 - \frac{\ln 2}{t_{1/2}} \right) \quad (21)$$

where $t_{1/2}$ is the half-life of neutrophils in the blood, as defined in the biological literature, and is assumed to be constant regardless of G-CSF levels (Lord 1989), though this could be easily modified. The kinetics of neutrophils in the tissues are not modeled in this work.

Neutrophils and G-CSF in the Circulating Blood

The elimination of neutrophils from peripheral blood follows a Poisson distribution, and can therefore be described as an exponential function (Cartwright, 1964). Therefore the rate of cells leaving this compartment is based on half-life determinations available in the literature. Since no direct cytotoxic effects of chemotherapy have been described for this compartment it is also modeled as a single pool of cells.

At the normal healthy level we have the following relationship:

$$G_{blood}^t = 0, p^t = \Pi, m_{\tau}^t$$

$$\frac{\Pi}{T} = m_{\tau}^t = o^t = \frac{n^t}{t_{1/2}} \times \ln 2$$

which reflects the stability of the steady state.

The kinetics of G-CSF is also modeled as an exponential distribution with a half-life of 3.5 hours (Stute, 1992) (Eq. 14).

The effects of G-CSF on the kinetics of the neutrophil lineage appear not to be a linear function of G-CSF administration levels. Since data provided in the literature (Chatta 1994) only refers to two doses (30 and 300 μ gram/kg body weight) we can only speculate on the effects of other levels of G-CSF. After trial and error analysis, it was found that assuming that the effects of the 300- μ gram dose are the maximal, at the 30- μ gram its effects are about 30% of the maximum.

Reference is now made to Figs. 12A and 12B, which are graphical illustrations of the effects of G-CSF at the two doses. The effects as a function of G-CSF level are connected piece-wise linearly. This way, the neutrophil levels observed clinically under both the 300 and the 30- μ gram protocols are obtained.

II. LINEAR IMPLEMENTATION OF THE MODEL

This model will later be incorporated into an optimization scheme that will have as its objective function both the aims of minimizing G-CSF administration and returning the neutrophil lineage to its normal levels.

Although the above-outlined model may be implemented in any number of optimization methods, linear programming was chosen because of its inherent advantages compared with other techniques, i.e. its ability to provide an optimal solution using partially analytical methods, and therefore

being more computationally tractable (Gill 1991). On the other hand, implementation of this model in linear programming carries with it the disadvantage that certain computations must be approximated linearly since they cannot be performed directly using linear methods. Thus, we shall
 5 compare the 'closeness' of the solution obtained through linear programming will be compared with that obtained through another, non-linear method of optimization.

The significant parts of the model that must be modified due to the linear programming implementation are the sections in which multiplication of

10 $\{(x_{\min}, y_{\min}, x_{\min} \cdot y_{\min}), (x_{\min}, y_{\max}, x_{\min} \cdot y_{\max}), (x_{\max}, y_{\min}, x_{\max} \cdot y_{\min}), (x_{\max}, y_{\max}, x_{\max} \cdot y_{\max})\}$ two variables is defined, since this operator is not itself linear. Therefore, multiplication is defined as an approximated value constrained within piecewise linear constraints that most closely bound the product within a four-faced polyhedron in 3-dimensional space whose vertices are

15 Where $x_{\min}, x_{\max}, y_{\min}, y_{\max}$ are the constant biologically defined minima and maxima of x and y .

$$M(x, y) \begin{cases} \geq y_{\min} x + x_{\min} y - x_{\min} y_{\min} \\ \geq y_{\max} x + x_{\max} y - x_{\max} y_{\max} \\ \leq y_{\min} x + x_{\max} y - x_{\max} y_{\min} \\ \leq y_{\max} x + x_{\min} y - x_{\min} y_{\max} \end{cases}$$

(22)

Multiplication may also be approximated with variations on the linear least squares method, by finding one plane that's closest to the four vertices
 20 defined.

The other functions that need to be defined linearly are those concerning the pharmacodynamics of G-CSF. Due to the nature of these functions (either non-increasing convex or non-decreasing concave), these effects are implemented as piece-wise linear functions whose breakpoints are the doses for which actual experimental data is available (Chatta 1994). Note that the effects of G-CSF on each of the kinetic parameters have not been determined in a detailed manner by experimentalists. Rather its effects over a few dose levels on the neutrophil blood counts and the size of the morphologically different mitotic compartments and the post mitotic compartment have been determined. From these data, the effects of G-CSF on the actual kinetic parameters (probability of mitosis, transit time and inflow of cells into the myeloblast compartment from stem cell progenitors) has been reconstructed at the dose levels available in the literature. These points are then connected linearly to obtain piecewise linear functions relating G-CSF levels to their effect on those parameters. Further experimental data in the future could be used to produce more accurate functions.

At the amplification points within the mitotic compartment, the linearly approximated multiplication operator (Eq 22) is used instead of the product defined in Eq. 16.

At points where no amplification occurs the quantity from one compartment is simply transferred to the next according to the following Equation:

$$m_{n+1}^{t+1} = m_n^t$$

$$m_n^0$$

(23)

Values are set according to the steady state values of the mitotic compartment, or are depleted according to the kill function of the chemotherapy.

5 The flow out of the post mitotic compartment (Eq. 20) is similarly defined as a linear approximation of a product.

3. Formulation of the Model as an Optimization Problem for Linear Programming

The simulation spans a finite number of discrete time steps denoted by T .

10 We define as the control variable the vector that represents G-CSF administration at every given hour t , $G_{adm}^t \in \{1..T\}$

The objective function is defined as maximization of the following expression:

$$\sum_{t=1}^T (\beta^t \cdot p^t - G_{adm}^t) \quad (\text{Eq. 24})$$

15 where p^t is the number of cells in the post mitotic compartment at time t , and β^t is a scalar weighting coefficient. The logic for formulating the objective function this way is that the ability to maintain the post mitotic compartment's steady state size for a prolonged period of time is sufficient for rehabilitation of the neutrophil lineage as a whole. Also, our goal is to minimize the total administered quantity of G-CSF. β^t is introduced to allow us to factor in both these goals in one objective. Also, this would allow a different weight to be given for certain times, e.g. were it determined (by clinicians) that the later states of the post-mitotic compartment should be weighted more than the first

20

ones. Obviously this is only one of the possible formulations of the objective function as defined in the previous section.

The pharmacokinetics and pharmacodynamics of G-CSF that were defined generally in the mathematical model are defined piecewise linearly. 5 Some of the considerations that we put into formulating these functions were based directly on experimental evidence (elaborated in the main body of text). We note however, that actual experimental data regarding the direct effects of G-CSF on the kinetic parameters in which this model is interested is rather scant. Therefore, some formulations were conducted through partly analytic 10 and partly trial-and-error methods.

The formulation of the model in piecewise linear terms will allow use of this model as a clinical tool in three ways. First, the model will determine the effectiveness of various protocols suggested by clinicians prior to their actual 15 use on human patients. Second, the model allows computation of the optimal protocol in a given situation of neutrophil counts, so that the neutropenic period following chemotherapy is either shortened or completely avoided at a minimal cost and exposure to G-CSF. Third, the model serves as a constituent in a broader framework of clinical tools that will compute the most 20 optimal treatment plan for chemotherapy and growth factors. These uses should help clinicians administer more rational treatment to their patients minimizing both suffering and medical costs.

Amplification at the exit	Mean transit time (hours)	Size (10^6 cells/kg weight)	Compartment
2 ⁺	24 ⁻	0.139 [*]	Myeloblasts
2 ⁺	48 ⁻	0.558 [*]	Promyelocytes
1.5 ⁺	48 ⁻	1.4 [*]	Myelocytes
1	160 [*]	5.84 [*]	Post mitotic
0	10.96 [*]	0.4 [*]	Neutrophils

Table 1. Kinetics under steady state conditions in healthy humans.

^{*}Dancey, 1976.

^{*}Dresch, 1986.

^{*}Calculated based on the steady state assumption as elaborated in the main text.

EXAMPLE 3: Cancer and Treatment with Cytotoxic Drug Delivery

Introduction

Cancer is the second leading cause of mortality in the US, resulting in approximately 550,000 deaths a year. There has been a significant overall rise
5 in cancer cases in recent years, attributable to the aging of the population. Another contributing factor to the rise in the verifiable number of cases is the wider use of screening tests, such as mammography and elevated levels of prostate specific antigen (PSA) in the blood.

Neither better detection nor the natural phenomenon of aging,
10 however, can entirely explain the increase in new cases of tumors. Meanwhile, other cancers, like brain tumors and non-Hodgkin's lymphoma, are becoming more common. Their increase could reflect changes in exposures to as yet unidentified carcinogens. Current trends suggest that cancer may overtake heart disease as the nation's no. 1 killer in the foreseeable future. As gene
15 therapy still faces significant hurdles before it becomes an established therapeutic strategy, present control of cancer depends entirely on chemotherapeutic methods.

Chemotherapy is treatment with drugs to destroy cancer cells. There are more than 50 drugs that are now used to delay or stop the growth of
20 cancer. More than a dozen cancers that formerly were fatal are now treatable, prolonging patients' lives with chemotherapy.

Treatment is performed using agents that are widely non-cancer-specific, killing cells that have a high proliferation rate. Therefore, in addition to the malignant cells, most chemotherapeutic agents also cause severe side-
25 effects because of the damage inflicted on normal body cells. Many patients

develop severe nausea and vomiting, become very tired, and lose their hair temporarily. Special drugs are given to alleviate some of these symptoms, particularly the nausea and vomiting. Chemotherapeutic drugs are usually given in combination with one another or in a particular sequence for a relatively
5 short time.

Chemotherapy is a problem involving many interactive nonlinear processes which operate on different organizational levels of the biological system. It usually involves genomic dynamics, namely, point mutations, gene amplification or other changes on the genomic level, which may result in
10 increasing virulence of the neoplasia, or in the emergence of drug resistance. Chemotherapy may affect many events on the cellular level, such as cell-cycle arrest at different checkpoints, cell transition in and out of the proliferation cycle, etc. Chemotherapy may also interfere with the function of entire organs, most notably, with bone marrow blood production. In recent years molecular biology
15 and genetics has made an important step forward in documenting many of these processes. Yet, for assessing the contribution of specific molecular elements to the great variety of disease profiles, experimental biology must be provided with tools that allow a formal and systematic analysis of the intricate interaction between the genomic, cellular and cell population processes in the
20 host and in the disease agent. This system is so complex that there is no intuitive way to know how small changes in the drug protocol will affect prognosis. But in spite of this intricacy, attempts to improve chemotherapy have been carried out by "trial and error" alone, with no formal theory underlying the application of specific drug schedules. Such an approach "is apt to result in no

improvement, only discouragement and little useful information for future planning" (Skipper, 1986).

The treatment of cancer by cytotoxic drug (or drug combination) delivery is addressed. In this model, two generic types of cells are considered: host cells and target cells. Target cells are, in fact, the tumor. Both types of cells may be damaged while exposed to chemotherapy. The aim is to obtain the most suitable treatment protocol according to specified conditions and limitations. It is assumed that the cell dynamics are deterministic and known, and that both types of cells are sensitive to chemotherapeutic agents in certain known period of the cell-cycle phases. If a cell is exposed to chemotherapy during part of its critical phase, there is a chance that it will be eliminated, blocked or affected in any other known way. The description of the dynamics of the delivered drugs is assumed to be known as well.

In order to achieve the goal optimization process is applied to the model. The optimization module uses the model predictions in order to search for the suitable solution to posted optimization problem. Precise defining of optimization objectives as well as the relevant parameters adjustment is done according to the settings defined by user/operator for every special case. The method can be applied in general cases as well as in specific ones.

2. Model of Biological System

The basic layer of the model incorporates a description of age distribution of cycling cells and number of resting (quiescent) cells. The term

"age of the cell" here refers to chronological age starting from the conventional beginning point of mitotic cycle.

Reference is now made to Fig. 13, which is a schematic illustration of the tumor cell cycle layer. The whole cycle is divided into 4 compartments, or stages (G_1 , S , G_2 and M). Each compartment is divided into equal subcompartments, where i^{th} subcompartment in each stage represents cells of age i in the particular stage (i.e. they have spent i time-steps in this stage). The quiescent stage is denoted G_0 . The cell cycle follows a direction as shown by arrows (#). Thus, cells enter each stage starting with the first subcompartment, denoted G_1 .

The model can be described mathematically as follows: Let T_k denote the maximum duration of k^{th} stage in the cycle. Let $\bullet t$ denote the time resolution of the model in discrete time steps. $X_k^i(t)$ is a function, which represents the number of cells in stage k in the i^{th} sub-compartment, at time t to $t+\bullet t$. Both time and age are measured in the same unit, in this case, hours. Let $Q(t)$ represent the number of resting cells at time t to $t+\bullet t$. $\text{Trans}(k,i,t)$ represents the probability that a cell of age i in the stage k will move to the next $(k+1)$ compartment. Cells entering the new stage always start from the first subcompartment, i.e. from $i=1$. This probability may change with time, representing the influence of conditions on cycle length distribution.

By definition, the cell cannot remain more than T_k timesteps in the k^{th} compartment, as described in the following equation.

$$\forall k : \text{Trans} (k, T_k) = 1$$

The restriction point (R-point) represents a cell's commitment to complete the mitotic cycle. Let T_R denote the age at which the cell passes

through the restriction point in G1. Only cells in G₁ with $I < T_R$ can the cycle (in the absence of a drug).

The total number of proliferating cells $P(t)$ can be calculated as follows:

$$P(t) = \sum_{k=G_1, S, G_2, M} \left(\sum_{i=1}^{T_k} x_k^i(t) \right)$$

In every time interval, quiescent cells may return to the proliferation pool. Alternatively, proliferating cells may change their state to become quiescent if and only if they are in the G1 stage and at age i , where $T_R \cdot i > 0$. To describe this process we introduce the function $G_{1 \rightarrow 0}(i, t)$ which describes the number of G1 cells in age i which become quiescent during time interval $[t, t + \Delta t]$. This function may receive negative values, accounting for cells that return from resting to proliferation.

As we assume that the exit to quiescence can occur only prior to the R-point (even in cancer cells), and that a resting cell that returns to proliferation enters the cycle at T_0 , it can be stated:

$$\forall i > T_R, \forall t : G_{1 \rightarrow 0}(i, t) = 0$$

It must be noted that this function is not dependent on i and t solely. Its value is determined according to current cell distribution and all the general parameters that characterize the described cells group. The same should be said about the values of $Trans$ vector that can change during the history of given population.

The model traces the development of described group of cancer cells using given parameters, by calculating the number of cells in each and every subcompartment according to the following stepwise equations:

$$x_k^i(t) = \begin{cases} x_k^{i-1}(t-1) \cdot [1 - Trans(S, i-1, t-1)], & 1 \leq i \leq T_k \\ \sum_{j=1}^{T_{k-1}} x_{k-1}^j(t-1) \cdot Trans(G1, j, t-1) \cdot [1 - G_{k-1}(i-1, t-1)], & i = 1 \end{cases}$$

10

15 for $k=G_2, M$, $k-1$ returns the previous stage (e.g. $G_2-1=S$).

These equations make it possible to calculate the number of cells in each subcompartment at every time interval $[t, t+1]$ starting from initial distribution (e.g. at time $t=0$). Since in this model cell ages are measured in absolute time units, these measurements refer to the chronological age of the cell, and not the biological age, whose units are relative to a maturation rate that differs from cell to cell. Consequently, in this model no cell can remain in the same age subcompartment after every time step. On the other hand, a fraction of the cells that leaves any subcompartment may be transferred to the first subcompartment of the next stage, according to probability vector

$Trans(k,i,t)$. This vector provides the ability to account for variability of cycle lengths while retaining a deterministic approach.

The behavior of the cell population in this model is completely controlled by two components: *Trans* vector, and $G1 \rightarrow G0$ function. These two functions determine uniquely the outcome of every single time step, and, consequently the result over long periods. Thus, they are referred to as "control functions". The values of these functions may be dependent not only on time and age of cells, but also on the current population state (or, generally, on the whole history of the population) as well as on the environment associated with a given cell group. However, those parameters are similar for all the cells in the group, implying that the model presented here is suitable for describing highly homogenous group of cells. Therefore, the basic layer of the model should give a realistic description for a uniform group of cancer cells for which environmental conditions and relevant biological properties are defined, in a way that will allow the construction of the control functions for the group.

2.2. The General Tumor Model

In the general approach the whole model is viewed as constructed from similar components, each of them derived from the basic structure described in the previous paragraph. Each component represents cells that are subjected to the same environmental conditions and, therefore behaves similarly (to be denoted *homogenous group*). The whole tumor is modeled as a union of many varying homogenous groups of cells, where the

development of each group can be accurately predicted (when local conditions are known).

This general model simulates progress of the tumor in discrete steps of time. At each step the number of cells in each subcompartment of each group is calculated according to the previous state, parameters of tumor, drug concentration, etc. The parameters of the tumor must include all the information that is relevant to prognosis. Some of these parameters are defined locally, e.g., those relating to the tumor's geometry. For this reason the representation of the spatial structure will be included.

The cells will be able to pass between the groups during the development of the tumor. This allows the representation of the changes in the local conditions during the tumor evolution (e.g. forming of necrotic core, improvement in "living conditions" in vascularized regions, etc.). In addition, all the parameters of the tumor may change in accordance with the dynamics of the cancer.

The calculation of the tumor development over time will be done by stepwise execution of the described simulation and can be used to predict the outcome of the treatment or in fitness function for search algorithms.

20

2.3. From General to Individual Tumor Model

When the general theoretical description of the model is accomplished, the model is fitted to represent the actual tumors. We render it patient-specific by adjusting all the parameters that determine the behavior of the modeled

25

tumor to those of the real cancer in the patient's body. In order to accomplish this task we will establish the connections between mathematical parameters (most of them will have direct biological implication) and every kind of data that is practically obtainable in the clinic. These connections may be defined
5 through research on statistic correlation between different parameters (including genotype-phenotype correlation), or using advanced biochemical research (which may establish quantitative relations).

Thus defined, the model will be able to give realistic predictions for treatment outcomes either for specific patient or for a broad range profiles of
10 patients and diseases. This tool can serve to perform the prognosis of either an untreated cancer patient, or as a basis for treatment modeling as is described below.

15 **3. Introducing Pharmacology**

In order to simulate cancer treatment we add to the above model the pharmacologic component. We model pharmacokinetics as well as pharmacodynamics for specific anticancer drugs. We begin by representing
20 cell-cycle specific drugs, however the model implies no restriction on the type of drugs to be employed.

We model the distribution of the drug in and around the tumor as well as in the blood (the drug kinetics). For this purpose, we use the suitable model, defining it precisely for every certain type of the drug. The
25 concentrations of drug in the body are calculated at every time step in

accordance with the drug administration specified by the protocol, and different processes that define drug kinetics in the body.

The dynamics of the drug are represented through the direct influence of the drug on tumor cells. The effects on the proliferating cells are mostly blocking the cycle in different stages (which can be modeled as cell arrest) and cell death (immediate or after being in the block). Cell-cycle specific drugs are believed to have no direct influence on quiescent cells, but can affect them indirectly by killing proliferative cells and therefore changing local conditions. Where additional types of drugs added to the model, their effect on any kind of cells may be too modeled as killing certain fraction of cells (which is dose-dependent) or changing the behavior of the cells.

Additional phenomena that may prove significant in drug kinetics and dynamics (e.g. rate of absorption by the cells, development of tumor resistance to specific drug, etc.) can be introduced into the model to make it as realistic as needed.

The description of the drug in the model is done in terms of quantitative functions, which enable to calculate the drug amounts at certain locations and the tumor response to it at every time step. In the general case, these functions include parameters that depend on the specific data (drug type, body parameters, characteristic of the tumor, etc.) and can be determined in given situation (patient/case). The relation between clinical data and these parameters can be established in the ways similar to those described for the cancer model.

The combination of cancer model with the drug model described above makes it possible to predict the outcome of the treatment, given the relevant

parameters for the drug, the cancer and the patient. Again, the prognosis may be made for specified cases as well as for broad profiles of patients or disease. This simulation also serves to build the fitness function used for the optimaization objectives.

5

4. Combining with minimizing host toxicity.

Although an accurate predictive tool, the model that represents
10 chemotherapy of tumor alone cannot be used in optimization, for it posts no
constraint on the choosing of the treatment. Actually, this model implies using
as much drug as possible until the final elimination of the tumor; while in the
live system the toxicity of the drug is the most important constraint limiting the
treatment. In most cases of anticancer chemotherapy the dose-limiting
15 toxicity is bone marrow suppression, the two most sensitive bone marrow
lineages being granulopoiesis and thrombopoiesis. Accordingly, those two
were chosen as an example and are modeled separately and in a similar way
to predict the negative effect of the chemotherapy on them. These models
reconstruct the damage caused by the chemotherapy to the bone marrow
20 cells and the recovery of these lineages (treated by specific growth factors).

Thus, the whole system is capable of predicting the result of
chemotherapy treatment for the tumor as well as for bone marrow cells,
allowing the use of the protocols that combine anticancer drugs and growth
factors for healthy cells.

Chemotherapy toxicity to any other normal host cell population can be similarly taken into account, if it is defined as relevant for dose and schedule optimization.

5

VI. INDIVIDUALIZATION OF THE MODELS

Due to a great degree of heterogeneity between malignant tumors (even among similar tissue types) and between patients, it would be advantageous to adjust the treatment protocol to the individual case. This individualization
10 procedure includes three aspects:

- 1) individual parameters of tumor dynamics
- 2) individual parameters of patient-specific drug pharmacokinetics
- 3) individual parameters of the dynamics of dose-limiting normal host tissues.

15 Relevant data concerning individual cases can be obtained by research on statistic correlation between different parameters (including genotype-phenotype correlation), or using advanced biochemical research (which may establish quantitative relations). In the general model, important dynamic parameters are estimated from experimental studies conducted in certain
20 patient populations. Any of these parameters, when available on the per patient basis, can be individualized, while those that are unavailable can be left as a population-based figure. This approach allows continuous increase in the degree of individualization of the treatment protocols with progress in the technology of parameter evaluation (e.g., oncochips).

All different parameters may then be adjusted, which will result in an adjusted array of models to be simulated. Parameters may include many different factors, which are adjustable according to the needs of a pharmaceutical company for general use of the treatment, or may even be
5 individualized for use by a specific clinician for a particular individual. Examples of parameters may include, but are not limited to age, weight, gender, previous reaction to treatment, desired percentage of healthy body cells, desired length of treatment protocol, pathologic or cytologic specifics, molecular markers, genetic markers etc.

10 In order for the system to be user-friendly, all possible parameters are termed in ways that are easy for the user to understand.

Once all the parameters are set, an array of solutions is produced based on the input parameters. A number of possible protocols can be set (is thus generated by the computer). a fitness function is applied, which results in
15 scores for each of the proposed solutions.

GENERATION OF PROTOCOL SPACE

Refer back to Fig. 2. This model makes it possible to check any given
20 treatment protocol and to choose a very good one according to user's criteria. The user may be a physician, a drug developer, a scientist, or anyone else who may need to determine a treatment protocol for a drug. The specific parameters may include several categories, such as individual patient characteristics and/or medical history, needs of a specific user (research,

efficacy, treatment, etc.), and other particulars (such as maximum length of treatment, confidence level, etc.).

. That is, an array of possible treatment protocols is created from which
5 the optimal treatment protocol can then be chosen. It should be noted that the method does not imply the fitness estimation for all possible protocols. The use of operation research allows a much more sophisticated, yet resource saving procedure.

An example of this procedure will be described as it relates to cancer
10 treatment by chemotherapy, as described in the third embodiment of the invention above. However, it should be noted that a similar procedure may be performed in any of the embodiments.

The procedure implements cell growth and cell death procedures, as defined in the detailed model above. There are certain pre-defined
15 parameters, including the lengths of the host and target life-cycles, the lengths of their critical phases, and a resolution factor, that determines the length of a single time unit. The user is asked to define an action (treatment or non-treatment). Simulation of cell growth and death is then performed for the single time unit. This procedure is repeated until the end of the total
20 simulation. Alternatively, the choice of treatment or non-treatment is made by the processor, with many possible permutations considered. In that case, the protocol space would be very large, and the resolution would depend on the (selected) length of the time unit (and computer capacity)

There are two procedures: one for growth simulation during treatment and one without. The array in which the numbers of cells are kept is updated once per time unit, whether with or without treatment present at that time.

5

VII. Defining the Fitness Function

The fitness function is an important tool in Operation Research. In this case of protocol optimization, it allows the comparison between a number of different protocols each one of them scoring differently with respect to various objectives that can be set by the developers or by the users and identifying the protocol for which the highest weighted score is predicted. The fitness function calculates for any given protocol its relative efficacy ("score" or "fitness"), thus enabling a definite decision of the best protocol from a given set of protocols.

15 In different cases, different objectives can be formulated. There are several settings in which such a model can be used, including but not limited to:

One) clinical practice- where objectives can change depending on type of disease, condition of the patient, purpose of treatment, etc.

20 Two) pharmaceutical company- where objectives can be aimed at finding the therapeutic window and an optimal schedule.

Three) scientific setting- research oriented objectives can be aimed at.

In each case, a particular fitness function can be formulated, reflecting all given requirements. Thus, in any particular case one can compare

between different protocols and obtain the most suitable to his/her special purposes and needs.

Examples for some alternative objectives are given:

1. The smallest number of drug dosings required for achieving any given aim.
2. The lowest total drug dose required for achieving any given aim.
3. The minimal total amount of drug needed for rehabilitation.
4. The smallest deviation from the baseline at normal cell population count (e.g., platlet nadir) after chemotherapy or another cell-suppressive treatment.
5. The shortest period of disease (e. g.,thrombocytopenia).

Using the fitness function it is possible to a) estimate the efficacy of a given protocol, b) search for the solution of an optimization problem, i.e., predict which protocol will be best of many potential protocols considered for curing/relieving the patient.

VIII. Solving the Optimization Problem

The optimization problem is stated using the described models: to find the protocol for drug administration (with option to growth factor administration) which maximizes the given fitness function.

As explained above, we define the fitness function according to the user requirements. For example, the goal of the treatment may be defined as minimizing the number of cancer cells at the end of the treatment, minimizing

the damage to the BM cells throughout the treatment or at its end, and curing the patient (where cure is defined precisely) as quickly as possible. Note that the fitness function may also include goals such as maximizing life expectancy, minimizing cost of treatment, minimizing treatment hazards and/or discomfort etc. Generally, the aim of optimization is to find the best protocol, i.e. the protocol that generates the best value of fitness. Customarily, this is achieved by mathematical analysis. However, mathematical analysis is restricted to over simplified models, whereas, in order to accommodate biologically realistic parameters, the described models are very complex and, therefore, cannot be solved analytically. On the other hand, the practical purpose of the treatment is not to find *the best possible protocol* (i.e., the global optimum) but "only" one that will suit the user's objectives, even if its fitness is not absolutely the best (i.e., the local optimum). For this reason we can be satisfied with the solution that can be shown to promise the pre-defined objectives.

Hence, the optimization problem may be reformulated as follows: for given initial conditions, find the treatment protocol which will fulfill the user's requirements (e.g. curing a patient according to given definitions of cure) and subjected to given limitations (e.g. treatment duration, drug amounts, etc.). To this end it is not compulsory to find **the** global solution. It is enough, with regards to objectives and limitations, to perform search, using search algorithms, in certain regions of the protocols' space, and find the local maxima of the fitness function. After determining the locally best protocols, we can verify that they serve one's objectives and check them numerically for stability.

Such a strategy can be used for identifying patient-specific treatment, as well as in the general case, where only the profile of the disease and the drug are specified. If more patient-specific data are supplied, the solution will be tailored more specifically. On the other hand, the optimization program
5 could propose general recommendations for the protocol types for certain kinds of disease, treated with a certain kind of medication.

It will be appreciated that the present invention is not limited by what has been described hereinabove and that numerous modifications, all of which fall within the scope of the present invention, exist. For example, while the
10 present invention has been described with respect to certain specific cell lineages, the concept can be extended to any other lineage and treatment protocol which can be detailed mathematically (e.g., viral or bacterial diseases). Furthermore, certain assumptions were necessarily used in computing the mathematical models of the embodiments. Values and equations based on
15 these assumptions can be changed if new information becomes available.

It will be appreciated by persons skilled in the art that the present invention is not limited by what has been particularly shown and described herein above. Rather the scope of the invention is defined by the claims which follow:

What is claimed is: [independent claims listed now, dependent claims to follow] (Note that we are not in a position to revise the claims. Z. Agur)

1. A system for individualized optimization of a treatment protocol, the system comprising:

5 a system model comprising:

a model of a biological process; and

a mathematical model of treatment effects on said biological process;

a plurality of treatment protocols;

10 means for adding individualized parameters to said system model,

whereby said system model is modified based on said individualized parameters; and

a selector for selecting an optimal treatment protocol from said plurality of treatment protocols based on modification of said system model.

15 2. A system for identification of optimal treatment protocols using heuristic analysis, the system comprising:

a biological model;

a plurality of treatment protocols included within said model, thereby providing a plurality of treatment models, wherein said treatment models
20 provide effects of said treatment protocols on said biological model; and

heuristic means for identification of said optimal treatment protocol from said treatment models.

What is claimed is: [independent claims listed now, dependent claims to follow] (Note that we are not in a position to revise the claims. Z. Agur)

1. A system for individualized optimization of a treatment protocol, the system comprising:

5 a system model comprising:

a model of a biological process; and

a mathematical model of treatment effects on said biological process;

a plurality of treatment protocols;

10 means for adding individualized parameters to said system model,

whereby said system model is modified based on said individualized parameters; and

a selector for selecting an optimal treatment protocol from said plurality of treatment protocols based on modification of said system model.

15 2. A system for identification of optimal treatment protocols using heuristic analysis, the system comprising:

a biological model;

a plurality of treatment protocols included within said model, thereby providing a plurality of treatment models, wherein said treatment models
20 provide effects of said treatment protocols on said biological model; and

heuristic means for identification of said optimal treatment protocol from said treatment models.

3. A system for presenting a individualized model of a biological process, the system comprising:

a processor for generating a model of a biological process;

a plurality of experimental data, included within said model; and

5 means for including individual data into said processor, thereby providing said individualized model of said biological process.

4. A system for prediction of outcomes of a treatment protocol, the system comprising:

10 5. A system for describing treatment effects on a biological process

6. A method for individualized optimization of treatment, the method comprising the steps of:

providing a biological model;

inputting parameters into said model;

15 computing treatment protocols for said model within said parameters;

applying a fitness function to said treatment protocols; and

choosing an optimal treatment protocol based on said fitness function.

20 7. A method for optimization of a treatment protocol, the method comprising the steps of:

providing a variable representing an amount of medication administered;

providing behavior characteristics of said administered medication;

providing a model of a cell line predicting effects of said administered medication on said cell line;

calculating a

determining a treatment protocol

5 8. * A system for prediction of outcomes of treatment of thrombocytopenia by Thrombopoietin (TPO), the system comprising:

9. * A system for prediction of outcomes of treatment of neutropenia with Granulocyte colony stimulating factor.

10 10. A system for individualized optimization of treatment of neutropenia, the system comprising:

a system model comprising:

a mathematical model of a neutrophil lineage; and

a mathematical model of effects of treatment on said neutrophil lineage;

15 a plurality of treatment protocols;

means for adding individualized parameters to said system model, whereby said system model is modified based on said individualized parameters; and

20 a selector for selecting an optimal treatment protocol from said plurality of treatment protocols based on modification of said system model.

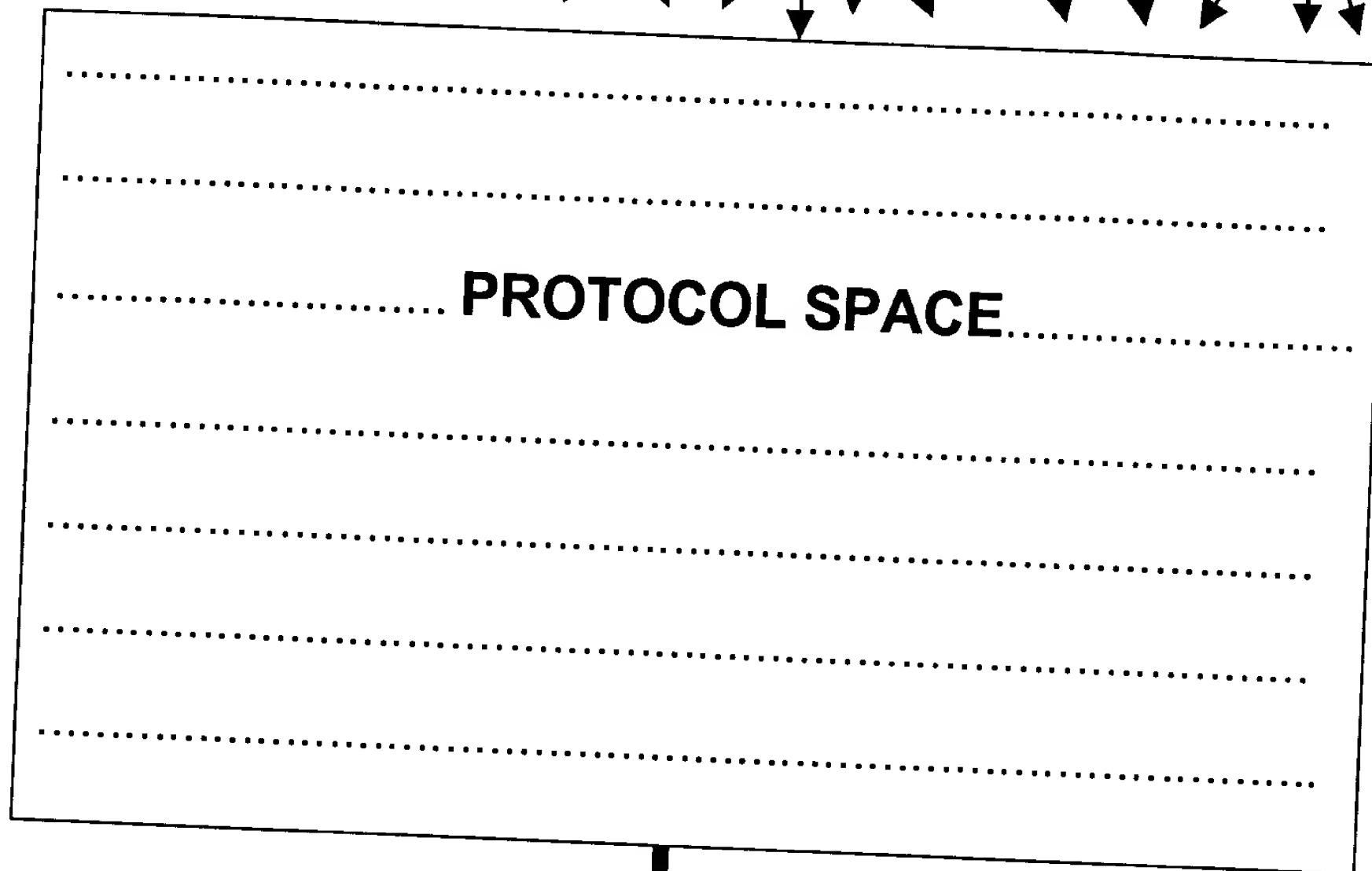
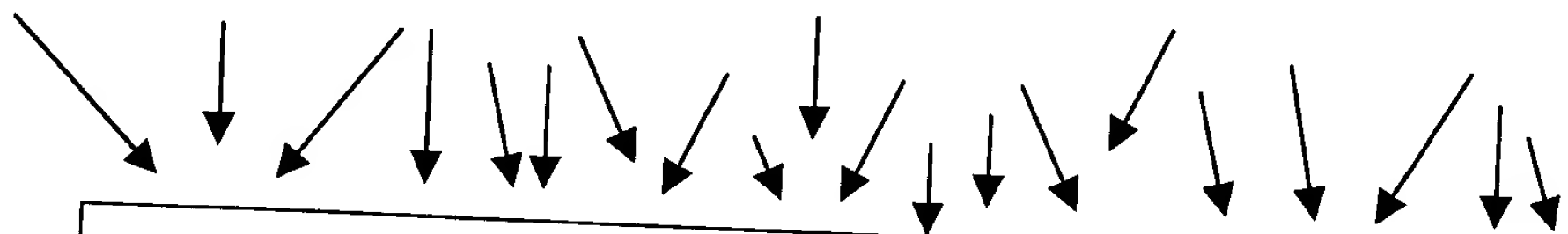
11.

Figures

5

CONCEPT

DETAILED PARAMETERS



OPTIMAL TREATMENT PROTOCOL

10

Fig. 1

15

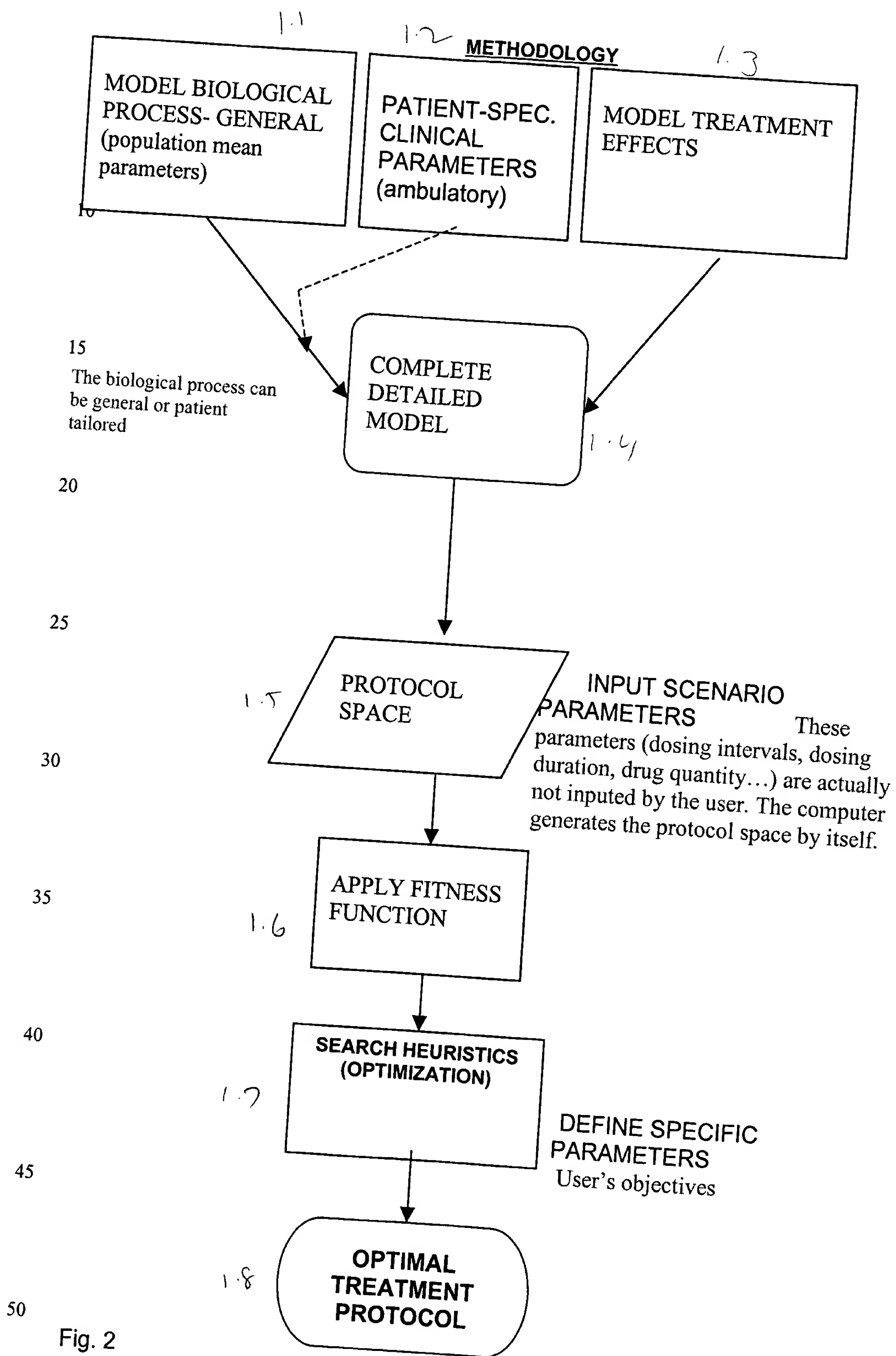


Fig. 2

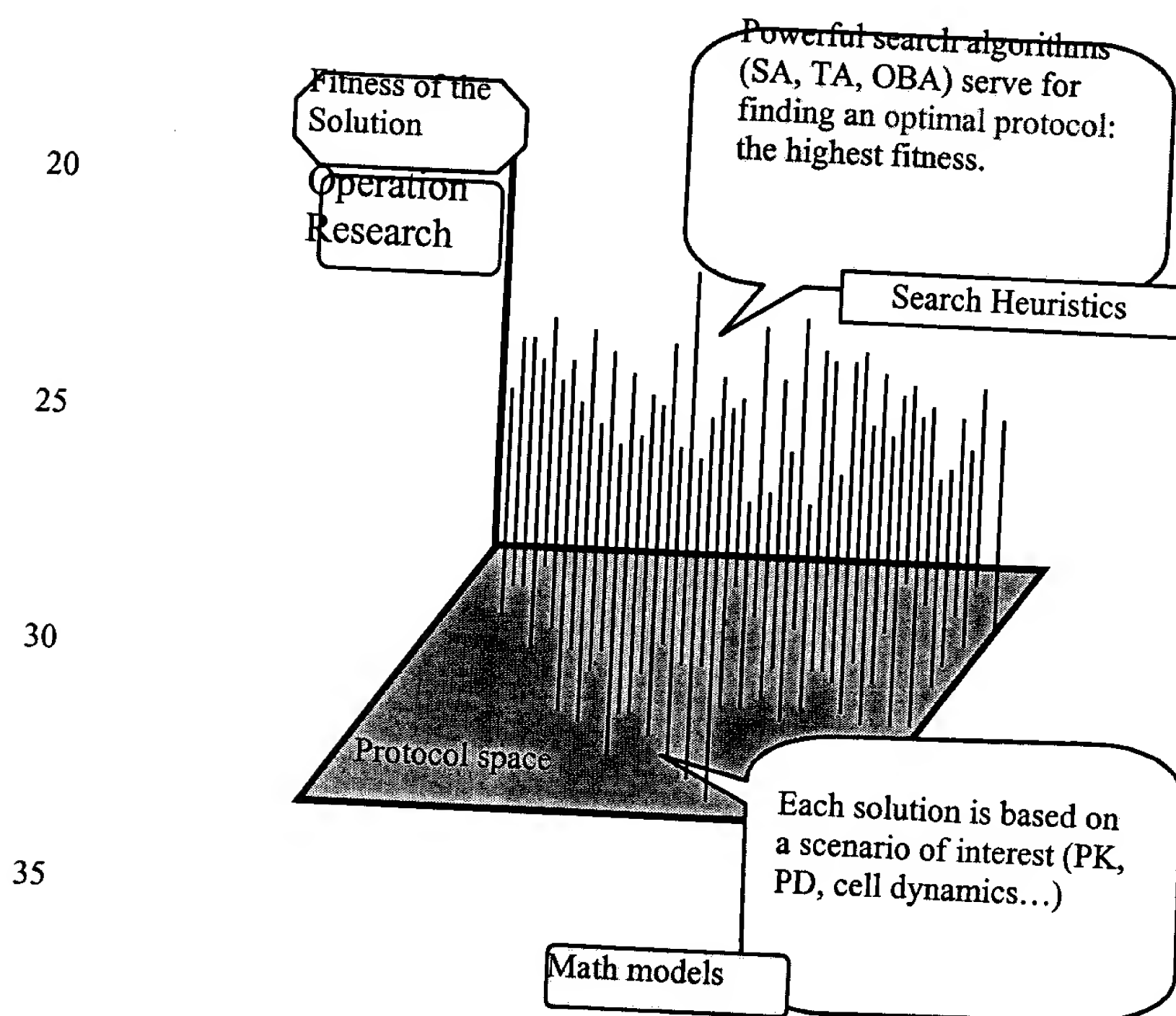
METHODOLOGY (2)

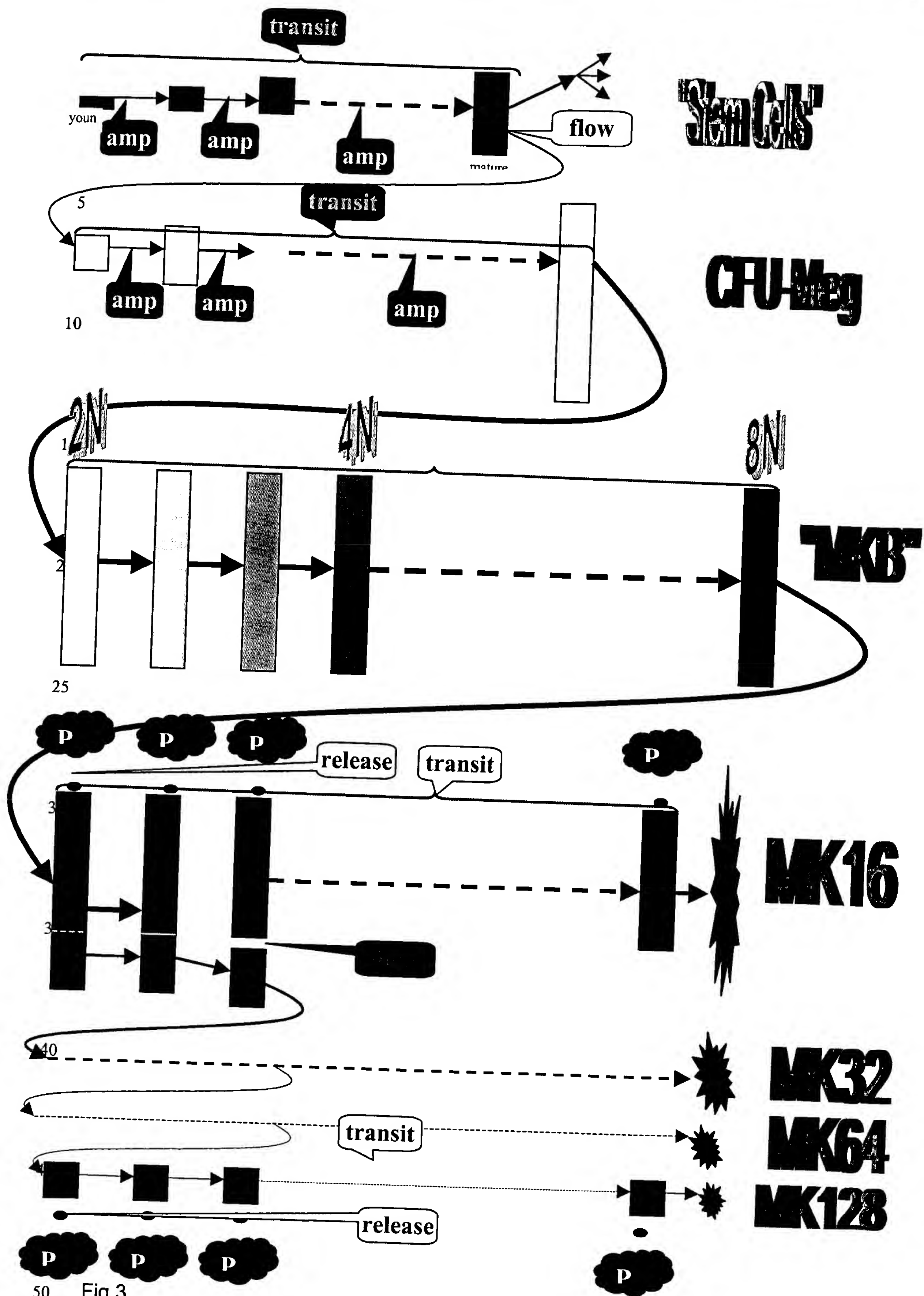
5

10

Attempting to optimize some instance of
a chemotherapy problem with a given
set of solutions...

15





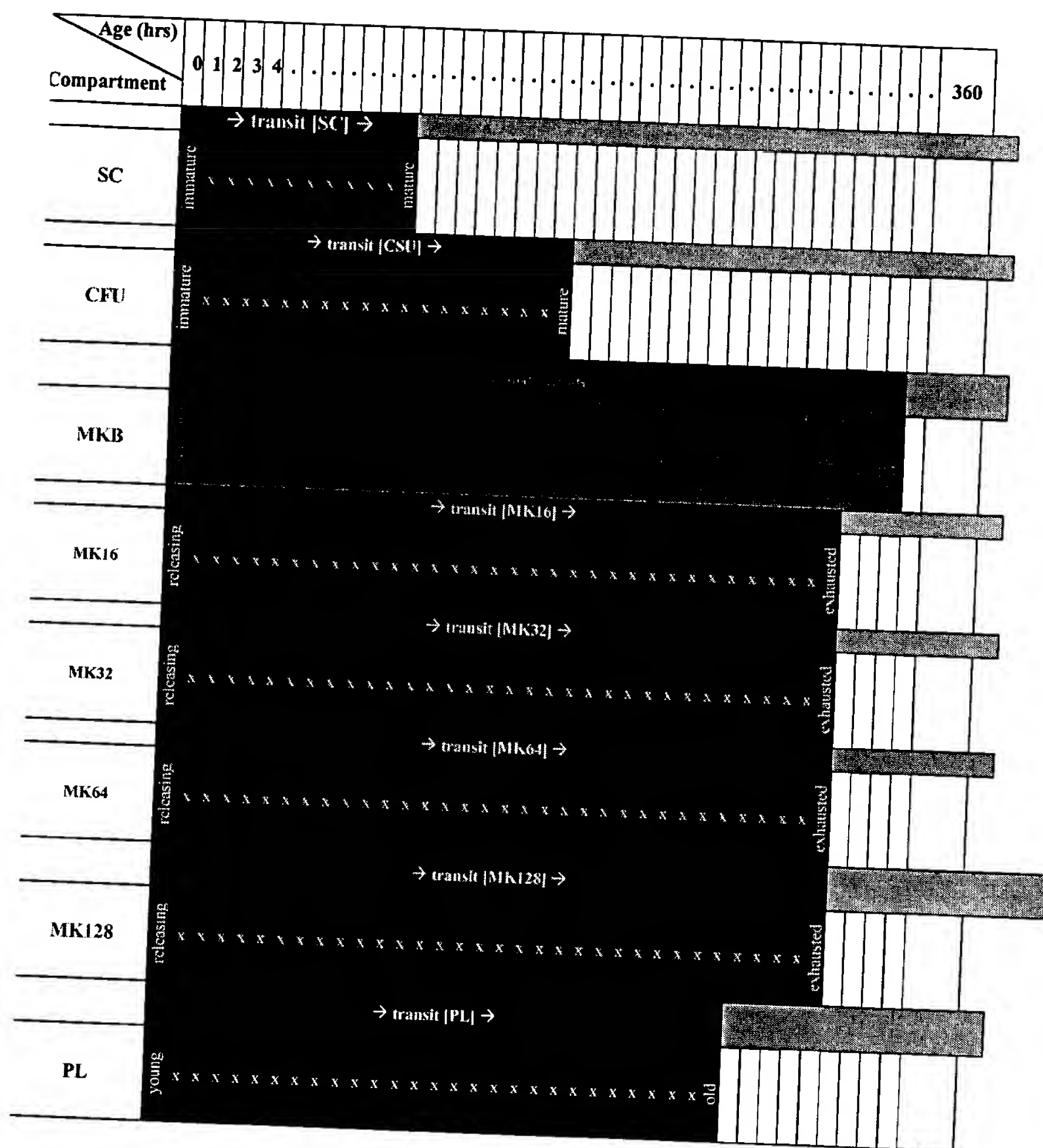
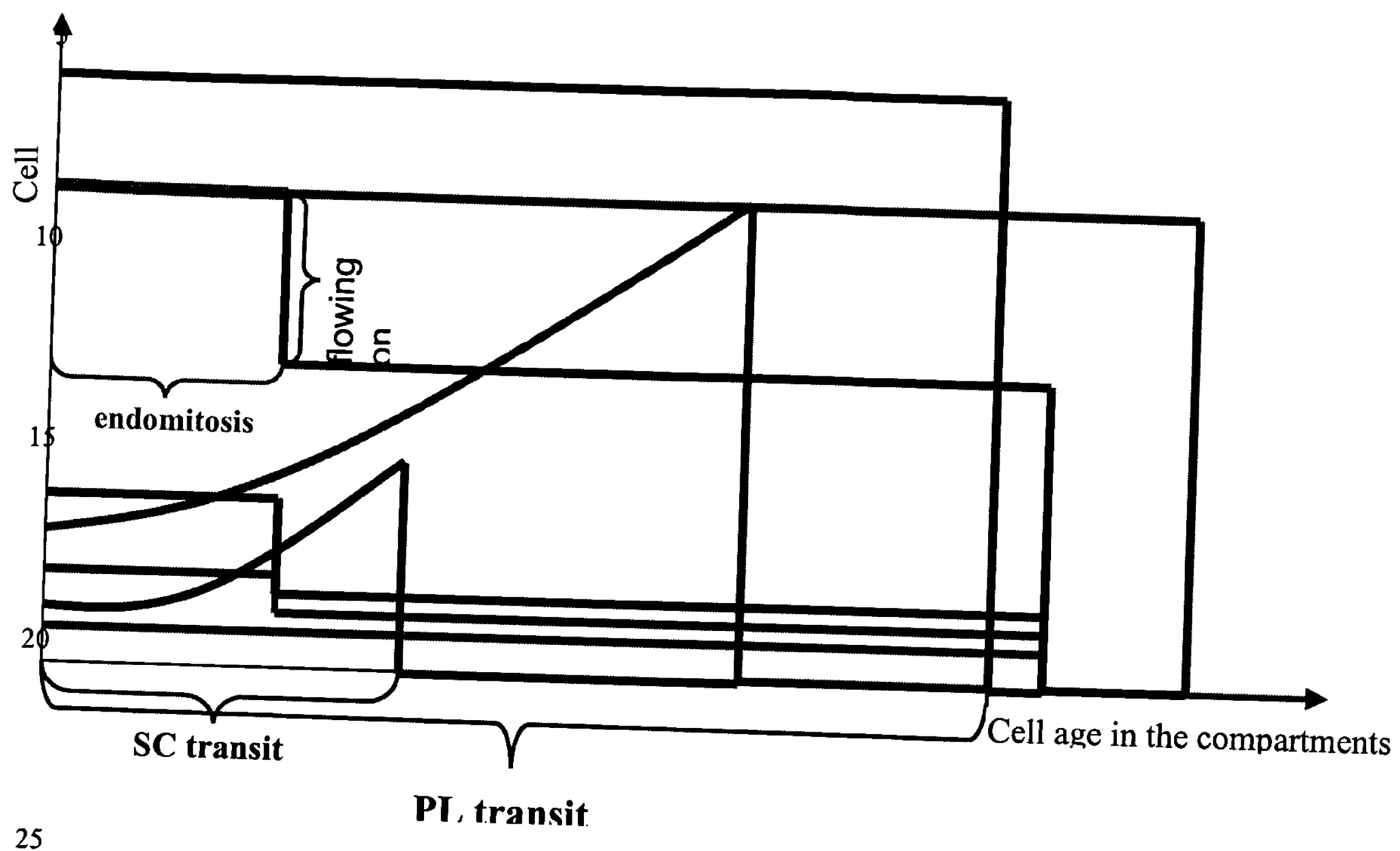


Fig 4



25

Fig 5

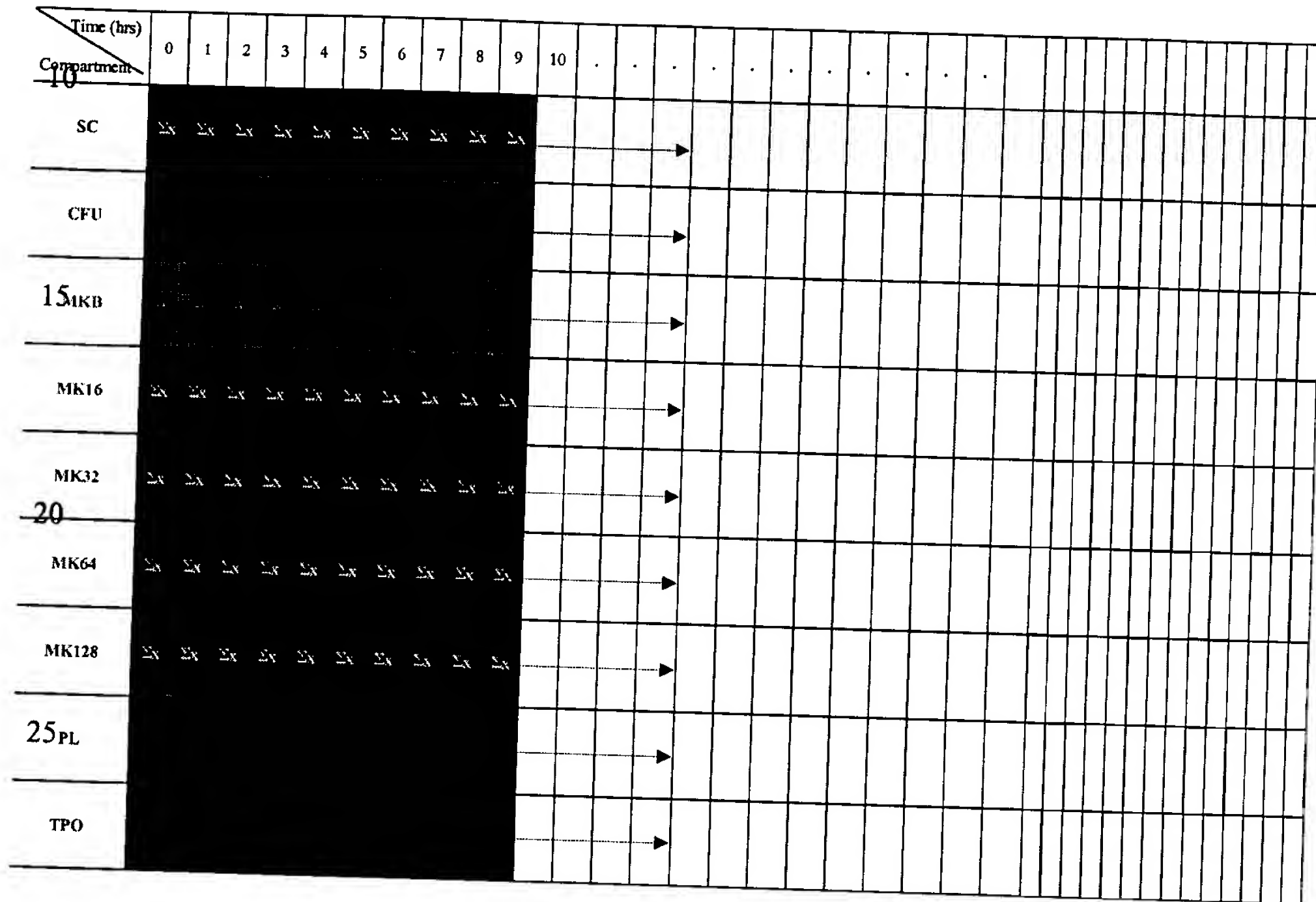


Fig. 6

Fig 7

Simulations showing that if the protocol is pre-calculated then a similar or a higher efficacy can be obtained using 4-fold reduced total dose of TPO.

5

TPO use in healthy donors:

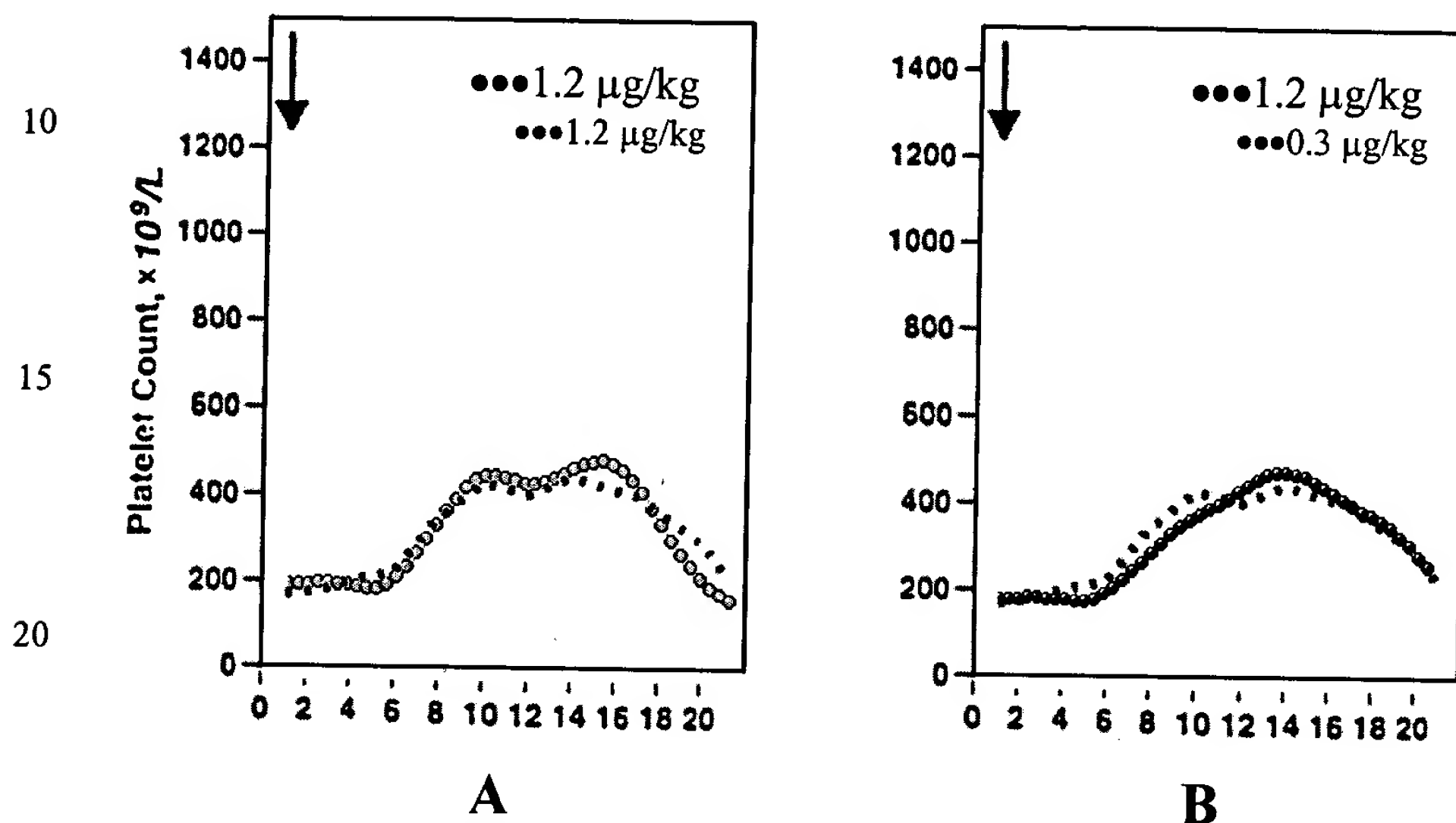


Fig. 8: TPO given to healthy donors- Results of TPO clinical trials from recent research on healthy platelet donors, as compared to our computer simulation results. Arrows indicate the start of TPO treatment. (A) Comparison of experimental data from published articles¹ (black) and our model simulation (green), in both TPO was given as a single IV dose of 1.2 µg/kg on day 0. (B) Comparison of the same experimental data (black) and our proposed TPO administration protocol; the total dose in the simulated protocol was 0.3 µg/kg (blue).

TPO use in patients receiving chemotherapy:

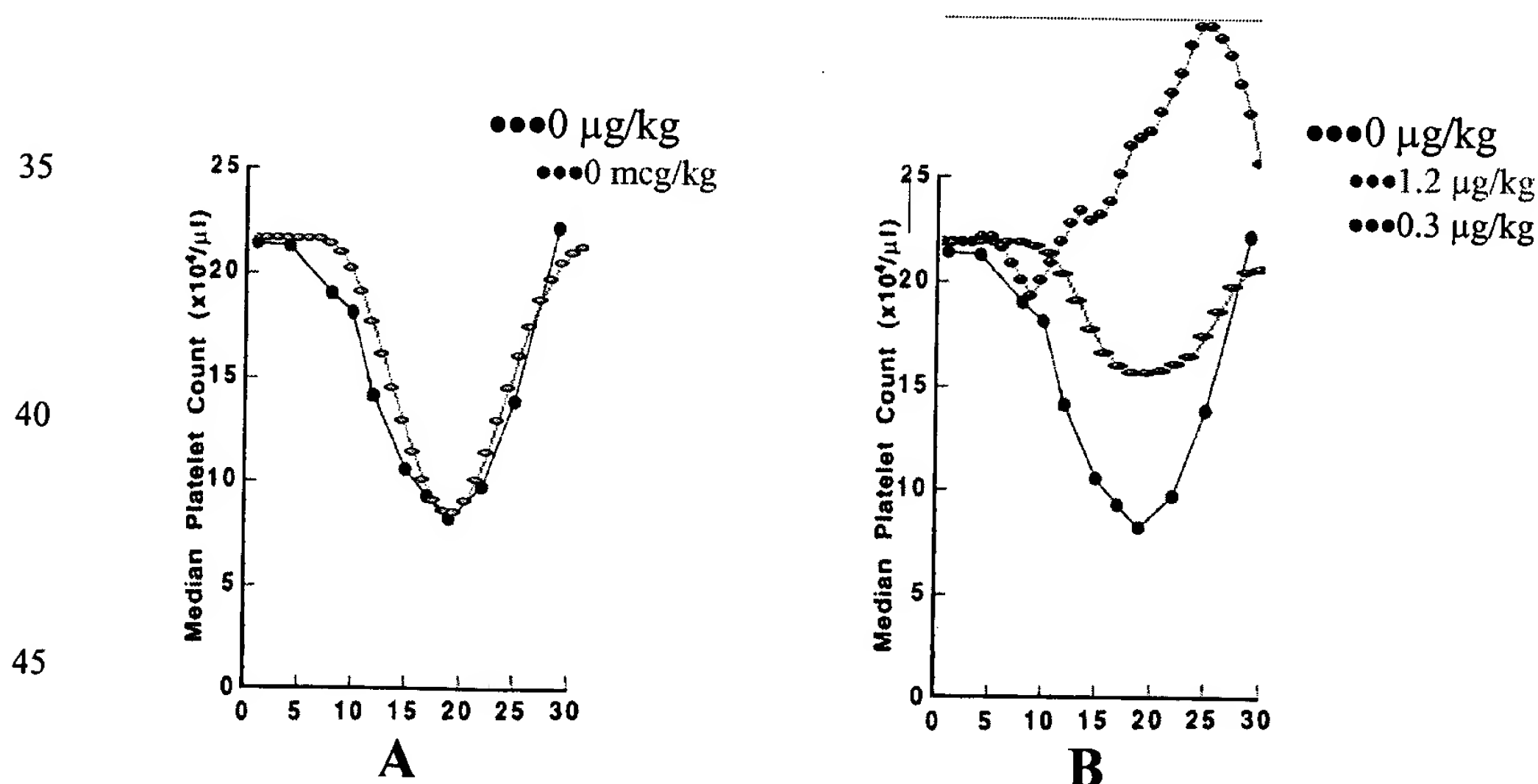


Fig. 9: TPO with chemotherapy- (A) Results of clinical trials from recent research on thrombocytopenia induced in patients receiving single carboplatin chemotherapy² on day 0 (black), as compared to our model simulation of these results (green). (B) The same experimental data (black); simulations of the same experiment, with addition of "conventional" TPO protocol of a single IV dose of 1.2 µg/kg on day 0 (olive); simulations of the same experiment under our proposed protocol that totals 0.3 µg/kg (blue).

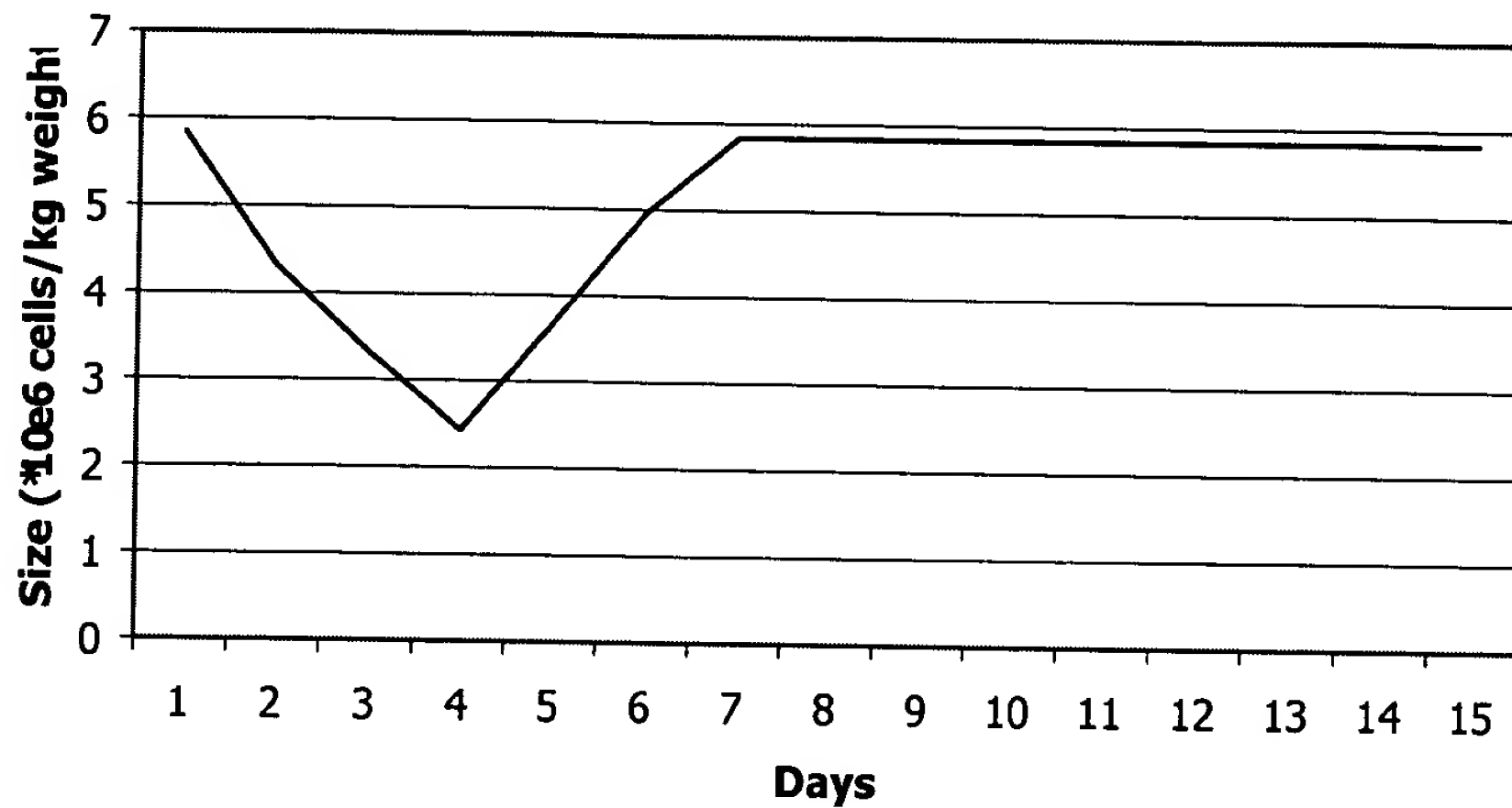


Fig 11

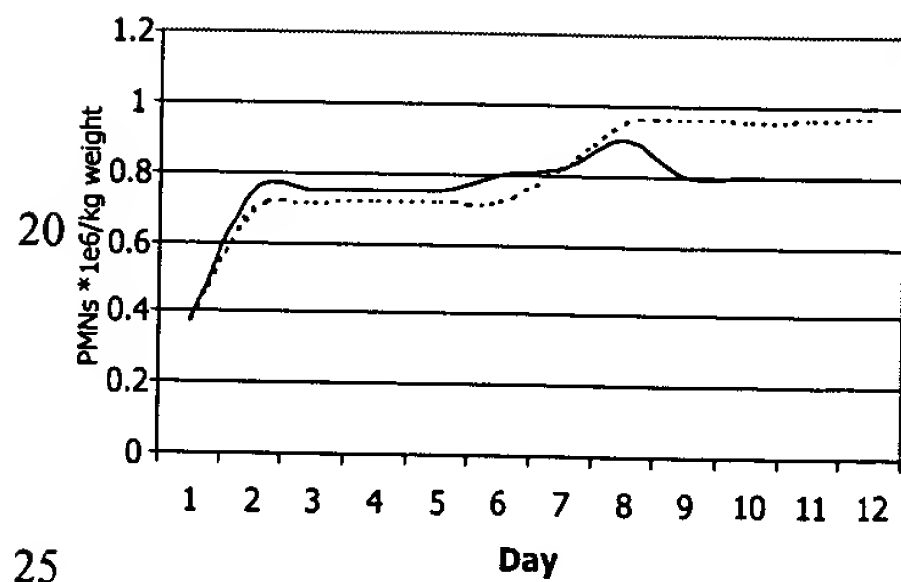


Fig 12a

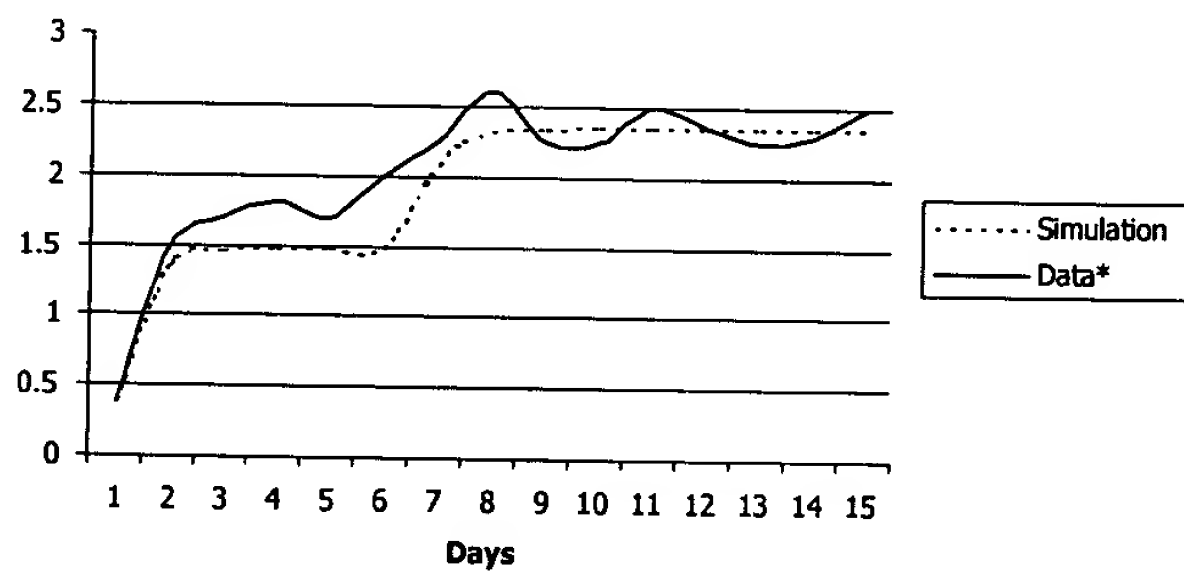


Fig 12b

Computer Simulator of Human Thrombopoiesis.

Contents:

- 1. Abstract**
- 2. Introduction**
 - 1) Demand for the work**
 - 2) Biological system**
 - One) Thrombopoiesis**
 - Two) Thrombopoietin**
- 3. Methods**
 - 1) The structure of the model**
 - One) The cells participating in thrombopoiesis**
 - Two) The role of TPO**
 - (a) TPO concentration**
 - (b) TPO effect on amplification rate**
 - (One) SC**
 - (Two) CFU-Meg**
 - (c) TPO effect on transit time**
 - (One) SC**
 - (Two) CFU-Meg and MKB**
 - (d) TPO effect on cell flow between compartments**
 - Three) The program structure**
- 4. Parameter determination**
- 5. Results**
- 6. Discussion**
- 7. References**

Abstract [\[return to Contents\]](#)

Thrombocytopenia is a common hazardous blood condition, which may appear in different clinical situations, including cancer chemotherapy, where it represents a major dose limiting side effect. For this reason, and due to the constant demand of platelet harvesting for transfusions, a specific control of blood platelet counts is strongly needed.

Recently, such a thrombopoiesis-controlling cytokine, thrombopoietin (TPO), was isolated and its human recombinant analog is now available. In order to accelerate a search for the most effective TPO treatment protocol, and to reduce the investigation costs (including number of potentially endangered patients), we offer a mathematical model, which is implemented as a computer simulation. Our model reproduces the dynamics of the human thrombopoietic lineage in the bone marrow, of platelet counts in the periphery, and effects of TPO administration on them.

Using this model, we are able to develop general and patient-specific optimal protocols of TPO administration for minimizing post-chemotherapy thrombocytopenia and for maximizing platelet harvest in platelet donations, while reducing TPO treatment cost.

Introduction [\[return to Contents\]](#)

Aim [\[return to Contents\]](#)

The most harmful dose-limiting side effect of cancer chemotherapy is the severe suppression of the hemopoietic system. This results in a state of immune deficiency and reduced blood coagulation as granulocyte and platelet counts fall drastically.^{1, 2} Therefore, post-chemotherapy rehabilitation of hemopoietic system is of great importance. However, most of the growth factors that are currently used (e.g., EPO, G-CSF) are almost impotent in stimulation of thrombopoiesis. This led to an intense search for specific thrombopoiesis-stimulating factors in the previous decades. This search was motivated also by the constant demand for platelet donations for transfusions to thrombocytopenic patients.

Recently, such thrombopoiesis stimulating cytokine, thrombopoietin (TPO), was isolated, and its synthetic analogs became available, and are under clinical investigation.^{2, 3, 4, 5, 6} These compounds were shown to have the same biological activity as TPO, thus the term hence the

The term TPO will be used without distinguishing between its different forms and analogs. It was shown to have a wide spectrum of useful effects, almost without adverse ones.

Most authors that studied TPO effects on thrombopoiesis emphasize the critical role of the TPO administration protocol in chemotherapy-associated treatment and in platelet harvesting.^{2, 4, 7, 8, 9, 10} However, the data accessible for selecting the proper protocol is very insufficient, because of TPO's recent discovery. Therefore, it is of special interest and importance to model thrombopoiesis and TPO effects on it

mathematically. An implementation of such a model as software may accelerate a search for the most effective TPO treatment protocol.

In this work we build such a mathematical model and implement it as a computer simulation that imitates a course of patient's bone marrow progression (particularly, compartments relevant for platelet production), peripheral platelet counts, and TPO concentration changes in the system for a period of several years. Both cell-suppressive treatment (chemotherapy, for example) and exogenous TPO administration, are considered in our model. The model allows their introduction concurrently, in any possible combination and timing.

Currently, our model enables a search for an optimal protocol by trial-and-error. An additional module is to be implemented shortly, which will use Operation Research tools while running the simulations, to find the best protocol. The great contribution to the traditional biological and clinical experiments is its cost and time reduction, and the decrease in need for experiments on animals and/or humans. Additionally, the optimal protocol search may be accelerated by some analysis of model tendencies.

Modeled biological system [return to [Contents](#)]

Thrombopoiesis [return to [Contents](#)]

[~~REFERENCE to a textbook of hemo/thrombopoiesis (to look for them in (50))~~
Review of thrombopoiesis see in (35); additional data see in (11, 12, 13, 31, 31-Kuter et al (1997)); brief review see below(31): Brancheg et al (1975)(?), Kuter et al (1997);
]

Like all other hemopoietic lines, the thrombopoietic line originates from poorly differentiated, multipotential cells, that are capable of some division and self-reconstitution.^{34,31, 35} Such bone marrow cell compartments as pluripotential hemopoietic stem cells and common myeloid progenitor cells (CFU-GEMM) have more or less these characteristics.³⁵

Gradually, the cells become more and more differentiated and thus committed to the thrombopoietic line. At this stage they proliferate extensively. Colony-forming Units – megakaryocytes (CFU-Meg) is an example of such compartment. Sometimes ~~the~~ burst-forming units – megakaryocyte (BFU-Meg), promegakaryoblasts or the megakaryoblasts³⁴ ~~compartments~~ are considered as having the ~~same~~ similar properties.^{31, 35}

The committed ~~thrombopoietic~~ megakaryocytopoietic cells, megakaryocyte precursors, go through several stages of maturation when the proliferation is impossible. However, megakaryocyte maturation is somewhat different from that of other hemopoietic lines. Here, along with cytoplasmic maturation, cell nuclei undergo mitotic events. However, although the DNA material of these cells doubles, cell division does not happen. Such incomplete mitosis is termed endomitosis or endoreduplication. Consequently, the cell becomes poliploid with 2N, 4N, 8N, etc., amount of DNA. Some authors call the cells with 2N to 4N chromosome number promegakaryoblasts, others call them megakaryoblasts or; ~~others call them immature megakaryocytes~~^{34, 31, 35}.

Usually, megakaryocytes do not start to release platelets until they reach the ~~8N~~ to 16N state.^{11, 35} Then they begin to create demarcation membranes that envelop cytoplasm fragments generating platelets. The platelets are released into the blood stream. A small fraction of the megakaryocytes do not cease their endoreduplication at the 16N-stage, but rather continue with one or more additional endomitoses and get thus a ploidy of 32N or more.^{34, 31} The amounts of cytoplasm, cell volume and the ability to release platelets increase proportionally to the cell ploidy.^{12, 13}

Thrombopoietin [return to [Contents](#)]

The major sites of TPO production are the liver and the kidneys. TPO is also produced in the spleen and the bone-marrow, but the production rate in these organs is significantly lower (5 times in mice) than in the former (???).^{2, 14, 15, 16, 32} Some authors also find low TPO production in many other sites in the body.^{15, 32} The rate of liver and kidney TPO production is constant under thrombocytopenia and thrombocytosis of every examined severity.^{2, 14, 15, 16} Spleen and bone-marrow production, on the other hand, is inversely related to the megakaryocyte and platelet mass.^{2, 14} However, these changes are extremely small compared with total TPO production, and are therefore considered negligible. The possibility of high local TPO concentration in these organs, in which megakaryopoiesis occurs, was rejected by experiments that showed that TPO concentration in the bone marrow equals that in the peripheral blood.¹⁷ Normal TPO concentration varies significantly between healthy subjects.³⁴ However, intraindividual variation in steady state TPO concentration is relatively low.³⁴

TPO-receptors on the platelet and megakaryocyte surfaces are the main TPO-clearance mechanism, and thus their major regulation mechanism. Hence, TPO concentration is inversely related to the total platelet and megakaryocyte mass.^{2, 5, 17, 18, 19, 20, 32}

The effects of TPO on the thrombopoietic line can be divided into three kinds: (i) stimulation of proliferation of the megakaryocyte progenitors which have an ability to proliferate;^{7, 9, 21, 22, 23, 31, 32, 33} (ii) stimulation of maturation of megakaryocyte progenitors;^{7, 22, 31, 32, 33} (iii) induction of an additional endomitosis of already mature megakaryocytes that leads to the increase in the average megakaryocyte ploidy^{3, 21, 22, 23, 31, 33}. These effects are mediated through the same TPO receptor.¹⁹ However, the mechanisms underlying these effects may be different. Hence, it seems possible that one of them may be introduced when another is saturated, at least partially.

Methods [return to [Contents](#)]

Model Structure [return to [Contents](#)]

The search for the best protocol of TPO administration was divided into two major parts: 1) creation of the model and computer simulation, which closely imitate thrombopoiesis of any given individual under different circumstances detailed below; 2) producing the module that can generate the best protocol for general purposes, as well as for the specific patient, according to a criterion specified by a physician, a scientist, a pharmacologist, or any other user. The optimization scheme uses a flexible fitness function, and is based on the results of simulation supplied by the first part. This paper will discuss only the first part.

First, we had to generate a scheme of thrombopoiesis that can be expressed mathematically. This scheme has to include certain biological mechanisms and parameters in order to be able to give a realistic prediction (Fig. 1 – ???).

Scheme of the Thrombopoiesis Model [\[return to Contents\]](#)

We divided the entire thrombopoietic lineage into eight compartments. The first, called abstractly “Stem Cells” (SC), refers to all bone marrow hemopoietic progenitors that have an ability to differentiate into more than one line (e.g., pluripotential stem cells, CFU-GEMM, etc). Cells of this compartment in our model proliferate, mature, and then differentiate into megakaryocyte progenitors or other precursors, or give rise to “new” stem cells. Although the consideration of the last process, i.e. the renewal of the stem cells by “new” ones, is not completely correct biologically^{36, 37}, it may serve as an acceptable assumption since we do not elaborate the characteristics of this population in details.

Cell death through apoptosis may have a significant effect on cell numbers in the proliferating compartments.³¹ However, we do not consider this process separately, but rather include its effect together with the effect of cell proliferation into total amplification of cell number (s_c) in a specific compartment. As far as we know, there is no data about significant apoptosis in the non-proliferating megakaryocytic compartments. We therefore disregard apoptosis in these compartments.

Kinetic data regarding the various sub-populations of the stem cell compartment (i.e. rates of proliferation, maturation and self-renewal) is rather scarce. We therefore assume one homogeneous stem cell compartment with biologically acceptable parameters. Based on some works that showed that probabilities of stem cell differentiation into one or another hemopoietic lineage are constant,^{24, 25, 26, 78} we assumed that a proportion of mature stem cells that flow into the megakaryocytic lineage (s_c) is fixed. The same was assumed about stem cell self-renewal. Thus, after the cells spend a defined transit time in the Stem Cell compartment (s_c), certain constant fraction of them returns to their “young state”, i.e. starts their passage through the SC compartment again. Another fraction (s_c , also constant) passes into the next compartment ~~called~~ named “CFU-Meg”. The remaining “stem cells” are supposed to go to hematopoietic lineages other than megakaryocytic.

By the name CFU-Meg (Colony-Forming Units – Megakaryocytes), we refer to all the cells that are already committed to the megakaryocyte line but are still capable of proliferation. Cells of this compartment in our model, like those of the previous one, spend some time multiplying at their own amplification rate CFU and maturing before they lose their proliferative ability and pass to the megakaryoblasts (MKB) compartment.²⁷ The time they spent in CFU-Meg compartment is CFU .

The MKB compartment in our model includes all the cells that have lost their ability to proliferate, but are not sufficiently mature to release platelets. We assume that megakaryocytes do not start to release platelets until they reach the 16N-ploidy phase.¹¹ Thus, “megakaryoblasts” is more of a conceptual name; it refers to the 2N, 4N and 8N cells of the megakaryocyte lineage that cannot divide, at all stages of cytoplasmic maturity. 16N-megakaryocytes, before they start to release platelets, are also included in this compartment. After these cells spend their designated transit time

(τ_{MKB}) in the MKB compartment, they move to the next bone marrow compartment, termed MK16.

The cells of the MK16 compartment are megakaryocytes of 16N-ploidy class. They release platelets at a constant uniform rate (r_{MK16}) until they exhaust their capacity (C_{MK16}) and then are disintegrated.^{12, 43, 27} We assume that the cell volume is in linear relation with megakaryocyte ploidy based on some evidences from literature.¹² Hence, we assume that all 16N-megakaryocytes have the same volume at the start of their path through the compartment and, thus, the same platelet-releasing capacity (C_{MK16}). Therefore, we suggest that all platelet-releasing 16N-megakaryocytes spend the same transit time (τ_{MK}) until they are exhausted and disintegrated.

However, not all 16N-megakaryocytes are destined to this fate in our model. Part of them (τ_{MK16}) does not participate in platelet release, but continue with another endomitosis and became 32N-megakaryocytes. These constitute a distinct compartment, MK32. Hence, after the cells spend the period needed for additional endomitosis (τ) in MK16 compartment, a certain fraction of them leave it and pass to the next one.

32N-megakaryocytes also release platelets. The rate of platelet release is constant for every compartment and proportional to the ploidy-state of the megakaryocytes in it.^{12, 13} Thus, 32N-megakaryocytes release platelets at the rate r_{MK32} , which is twice that of the 16N-megakaryocyte. However, we suggest that 32N-megakaryocytes are not exhausted sooner than the 16N class since they have twice the volume and platelet-releasing capacity (C_{MK32}). Consequently, we assume that all platelet-releasing megakaryocyte compartments have the same transit time (τ_{MK}).

Again, a fraction of the cells (τ_{MK32}) is not engaged in platelet formation, but continues to the 64N-stage. We assume that the additional endomitosis takes the same time (τ) as in the MK16 compartment. 64N-megakaryocytes continue this behavior, and a certain fraction of them (τ_{MK64}) becomes 128N-cells.^{31, 34} The time needed for an additional endomitosis remains the same (τ). ~~Normally, 64N and 128N megakaryocytes are not found in humans. [REFERENCE] However, these cells were detected in human bone marrow in some abnormal conditions. [REFERENCE] Therefore, we included these compartments in our model, but in the normal state the number of cells in them is negligible. According to current knowledge, megakaryocytes of greater ploidy classes were not encountered in human.~~

Finally, a platelet (PL) compartment is introduced into our model. This is not a bone marrow compartment, but rather the platelet pool in the peripheral blood. Platelets, which are released from megakaryocytes of 16N-, 32N-, 64N-, and 128N-ploidy classes, enter this compartment. There are two mechanisms of platelet elimination from circulation: By age-dependent destruction and by the normal utilization ~~directed at (???) in order to maintaining~~ the integrity of blood vessels.^{23, 28} The first mechanism is reflected as platelet disappearance after they spend their designated transit time (τ_{PL}) in the PL compartment. The second one is rather age-independent and it is reflected as constant platelet efflux (d) throughout all platelet age-stages.

TPO EFFECTS [\[return to Contents\]](#)

Having thus formulated the compartment model for thrombopoiesis, we still have to define the effects of TPO on it (Fig.1). As was mentioned before we can divide the effects of TPO to three levels. These could be expressed in terms of dependence of the following parameters on TPO concentration: (i) amplification rate (), (ii) the rate of cell maturation or, alternatively, transit time through given compartments (), and (iii) the fraction of megakaryocytes of a given ploidy that undergoes an additional endomitosis and passes to the next ploidy class (). ~~Neither~~ For simplicity we assume that neither the rate of platelet release per given megakaryocyte (r); nor the rate of platelet utilization (d) is dependent on TPO concentration in our model.²⁹ ~~—[REFERENCE]~~ First, we shall define the pharmacokinetics of TPO.

TPO concentration. [\[return to Contents\]](#)

Many works have shown that recombinant human full-length TPO, as well as its truncated form rHuMGDF, are fully active biologically. [REFERENCE] Therefore, in our model we simply add exogenously administered recombinant protein to endogenously produced one in order to calculate actual TPO concentration (C).

The rate of TPO production in the main TPO production sites, i.e. liver and kidney, was shown to be constant under thrombocytopenia or thrombocytosis of any severity.^{2, 14, 15} However, the level of TPO mRNA in the sites like bone marrow and spleen, where it is produced at the significantly lower rate than in the liver and kidney, can change considerably.^{2, 14} Despite the apparent importance of spleen and bone marrow concentrations as megakaryopoiesis mainly occurs at these sites, it was shown that there is no significant difference between TPO levels in the bone marrow and in the peripheral blood.¹⁷ We therefore assume that the bone marrow and spleen production of TPO is negligible, and that endogenous TPO is produced at a constant rate (p).

The main mechanism that controls TPO concentration in the blood is receptor-mediated TPO uptake (u).^{2, 5, 17, 18, 19, 20}

Another mechanism, we assume, is non-specific TPO-receptor-independent clearance of TPO (l). We suggest that this mechanism is rather insignificant in normal state, when receptor-mediated TPO binding, endocytosis, and degradation (u) remove most of the TPO (it was shown experimentally in mice)³⁰. But when the amount of TPO (C) rises significantly above the ability of the receptor pool to remove it, the non-specific clearance (l) becomes important.

Thus the formula for TPO levels C at time $i+1$ is:

$$(1) \quad C_{i+1}^* = C_i + p + x_i - u_i - l_i \quad p, x_i, u_i, l_i \geq 0 \quad C_i > 0$$

where C_i is TPO concentration at the current hour (i); C_{i+1}^* is approximation of the TPO concentration at the next hour (detailed below); p is TPO produced per hour

endogenously; x_i is the addition to TPO concentration due to exogenous TPO administration; u_i is TPO removed from the blood by receptor-mediated binding; l_i is TPO cleared from circulation by non-specific mechanisms.

We assume that receptor-mediated TPO clearance depends on the total number of TPO receptors (n) and on the ability of each receptor to uptake TPO (a):

$$(2) \quad u_i = n_i \cdot a \quad n_i, a \geq 0$$

where n_i represents the receptor pool and a is TPO-clearing ability of the receptors, i.e. amount of TPO that each receptor removes per hour.

Both, megakaryocyte and platelet mass contribute to the total receptor number (n) and, thus, to the rate of TPO clearance (u).¹⁵ We assume that every platelet bears the same number of TPO receptors (m_{PL}). The receptor number on megakaryocytes, however, changes. Thus, the receptor pool (n) is:

$$(3) \quad n_i = \sum_{comp=1}^4 \left(\sum_{j=1}^{\lceil \tau_{comp} \rceil} (q_{comp,j,i} \cdot m_{comp,j}) \right) + q_{PL,i} \cdot m_{PL} \quad q_{comp,j,i}, q_{PL,i}, m_{comp,j}, m_{PL} \geq 0$$

where $comp$ (1 to 4) is one of the platelet releasing megakaryocyte compartments (MK16, MK32, MK64, MK128, respectively); j is the period (in hours) that a given megakaryocyte already spent in the specific compartment; $\lceil \cdot \rceil$ denotes rounded to an integer; $q_{comp,j,i}$ is the quantity of the megakaryocytes of the specific compartment ($comp$), which spent a given period (j) in it; $m_{comp,j}$ is the receptor number on given megakaryocyte; $q_{PL,i}$ is the platelet number; m_{PL} is the receptor number per platelet.

It is assumed that the number of TPO receptors on each megakaryocyte ($m_{comp,j}$) equals the number of platelets that the megakaryocyte is capable of releasing (c_{comp}) times the average number of receptors per every potential platelet (b).

$$(4) \quad m_{comp,j} = (c_{comp} - r_{comp} \cdot j) \cdot b \quad c_{comp}, r_{comp}, j, b \geq 0$$

where c_{comp} is the number of platelets that the megakaryocyte of the specific compartment $comp$ can release during its entire life-span (c_{omp}); r_{comp} is the rate of platelet release by the megakaryocyte; j is the period that this megakaryocyte already spent in this compartment; b is the number of receptor on the megakaryocyte per potential platelet.

We assume that the non-specific TPO clearance (l_i) is exponential, i.e. every hour some fraction (f) of a current amount of TPO (C_i) is removed from circulation:

$$(5) \quad l_i = f \cdot C_i \quad f \geq 0$$

where f is the coefficient of non-specific TPO clearance and C_i is the current TPO concentration.

Exogenous TPO is included in the model as a linear relation of the initial maximum TPO blood concentration (x_i) to the administered intravenous (IV) dose (s) (the relation coefficient is 0.0167)²¹:

$$(6) \quad x_i = 0.0167 \cdot s_i \quad s_i \geq 0$$

The state when TPO completely disappears from the blood seems very unlikely based on biological logic, so we restricted the lower limit of possible TPO concentration to certain minimum (positive). Thus, the equation (1) is modified to receive the full TPO concentration equation:

$$(7) \quad C_{i+1} = \max((C_i + p + x_i - a \cdot n_i - f \cdot C_i), \varepsilon) \quad \varepsilon > 0$$

In steady state, the TPO concentration (C) is constant.

TPO effects on amplification rate. [return to [Contents](#)]

In our model, there are only two compartments, SC and CFU-Meg, whose cells are capable of dividing. These compartments differ significantly from each other, thus, we shall discuss them separately. Cells of other model compartments do not proliferate, and so their amplification rate () equals 1 under all circumstances.

SC compartment. [return to [Contents](#)]

Since TPO is primarily a thrombopoiesis-stimulating cytokine, we assume that the cells, which are not committed to thrombopoietic line yet (the SC compartment in our model), are relatively insensitive to TPO, compared to committed megakaryocytic cells. In our model this is considered as a threshold () in TPO concentration. Only above this threshold () TPO affects stem cells. As long as TPO remains below the threshold (), stem cells in the model are regulated by intrinsic TPO-independent mechanism that keeps the size of their population almost constant.

Thus, below the threshold () , SC amplification rate (α_{SC}) is determined hourly depending on the current number of cells in the SC compartment. It seems biologically reasonable that the dependence equation is a sigmoidal function where α_{SC} changes from 1 (i.e., no amplification, the cell number remains the same) when the cell number approaches infinity, up to the maximal value α_{SCw} when the cell number approaches zero. The increase in amplification rate (α_{SC}) is relatively gradual as long as the cell number (q_{SCi}) exceeds certain critical value (we assumed it to be a fraction (v) of the normal cell number (q_{SCnorm})). However, when the cell number falls below this threshold, α_{SC} begins to increase rapidly in order to restore the SC compartment as soon as possible. We assume that at normal cell numbers (q_{SCnorm}), α_{SCi} should be a fraction (y) of its maximal value α_{SCw} . Following is an example of such equation:

$$(8) \quad \alpha_{SC,i+1}^{*}(q_{SC,i}, C_i) = \begin{cases} \left(\alpha_{SCw} - 1 \right) \cdot \frac{1}{\left(\frac{1}{y} - 1 \right) \cdot \left(\frac{q_{SC,i}}{q_{SCnorm}} \right)^{S_1} + 1} + 1, & q_{SC,i} \geq v \cdot q_{SCnorm} \\ \alpha_{SCw} - \left(\alpha_{SCw} - \alpha_{SC}^{\sim} \right) \cdot \left(\frac{q_{SC,i}}{v \cdot q_{SCnorm}} \right)^{S_2}, & q_{SC,i} < v \cdot q_{SCnorm} \end{cases}$$

$$\alpha_{SC}^{\sim} = \left(\alpha_{SCw} - 1 \right) \cdot \frac{1}{\left(\frac{1}{y} - 1 \right) \cdot v^{S_1} + 1} + 1$$

$$\left. \begin{array}{l} q_{SC}, S_{1,2}, \theta \geq 0 \\ \alpha_{SCw} \geq 1 \\ 0 < y, v \leq 1 \end{array} \right\}$$

where $\alpha_{SC, i+1}^*$ is the amplification rate calculated based solely on the cell number; $\alpha_{SC, w}$ is the maximal possible rate of cell amplification in the SC compartment when TPO concentration (C_i) is below the threshold (θ); $q_{SC, i}$ is a quantity of cells in the SC compartment; $q_{SC, norm}$ is the normal quantity of cells there. S_1 and S_2 are the sensitivity coefficients in the regions of $q_{SC, i}$ higher or lower than the critical value ($vq_{SC, norm}$), respectively. These values determine the sensitivity of the mechanism that links the amplification rate (α_{SC}) with the cell number ($q_{SC, i}$). In other words, they determine the steepness of the dependence curve in the corresponding regions. High S_1 or S_2 mean that α_{SC} changes significantly due to slight changes of q_{SC} , and low S_1 or S_2 mean that α_{SC} remains relatively constant whatever the changes of q_{SC} are. Distinguishing between S_1 and S_2 allows us to force the amplification rate (α_{SC}) to grow rapidly as the cell number ($q_{SC, i}$) falls below the critical value, thereby increasing the resistance of the system to further cell number ($q_{SC, i}$) decay. Although the symbols S_1 and S_2 appear in several equations, their values are specific for every equation.

We suggest that TPO concentration (C) increase above the threshold (θ) should occur in severe platelet and/or megakaryocyte deficiency, or when TPO was administered exogenously. We assume that at these circumstances, TPO further increases the rate of cell amplification in the "Stem Cell" compartment (α_{SC}). We assume also that the increase is proportional to the difference between actual TPO concentration (C_i) and the threshold (θ). Thus, TPO effects appear gradually from the zero increase, when TPO concentration (C_i) equals the threshold (θ). Saturation of the mechanisms of TPO effect is reflected in the concavity of the effect function.

The following is an example of such a function:

$$(9) \quad \alpha_{SC, i+1}(q_{SC, i}, C_i) = \alpha_{SC, i+1}^*(q_{SC, i}, C_i) + t \cdot \ln(C_i - \theta + 1) \quad t, \theta \geq 0$$

$C_i > \theta$

where $\alpha_{SC, i+1}^*$ is the same expression as in equation (8), i.e. amplification calculated based on a TPO-independent mechanism, and the second operand is the TPO-related contribution to the amplification rate ($\alpha_{SC, i+1}$). t determines the steepness of the dependence curve (t is non-negative). Although the symbol t appears in several equations, its value is specific for every equation. We add one to the \ln argument in order to ensure positivity of the \ln result.

CFU-Meg compartment. [return to Contents]

In contrast to the cells of the SC compartment, we assume that cells of this compartment are fully sensitive to TPO and respond to the absolute TPO concentration (C_i), not to its difference with a threshold ($C_i - \theta$). In our model, they have no TPO-independent proliferative mechanism, and cease to proliferate when

deprived of TPO. On the other hand, when TPO concentration (C_i) in the system increases, CFU does not rise to infinity, but rather gradually reaches saturation, which also seems reasonable biologically. At normal TPO concentrations (C_{norm}), we assume CFU to be a fraction (h) of its maximal value (CFU_{max}). Thus an equation that describes the relation of the amplification rate of CFU-Meg cells (CFU) to TPO concentration (C_i) represents a sigmoidal function with CFU equaling 1 when TPO concentration (C_i) is zero, passing through h times CFU_{max} when TPO concentration is normal (C_i), and approaching an asymptote in CFU_{max} when TPO concentration (C_i) approaches infinity. In addition, in order to enable the system to be sensitive both to the regulation by endogenously produced TPO and to the effect of the exogenously administered drug, it was assumed that the function changes relatively rapidly in the region of normal TPO concentration (C_{norm}) and with a much smaller rate when a TPO concentration (C_i) is somewhat higher than normal (C_{norm}). The following is an example of such a function:

$$(10) \quad \alpha_{CFU, i+1}(C_i) = (\alpha_{CFU_{max}} - 1) \cdot \left(1 - \frac{1}{\frac{1}{\frac{1}{h} - 1} \cdot \left(\frac{C_i}{C_{norm}} \right)^t + 1} \right) + 1 \quad \begin{cases} C_{norm} > 0 \\ t \geq 0 \\ 0 < h \leq 1 \end{cases}$$

where CFU_{i+1} is an amplification rate of the CFU compartment; CFU_{max} is a maximal value of amplification rate there; C_{norm} is normal TPO concentration; t is the parameter that determines the steepness of the dependence curve.

TPO effects on transit time. [return to [Contents](#)]

For the reason noted earlier, we assume that all platelet-releasing megakaryocyte compartments have the same transit time (M_K). We assume that neither the relation of megakaryocyte volume (and thus, its platelet releasing capacity c_{comp}) nor of its rate of platelet release r_{comp} to megakaryocyte ploidy, is affected by TPO. Therefore, the transit time (M_K) through the noted compartments is constant. Platelets also spend in average a constant time in the circulation (PL), which is not affected by TPO concentration (C_i).

In contrast, the transit times of the SC, CFU-Meg, and MKB compartments (SC , CFU , MKB , respectively) are functions of the micro-environmental conditions. Since cells that are far from maturation are not expected biologically to undergo a sudden shift to maturation, it seems that these functions determine the value the transit time should approach, rather than the actual transit time. The actual transit time changes gradually: every hour it changes by $\frac{1}{2\pi\pi}$ hours towards the function-determined value. Thus, we will mean the value, that transit time approaches rather than the transit time itself when speaking about transit time () calculations below.

SC compartment. [return to [Contents](#)]

We assume that regarding transit time (s_c), the SC compartment differs from others in the same way as regarding amplification rate (s_c). It means that the cells of

this compartment respond to TPO only when its concentration (C_i) rises above a threshold (θ). This threshold (θ) is the same as for the amplification rate (λ_{SC}). Below the threshold (θ) SC transit time (τ_{SC}) is assumed to be regulated by a TPO-unrelated mechanism dependent on the current cell number ($q_{SC,i}$) only. The function of this dependence changes the transit time (τ_{SC}) from its minimal value ($\tau_{SC,u}$) when the cell numbers ($q_{SC,i}$) approach infinity, through the normal value that is greater than the minimal one by factor g , up to the highest value ($\tau_{SC,max}$) ~~is limited-determined~~ solely by biological reasons. This means that when the cell number in SC compartment ($q_{SC,i}$) is high, the cells will pass rapidly to the next compartment, thus reducing the SC one; and they will remain longer in the SC compartment when their number ($q_{SC,i}$) is low, thus repopulating it. This manner of regulation seems reasonable biologically.

We suggest that similar to the amplification rate (λ_{SC}), the transit time (τ_{SC}) in the range of very low cell numbers ($q_{SC,i}$) (lower than a certain fraction (ν) of the normal ($q_{SC,norm}$)), is very sensitive to further cell number decrease, and grows rapidly, thereby resisting compartment exhaustion. This fraction (ν) is the same as for the SC amplification rate.

Following is an example of such a function:

$$(11) \quad \tau_{SC,i+1}^*(q_{SC,i}, C_i) = \begin{cases} \tau_{SC,u} \cdot \left(1 + (g-1) \cdot \left(\frac{q_{SC,norm}}{q_{SC,i}} \right)^{S_1} \right) & , \quad q_{SC,i} \geq \nu \cdot q_{SC,norm} \\ \tau_{SC,max} - (\tau_{SC,max} - \tau_{SC}^*) \cdot \left(\frac{q_{SC,i}}{\nu \cdot q_{SC,norm}} \right)^{S_2} & , \quad q_{SC,i} < \nu \cdot q_{SC,norm} \end{cases}$$

$$\tau_{SC}^* = \tau_{SC,u} \cdot \left(1 + (g-1) \cdot \frac{1}{\nu^{S_1}} \right) \quad \begin{cases} S_{1,2} \geq 0 \\ \tau_{SC,u} > 0 \\ g \geq 1 \\ 0 < \nu \leq 1 \end{cases}$$

where $\tau_{SC,i+1}^*$ is the transit time calculated based on cell numbers ($q_{SC,i}$) only, i.e. when TPO concentration (C_i) remains below the threshold (θ); $\tau_{SC,u}$ is the minimal possible transit time through SC in these circumstances; ν is the fraction of normal cell number ($q_{SC,norm}$), below which the dependence of the transit time ($\tau_{SC,i+1}^*$) on the cell number ($q_{SC,i}$) changes; S_1 and S_2 are the sensitivity coefficients in the regions of $q_{SC,i}$ lower and higher than $\nu q_{SC,norm}$, respectively.

If TPO concentration (C_i) in the model rises above the threshold (θ), the transit time (τ_{SC}) is assumed to shorten in a dose dependent manner. As for the amplification rate (λ_{SC}), its decrease is presumed to be proportional to the difference between actual TPO concentration (C_i) and the threshold (θ). However, a shortening of the transit time (τ_{SC}) down to zero by TPO is biologically illogical, so we suggest that the transit time (τ_{SC}) approaches some minimal value as TPO concentration (C_i) increases. In our model this minimum represents a fraction (k) of the transit time calculated on the basis of cell numbers ($\tau_{SC,i+1}^*$) as described earlier (equation (11)).

Following is an example of such an equation:

(12)

$$\tau_{SC,i+1} \begin{matrix} (q_{SC,i}, C_i) \\ C_i > \theta \end{matrix} = \tau_{SC,i+1}^* (q_{SC,i}, C_i) \cdot k \cdot \left(\frac{1}{t \cdot \left(\frac{C_i - \theta}{C^* - \theta} \right)^t + \frac{k}{1-k}} + 1 \right) \quad 0 < k \leq 1 \quad t \geq 0$$

where $\tau_{SC,i+1}$ is the transit time when TPO concentration (C_i) is higher than the threshold (θ); $\tau_{SC,i+1}^*$ is the transit time calculated on the basis of cell numbers as described in equation (11); k is the fraction of $\tau_{SC,i+1}^*$ that gives the minimum, which the transit time approaches as TPO concentration (C_i) increases; C^* determines the point of TPO concentration (C_i), around which the transit time (τ_{SC}) is the most sensitive to concentration (C) change; t determines the steepness of the dependence curve (t is non-negative). Multiplication by t enables to regulate the sensitivity to C_i with $t < 1$ in the same manner as when $t > 1$.

CFU-Meg and MKB compartments. [return to [Contents](#)]

We assume that the transit time parameters of these two compartments (CFU , MKB , respectively) are dependent solely on TPO and respond to the absolute TPO concentration (C_i), rather than to its difference with a threshold ($C_i - \theta$). As TPO level (C_i) drops, the cell passage through these compartments slows, i.e. transit time (τ_{comp}) increases up to the values limited solely by biological reasons ($\tau_{comp,max}$) (we suggest that the cells cannot stay in these compartments for an infinite period of time). On the other hand, when the TPO concentration (C_i) in the system increases, τ_{comp} does not shorten to zero, but rather asymptotically reaches $\tau_{comp,min}$, thus bounding the function from below. This also seems biologically reasonable, as the cells cannot move through the compartment in one instant. At normal TPO concentrations (C_{norm}), we set τ_{comp} to equal its normal value ($\tau_{comp,norm}$). In addition, in order to enable the system to be sensitive both to the regulation by endogenously produced TPO and to the effect of the exogenously administered drug, it was assumed that the function changes relatively rapidly in the region of TPO concentrations (C_i) lower than normal (C_{norm}) and with a smaller rate when a TPO concentration (C_i) is higher than normal (C_{norm}). The following is an example of such a function:

(13)

$$\tau_{comp,i+1} = \begin{cases} \tau_{comp,max} - (\tau_{comp,max} - \tau_{comp,norm}) \cdot \left(\frac{C_i}{C_{norm}} \right)^{t_1}, & C_i \leq C_{norm} \\ (\tau_{comp,norm} - \tau_{comp,min}) \cdot \frac{2}{\left(\frac{C_i}{C_{norm}} \right)^{t_2} + 1} + \tau_{comp,min}, & C_i > C_{norm} \end{cases}$$

$$\begin{cases} 0 < \tau_{comp,min} \leq \tau_{comp,norm} \leq \tau_{comp,max} \\ t_{1,2} \geq 0 \end{cases}$$

where *comp* is one of the aforementioned compartments (CFU-Meg or MKB); $\tau_{comp,i+1}$ represents the transit times through these compartments; $\tau_{comp,min}$, $\tau_{comp,norm}$, and $\tau_{comp,max}$ are the minimal, normal and maximal transit times when TPO concentration is normal; t_1 and t_2 determine the steepness of the dependence curve in the regions of C_i lower and higher than C_{norm} , respectively.

TPO effects on the fraction of cells that flow from one compartment to the next. [return to [Contents](#)]

The discussed parameter is the proportion of “mature” cells that passes to the next compartment at any given moment (φ). We designate as “mature” the cells that are potentially ready to pass to the next compartment but do not necessarily pass. As was noted earlier, we assume that the fraction of the SC compartment that commits to the megakaryocytic lineage (s_c) is constant and TPO-independent. From the two subsequent compartments, CFU-Meg and MKB, every mature cell is supposed to emerge to the next compartment in any case. Thus, TPO in our model does not affect in the first three compartments.

In contrast, the fraction of MK16-, MK32-, and MK64- megakaryocytes that continues with additional endomitoses and flows to the next compartment (φ_{comp}) is assumed to be in the range of 0 to 1 depending on TPO concentration (C_i). Because there is no compartment with ploidy greater than 128N, the megakaryocytes of the MK128 compartment do not flow to any other compartment.

The dependence of MK16, MK32, and MK64 parameters on TPO concentration assumed to be delayed with τ calculated based on TPO concentration that was before the period needed for one additional endomitosis ($C_{i-\mu}$). The reason for this is the assumption that the cells that enter a given megakaryocyte compartment first “decide” what they do, i.e. undergo another endomitosis and not participate in platelet release in this compartment, or alternatively, begin with platelet release and remain in this compartment until complete exhaustion. Thus, the cells that leave a compartment now were preprogrammed before they start an additional endomitosis.

In the model the dependence is expressed by a sigmoidal function with s set to 0 when TPO concentration (C_i) is 0, equaling the normal value (τ_{norm}) when TPO concentration is normal (C_{norm}), and approaching 1 asymptotically.

$$(14) \quad \varphi_{comp,i+1}(C_{i-\mu}) = 1 - \frac{C_{norm}^t \cdot \left(\frac{1}{\varphi_{comp,norm}} - 1 \right)}{C_{i-\mu}^t + C_{norm}^t \cdot \left(\frac{1}{\varphi_{comp,norm}} - 1 \right)} \quad 0 \leq \varphi_{comp,norm} \leq 1 \quad t, \mu \geq 0$$

where *comp* is one of the discussed compartments (MK16, MK32, or MK64); $\tau_{comp,i+1}$ is a parameter of these compartments; τ is the time needed for one additional endomitosis; $\tau_{comp,norm}$ is the value of τ_{comp} under normal TPO concentration (C_{norm}); t determines the steepness of the dependence function (t is non-negative).

The time needed for an additional endomitosis (τ) is assumed to be the same in the three relevant compartments (MK16, MK32, and MK64).

PROGRAM STRUCTURE [return to [Contents](#)]

Our model was built while trying to imitate real bone marrow physiology. Each compartment is subdivided into small sections that contain the cells of a specific age with a resolution of one hour. For example, the fifth age-section of the MKB compartment contains the cells which spent 5 hours in this compartment. Every hour, all the cells in the virtual bone marrow pass to the next age-section in the same compartment.

When the cells spend all the transit time predetermined for them in a given compartment, they pass to the beginning of the next compartment, i.e., every hour the cells that have just left each compartment fill the first age-section of the next one. The cells that leave the MK128 compartment disappear. The first age-section of the SC compartment is given a constant fraction of the number of cells exiting the compartment. The platelet releasing cells contribute platelets to the first age section of the PL compartment every hour.

The described structure is implemented as an array of 8 rows and 360 columns (Fig. 2). The 8 rows relate to 8 cell compartments, and the columns to the age sections, as we assumed that none of the transit time could exceed 360 hours. This array which will later be referred to as age-distribution, is refilled hourly according to the rules described above. The smoothened graphic representation of this array is shown in Fig. 3. Although the age-distribution array is useful in model investigation, this is not what physicians and biologists are interesting in. Rather the time course of the sizes of different compartments is required. Hence, in our simulation we file the hourly states of all the compartments and TPO concentration at all times. For this purpose, another array, which will later be referred to as time course is established in the model (Fig. 4). The rows in the array are cell compartments and the columns are the time steps of the simulation course. Every time-step of the simulation (one hour of "patient's life"), the number of cells in all age-sections is summarized for each compartment and the next column in the time-course array is filled. Thus, every cell in this array represents the total number of cells in a given compartment at a given time point.

There is an additional row in the time-course array that relates to the TPO concentration in the blood. TPO concentration is written down every time-step concurrently with the cell numbers. Example of it is shown in Fig. 5.

Parameter determination [return to [Contents](#)]

Our model is very flexible allowing the user to fit it to patients with diverse blood and bone marrow parameters. Real patients differ in their baseline platelet counts (q_{PLnorm})³¹ and numbers of bone marrow precursors ($q_{comp,norm}$), in the sensitivity of their stem cell "intrinsic" regulation mechanism (S -s), in their minimum and normal transit times ($S_{C,u,comp,norm}$) and maximal amplification rates ($S_{C,w,comp,max}$), rates of platelet release by megakaryocytes (r_{comp}), fractions that each megakaryocyte ploidy class contribute for additional endocytosis ($c_{omp,norm}$), and the time needed for endomitosis (τ). Furthermore, the baseline TPO level (C_{norm}), the rate of TPO production (p), receptor- and non-receptor-mediated TPO clearance (a and f),

the threshold of TPO effect on the SC compartment (θ), and the sensitivity of different cell parameters to TPO also differ between patients (t -s).³⁴

Since the aim of this work is to achieve the best fit of the model to each patient, the patient-related parameters should be determined individually for each patient. However, practically, it would be very difficult to predetermine many of these parameters for every patient. We calculated certain average parameters (Table 1), based, generally, on published data (see references in the Table). These averaged parameters are used as a framework, into which known individual characteristics are included. Thus, before the simulation of the specific patient is begun, the user should correct the parameters of the model as far as he knows the relevant information about the patient.

Usually, the known patient-related data are not parameters in the form defined by our model, but rather some kind of measurements obtained in the clinic (e.g., day and value of post-chemotherapy thrombocytopenia nadir, day and value of platelet peak after TPO administration, or even the change in the megakaryocyte modal ploidy following some perturbation). [REFERENCE] In this case, we analyze the available data to convert it into the model-compatible format.

Sometimes, the only available patient-related data is the graphic representation of patient's platelet course following some perturbation (e.g., cell-suppressive therapy or TPO administration). [REFERENCE] The data may also be a picture of the platelet course without any external perturbation (e.g., cyclic thrombocytopenia). [REFERENCE] In these cases we change the model parameters by trial-and-error until a good compliance of the model graphic output with the given patient's graphs is achieved. However, some kind of analysis is possible even in these cases, and the choice of the parameter sets for trying is not absolutely random.

Results [\[return to Contents\]](#)

We implemented the described model as a computer simulation that retrieves the changes that occur in the human thrombopoietic system (platelet counts, bone marrow precursor numbers, and TPO concentrations) over several years. The resolution of the simulation output is one hour. Time units and periods that we will speak of relate to the simulated patient's life, not to the running time of the program. The programming tools give the user the following features:

- 1) As was noted in the previous section, the user can set the baseline values and all other thrombopoietic parameters as far as he knows them about the patient before running the simulation.
- 2) The user (e.g., physician, scientist) can determine how long the simulation will run, from 12 hours up to several years.
- 3) The user can determine how frequently he wants the program to show him the course of a patient counts up to the moment. The frequency can change from every 12 hours to once during the overall period of the simulation.
- 4) The user can determine what resolution he would like to see the output graph, one hour or above.

- 5) The user can determine if he wants to see the graphical representation of the age distribution through the compartments at any moment of the simulation.
- 6) The user can simulate a cell-suppressive therapy at any moment while running the simulation by reducing one or several of the compartments by any value.
- 7) The user can simulate exogenous TPO administration at any moment while running the simulation by controlling:
 - dose height
 - number of dosings
 - frequency of dosings

The simulation tool has been carefully tested with respect to the published experimental results, and has proved to be well calibrated for averaged human thrombopoiesis. The technique for relatively fast modifications in order to fit a specific patient has been also developed. Fig. 6A and 7A show examples of the tool's output. Here we retrieve the *in vivo* platelet counts following TPO administration (Fig. 6A) and chemotherapy without TPO (Fig. 7A).

Discussion [\[return to Contents\]](#)

We built a model that simulates cell and platelet counts in the steady state, as well as after perturbations to the hematopoietic system, e.g., cell-suppressive therapy, recombinant thrombopoietin administration, etc. It is possible to simulate any protocol of drug administration and any hematological state of a patient, regarding his/her platelet count and number of bone marrow megakaryocytes and their precursors. The model is very flexible and can be adapted to many categories of patients, or healthy platelet donors. It can also be modified to fit species other than human. By providing specific parameters one can adjust the model so as to yield particular predictions about the thrombopoietic profile of an individual patient. We believe that platelet disorders, such as cyclic thrombocytopenia, can also be simulated in our model.

This model makes it possible to check any given treatment protocol and to choose the best one according to the user's criteria. As such, it strongly reduces the number of necessary clinical trials and lowers the risk of treating a patient with ineffective TPO protocol.

In the near future, we will operate an optimization program on our model. For any individual this modified program will select the best protocol out of an entire spectrum of possibilities. The criteria by which the optimization module determines an optimal treatment protocol may be one or several of the following (this list is just an approximation):

1. The smallest number of TPO dosings required for achieving any given aim.
2. The lowest maximal TPO dose required for achieving any given aim.

3. The minimal total amount of TPO needed for rehabilitation.
4. The smallest deviation from the baseline at platelet nadir after chemotherapy or another cell-suppressive treatment.
5. The shortest period of thrombocytopenia.

Fig. 6 and 7 show examples of the tool's output. Here we retrieve the experimentally obtained *in vivo* platelet counts following TPO administration (Fig. 6A) and chemotherapy without TPO (Fig. 7A). Most notably, we show that by use of our tool, it is possible (at least theoretically) to construct a TPO protocol that would reduce by 75% the amount of TPO currently used for chemotherapy patients, while maintaining the same thrombocyte rehabilitation pattern.

References [\[return to Contents\]](#)

1. Harker LA, Hunt P, Marzec UM, Kelly AB, Tomer A, Hanson SR, Stead RB: Regulation of platelet production and function by megakaryocyte growth and development factor in nonhuman primates. *Blood*. Mar 1996; Vol. 87(5); pp. 1833-1844.
2. Alexander WS: Thrombopoietin. *Growth Factors*. 1999; 17(1); pp. 13-24.
3. Kaushansky K: Thrombopoietin: the primary regulator of platelet production. *Blood*. Jul 1995; Vol. 86(2); pp. 419-431.
4. Vadhan_Raj-Raj S: Recombinant human thrombopoietin: clinical experience and *in vivo* biology. *Seminars Hem*. Jul 1998; Vol. 35(3); pp. 261-268.
5. Harker LA: Physiology and clinical applications of platelet growth factors. *Current Opinion Hematol*. 1999; Vol. 6; pp. 127-134.
6. Levin J: Thrombopoietin – Clinically realized? *New Eng J Med*. Feb 1997; Vol. 336(6); pp. 434-436.
7. Somlo G, Sniecinski I, ter Veer A, Longmate J, Knutson G, Vuk-Pavlovic S, Bhatia R, Chow W, Leong L, Morgan R, Margolin K, Raschko J, Shibata S, Tetef M, Yen Y, Forman S, Jones D, Ashby M, Fyfe G, Hellmann S, Doroshow JH: Recombinant Human thrombopoietin in combination with granulocyte colony-stimulating factor enhances mobilization of peripheral blood progenitor cells, increases peripheral blood platelet concentration, and accelerates hematopoietic recovery following high-dose chemotherapy. *Blood*. May 1999; Vol. 93(9); pp. 2798-2806.
8. Neelis KJ, Hartong SC, Egeland T, Thomas GR, Eaton DL, Wagemaker G: The efficacy of single-dose administration of thrombopoietin with coadministration of either granulocyte/macrophage or granulocyte colony-stimulating factor in myelosuppressed rhesus monkeys. *Blood*. Oct 1997; Vol. 90(7); pp. 2565-2573.
9. Murray LJ, Luens KM, Estrada MF, Bruno E, Hoffman R, Cohen RL, Ashby MA, Vadhan-Raj S: Thrombopoietin mobilizes CD34⁺ cell subsets into peripheral blood and expand multilineage progenitors in bone marrow of cancer patients with normal hematopoiesis. *Exp Hem*. 1998; Vol. 26; pp. 207-216.
10. Basser RL, Rasko JE, Clarke K, Cebon J, Green MD, Grigg AP, Zalcberg J, Cohen B, O'Byrne J, Menchaca DM, Fox RM, Begley CG: Randomized, blinded, placebo-controlled phase I trial of pegylated recombinant human megakaryocyte growth and development factor with filgrastim after dose-intensive chemotherapy in patients with advanced cancer. *Blood*. May 1997; Vol. 89(9); pp. 3118-3128.
11. Gordon AS : Regulation of hematopoiesis. N.-Y. 1970 Vol. 2, Section IX (textbook).
12. Harker LA, Finch CA: Thrombokinetis in man. *J Clin Invest*. 1969; Vol.48; pp. 963-974.

13. Harker LA: Thrombokinetics in idiopathic thrombocytopenic purpura. *Br J Haematol.* 1970; Vol. 19; pp. 95-104.
14. Sungaran R, Markovic B, Chong BH: Localization and regulation of thrombopoietin mRNA expression in human kidney, liver, bone marrow, and spleen using in situ hybridization. *Blood.* Jan 1997; Vol. 89(1); pp. 101-107.
15. Nagata Y, Shozaki Y, Nagahisa H, Nagasawa T, Abe T, Todokoro K: Serum thrombopoietin level is not regulated by transcription but by the total counts of both megakaryocytes and platelets during thrombocytopenia and thrombocytosis. *Thromb Haemost.* 1997; Vol. 77; pp. 808 - 814.
16. Nagahisa H, Nagata Y, Ohnuki T, Osada M, Nagasawa T, Abe T, Todokoro K: Bone marrow stromal cells produce thrombopoietin and stimulate megakaryocyte growth and maturation but suppress proplatelet formation. *Blood.* Feb 1996; Vol. 87(4); pp. 1309-1316.
17. Hsu HC, Tsai WH, Jiang ML, Ho CH, Hsu ML, Ho CK, Wang SY: Circulating levels of thrombopoietic and inflammatory cytokines in patients with clonal and reactive thrombocytosis. *J Lab Clin Med.* 1999; Vol. 134(4); pp. 392-397.
18. Stoffel R, Wiestner A, Skoda RC: Thrombopoietin in thrombocytopenic mice: evidence against regulation at the mRNA level and for a direct regulation role of platelets. *Blood.* Jan 1996; Vol. 87(2); pp. 567-573.
19. Alexander WS: Thrombopoietin and the c-Mpl receptor: insights from gene targeting. *Int J Biochem Cell Biol.* 1999 Oct; Vol. 31(10); pp. 1027-1035. [ABSTRACT]
20. Miyazaki M, Fujiwara Y, Isobe T, Yamakido M, Kato T, Miyazaki H: The relationship between carboplatin AUC and serum thrombopoietin kinetics in patients with lung cancer. *Anticancer Research.* 1999; Vol. 19; pp. 667-670.
21. Vadhan-Raj S, Murray LJ, Bueso-Ramos C, Patel S, Reddy SP, Hoots WK, Johnston T, Papadopolous NE, Hittelman WN, Johnston DA, Yang TA, Paton VE, Cohen RL, Hellmann SD, Benjamin RS, Broxmeyer HE: Stimulation of megakaryocyte and platelet production by a single dose of recombinant human thrombopoietin in patients with cancer. *Ann Intern Med.* May 1997; Vol. 126(9); pp. 673-681.
22. Wichmann HE, Gerhardt MD, Spechtmeyer H, Gross R: A mathematical model of thrombopoiesis in rats. *Cell Tissue Kinet.* 1979; Vol. 12; pp. 551-567.
23. Harker LA, Roskos LK, Marzec UM, Carter RA, Cherry JK, Sundell B, Cheung EN, Terry D, Sheridan W: Effects of megakaryocyte growth and development factor on platelet production, platelet life span, and platelet function in healthy human volunteers. *Blood.* 2000 Apr; Vol. 95(8); pp. 2514-2522.
24. Mayani H, Dragowska W, Lansdorp PM: Lineage commitment in human hemopoiesis involves asymmetric cell division of multipotent progenitors and does not appear to be influenced by cytokines. *J Cellular Physiol.* 1993; Vol. 157; pp. 579-580.
25. Golde DW: The Stem Cell. *Medicine.* Dec 1991.
26. Morrison SJ, Uchida N, Weissman IL: The biology of hematopoietic stem cells. *Annu Rev Cell Dev Biol.* 1995; Vol. 11; pp. 35-71.
27. Eller J, Gyori I *et al*: Modelling thrombopoiesis regulation – I: model description and simulation results. *Comput Math Applic.* 1987; Vol. 14 (9-12); pp. 841-848.
28. von Schulthess GK, Gessner U : Oscillating platelet counts in healthy individuals: experimental investigation and quantitative evaluation of thrombopoietic feedback control. *Scand J Haematol.* 1986; Vol. 36; pp. 473-479.
29. Harker LA, Marzec UM, Hunt P, Kelly AB, Tomer A, Cheung E, Hanson SR, Stead RB: Dose-response effects of pegylated human megakaryocyte growth and development factor of platelet production and function in nonhuman primates. *Blood.* Jul 1996; Vol. 88(2); pp. 511-521.
30. Fielder PJ, Gurney AL, Stefanich E, Marian M, Moore MW, Carver-Moore K, de Sauvage FJ: Regulation of thrombopoietin levels by c-mpl-mediated binding to platelets. *Blood.* Mar 1996; Vol. 87(6); pp. 2154-2161.

31. Swinburne JL, Mackey MC: Cyclical thrombocytopenia: characterization by spectral analysis and a review. *J Theor Medicine*. 2000; Vol. 2; pp. 81-91.
32. Rasko JEJ, Begley CG: Molecules in focus: The thrombopoietic factor, Mpl-ligand. *Int J Bioch Cell Biol*. 1998; Vol. 30: 657-660.
33. De Sauvage FJ, Carver-Moore K, Luoh S-M, Ryan A, Dowd M, Eaton DL, Moore MW: Physiological regulation of early and late stages of megakaryocytopoiesis by thrombopoietin. *J Esp Med*. 1996 Feb; Vol. 183: 651-656.
34. Tacke F, Schoffski P, Trautwein C, Martin MU, Stangel W, Seifried E, Manns MP, Ganser A, Petersen D: Endogenous serum levels of thrombopoietic cytokines in healthy whole-blood and platelet donors: implication for plateletpheresis. *Br J Haematol*. 1999; Vol. 105: 511-513.
35. Beutler E, Lichtman MA, Coller BS, Kipps TJ: Williams HEMATOLOGY. 5th edition McGraw-Hill, Inc. 1995; Chapter 118; pp. 1149-1161.
36. Schofield R, Lord BI *et al*: Self-maintenance capacity of CFU-S. *J Cellular Physiol*. 1980; Vol. 103: 355-362.
37. Rosendaal M, Hodgson GS, Bradley TR: Organization of haemopoietic stem cells: the generation-age hypothesis. *Cell Tissue Kinetics*. 1979; Vol. 12: 17-29.

APPENDIX B:

A Model of the Neutrophil Bone Marrow and Peripheral Blood Compartment under the Effects of Growth-Factors and its Use as a Tool for Optimizing Treatment with Granulocyte Colony Stimulating Factor (G-CSF)

Abstract

We present a mathematical model of the neutrophil compartment of the hemopoietic system. Our aim is to use this model as a basis for optimizing treatment with Granulocyte Colony Stimulating Factor (G-CSF) for patients undergoing myelosuppressive treatment. Therefore, we formulated the model as a piecewise linear system of equations, and implemented it in AMPL (A Mathematical Programming Language), thus guaranteeing the ability to use linear programming techniques in the treatment optimization effort.

Underlying our model are two main sources of information and validation: Firstly, the mechanism implemented in the model is in accordance with suggestions and experimental evidence available in the literature regarding the kinetics of the lineage. However, these suggestions are often broad-brush strokes allowing a considerable degree of freedom especially in view of conflicting evidence. Therefore, we used as a second source of information the data available in the literature regarding the effects of G-CSF on blood neutrophil levels, and insisted that our predictions be in close accordance with these data. This ensures that our model is in close accordance with both the qualitative and the quantitative aspects of the experimental data. Both aspects are essential for correctly predicting optimal treatment protocols.

Introduction

The neutrophil lineage originates in pluripotent stem cells that proliferate and become committed to the neutrophil lineage. These cells then undergo gradual maturation accompanied with proliferation through the three morphologically distinguishable mitotic compartments: Myeloblasts, promyelocytes and myelocytes. The myelocytes then mature and lose their capacity to proliferate, and thus enter the post mitotic compartment. In the post-mitotic compartment the cells continue their gradual maturation, which is not accompanied with proliferation through the three morphologically distinguishable sub-compartments: Metamyelocyte, band and segmented-neutrophils. Cells exit the various sub-compartments in the post-mitotic compartment and enter the blood as neutrophils. They then migrate from the blood to the tissues.

The Granulocyte-Colony Stimulating Factor (G-CSF) effects an increase in blood neutrophil levels primarily by increasing production in the mitotic compartment and shortening the transit time of the post-mitotic compartment. REVIEW G-CSF USAGE...

Thus, the first compartment of the mitotic pool (myeloblast) receives an inflow of cells from stem-cell precursors. The inflow of the other compartments receives the outflow from the previous one, subject to multiplication factors due to cell replication in the mitotic stages. For a review of granulopoiesis and experimental methods see Mary – 1984.

Models regarding granulopoiesis in normal humans and in humans with pathologies of the bone marrow were suggested previously in order to give a coherent description of the kinetics of granulocytes from experimental data (Cartwright – 1964, Mary – 1978, Rubinow – 1974). In recent years Schmitz et al. developed a kinetic simulation model for the effects of G-CSF on granulopoiesis (Schmitz – 1993), and used it for the analysis of administration of G-CSF to patients suffering from cyclic neutropenia (Schmitz – 1995). However, the data Schmitz rests upon for his model has been more accurately assessed in recent years by Price et al. (1998) and Chatta et al. (1996). Actual empirical data regarding compartment sizes and their transit times was not incorporated into their model despite the importance of these data (Dancey et al. 1976).

In this work we propose a mathematical pipeline model of the neutrophil lineage with and without the effects of G-CSF which rests on the latest experimental data available. Our work is **the first of its kind**, as far as we know, to have formulated the mathematical model in a way that would facilitate the process of finding optimal protocols for neutropenia induced by chemotherapy. We then formulate an objective function for reconstitution of a patient's bone marrow, and implement the optimization model as a linear programming problem. This will allow us to use it as a tool for predicting the optimal protocol for G-CSF administration to patients undergoing myelosuppressive chemotherapy.

In this article we shall present the mathematical model and its predictive power and discuss its possible applications for determining G-CSF treatment protocols for patients undergoing myelosuppressive treatment.

Tools and Methods

Since our long-term aim is to provide a tool for calculating optimized treatment schedules, we formulated the model with piecewise linear equations and implemented it in AMPL Plus software. AMPL is a comprehensive algebraic modeling language for problems in linear, nonlinear and integer programming. We used the AMPL language processor, which supports all the commands and syntax of AMPL.

The Mathematical Model

1. G-CSF

The effects of G-CSF on the neutrophil lineage are relayed in the model in three stages. The first is the administered amount of cytokine given at time t , which is marked: G_{adm}^t *administered*

The G_{adm} vector serves as the control variable of the subsequently described optimization programme, as the main objective of this work is the optimization of G-CSF administration. *kinetic behaviour*

The second stage represents the pharmacokinetic behaviour of G-CSF in circulation. It incorporates for instance the half-life of G-CSF, and could in the future be modified to express more of the effects of time on G-CSF activity. This level is marked G_{blood}^t

G-CSF is eliminated from the blood in a Poissonic manner (Stute, 1992):

$$G_{blood}^{t+1} = G_{blood}^t \left(1 - \frac{\ln 2}{\tilde{t}_{1/2}}\right) + G_{adm}^{t+1} \quad (\text{Eq.1.1})$$

Where $\tilde{t}_{1/2}$ is the half-life of G-CSF in the blood, and $G_{blood}^1 = G_{adm}^1$

We note, that recently data regarding the dependence of the half-life of G-CSF on the neutrophil counts has emerged (Terashi et al. 1999). In the absence of exact kinetics of G-CSF effects on the neutrophil lineage, we consider the half life to be constant, though this could easily be modified should more exact information emerge.

Note, that we set as zero the effects and level of the endogenously produced G-CSF, and that only exogenously produced G-CSF is considered to effect the kinetic parameters. If more empirical data regarding the production of endogenous G-CSF is made available, we could obviously incorporate it in this equation.

The third and final stage models the pharmacodynamic effects of G-CSF on the kinetic *dynamic* parameters. As will be elaborated subsequently the dependence of the various kinetic parameters of the neutrophil lineage on the level of G-CSF in the blood is assumed to be through either non-decreasing concave or non-increasing convex functions. This reproduces the effects of ~~s~~aturation that are seen in clinical studies on the effects of G-CSF (Duhrsen 1988), i.e. addition of G-CSF carries a lesser effect when its level in circulation is already high.

Mitotic Compartment

The mitotic compartment is divided into subcompartments. The k th subcompartment contains all cells of chronological age between $k-1$ and k hours, relative to the time of entry into the mitotic compartment. The number of cells in subcompartment k at time t is marked as m_k^t .

$$k \in \{1..\tau\}$$

$$m_1^t = \ell_1^t(G_{blood}^t) \quad (\text{Eq.1.2})$$

where τ is the transit time of the entire mitotic compartment. τ is assumed to be the same and constant for all cells entering the mitotic compartment.

Where l_1 is a vector reflecting the flow of newly committed cells into the mitotic compartment. The biological grounds for this definition is the existence of a myeloid stem cell reservoir, which is known to supply new committed cells to the mitotic compartment. However, the reservoir's actual kinetics are not very well explored empirically. We therefore fix l_1 to levels such that the overall size of the mitotic compartment as well as the kinetics of the neutrophils in circulation would match those obtained empirically.

Obviously, any new biological data could help define these kinetics more accurately within the framework of this model. We note that our results indicate that the assumption of a constant rate of stem cells flowing into the mitotic compartment in the absence of G-CSF is plausible.

For every $n \in \{1..\delta\}$, and for every t , amplification occurs at the exit from m_n^t :

$$m_{n+1}^{t+1} = m_n^t \cdot \alpha_n(G_{blood}^t) \quad (\text{Eq.1.3})$$

where:

α_n is a non-decreasing concave function of G-CSF levels in the blood, which determines the factor of amplification in the hourly subcompartment n . If for instance no amplification occurs at subcompartment n_0 at time then

$$\alpha_{n_0} = 1$$

$$\forall n, G_{blood}^t \quad 1 \leq \alpha_n(G_{blood}^t) \leq 2$$

The size of the morphological sub-compartments in the mitotic compartment at time t is determined as:

$$\sum_{n=n_0}^{n_1} m_n^t \quad (\text{Eq.1.4})$$

Where n_0 is the first hourly sub-compartment of a morphological sub-compartment and n_1 is its last hourly sub-compartment. Note, that the division into the morphological sub-

compartments will be used only for fine-tuning of the kinetic parameters with the use of experimental data.

The post mitotic compartment at time t is a single quantity of cells p^t , such that:

$$p^{t+1} = l_3(G_{blood}^t) \cdot p^t + m_\tau^t \quad (\text{Eq.1.5})$$

l_3 is a convex, non-increasing function of G-CSF levels in the blood, which takes values in the range of [0-1]. This definition entails $p^t > 0$.

We shall mark as o^t the outflow from the post mitotic compartment:

$$o^t = m_\tau^t + p^t - p^{t+1} \quad (\text{Eq.1.6})$$

The number of neutrophils in the circulating blood compartment at time t is marked n^t and is modeled as a single quantity of cells, such that:

$$n^{t+1} = o^t + n^t \left(1 - \frac{\ln 2}{t_{1/2}}\right) \quad (\text{Eq.1.7})$$

where $t_{1/2}$ is the half-life of neutrophils in the blood, as defined in the biological literature. $t_{1/2}$ is assumed to be held constant regardless of G-CSF levels (Lord 1989), though this could be easily modified. The kinetics of neutrophils in the tissues are not modeled in this work.

This model will be incorporated into an optimization scheme that will have as its objective function both the aims of minimizing G-CSF administration and returning the neutrophil lineage to its normal levels.

At $G_{blood}^t = 0$, $p^t = \Pi$, m_τ^t at the normal healthy level we have the following obvious relationship:

$$\frac{\Pi}{T} = m_\tau^t = o^t = \frac{n^t}{t_{1/2}} \times \ln 2 \quad (\text{Eq.1.8})$$

Which reflects the stability of the steady state.

2. Linear Programming Implementation

The above outlined model may be implemented in any number of optimization methods [1]. We chose to use linear programming because of its inherent advantages compared with other techniques, i.e. its ability to provide an optimal solution using at-least partially analytical methods, and therefore being more computationally tractable (Gill 1991). On the other hand, implementation of this model in linear programming carries with it the disadvantage that certain computations must be approximated linearly since they cannot be performed directly using linear methods. We shall therefore have to judge the 'closeness' of the solution obtained through linear programming with that obtained through another method of optimization that is not constrained with linear formulation.

The significant points in the model that have to be modified due to the linear programming implementation are wherever multiplication of two variables is defined, since this operator is not itself linear. We therefore define multiplication as an approximated value constrained within piecewise linear constraints that most closely bound the product within a four-faced polyhedron in 3-dimensional space whose vertices are

$$\{(x_{\min}, y_{\min}, x_{\min} \cdot y_{\min}), (x_{\min}, y_{\max}, x_{\min} \cdot y_{\max}), (x_{\max}, y_{\min}, x_{\max} \cdot y_{\min}), (x_{\max}, y_{\max}, x_{\max} \cdot y_{\max})\}$$

Where x_{\min} , x_{\max} , y_{\min} , y_{\max} are the constant biologically defined minima and maxima of x and y .

$$M(x, y) \begin{cases} \geq y_{\min} x + x_{\min} y - x_{\min} y_{\min} \\ \geq y_{\max} x + x_{\max} y - x_{\max} y_{\max} \\ \leq y_{\min} x + x_{\max} y - x_{\max} y_{\min} \\ \leq y_{\max} x + x_{\min} y - x_{\min} y_{\max} \end{cases} \quad (\text{Eq. 2.1})$$

Note, that multiplication may also be approximated with variations on the linear least squares method, by finding one plane that's closest to the four vertices defined (this should be tested).

The other functions that need to be defined linearly are those concerning the pharmacodynamics of G-CSF. Due to the nature of these functions (either non-increasing convex or non-decreasing concave), we implement these effects as piece-wise linear functions whose breakpoints are the doses for-which actual experimental data is available (Chatta 1994). Note, that the effects of G-CSF on each of the kinetic parameters were not determined in a detailed manner by experimentalists as far as we know. Rather its effects over a few dose levels on the neutrophil blood counts and the size of the morphologically different mitotic compartments and the post mitotic compartment was determined. From these we reconstructed the effects of G-CSF on the actual kinetic parameters (probability of mitosis, transit time and inflow of cells into the myeloblast compartment from stem cell progenitors)

at the dose levels available in the literature, and then connected these points linearly to obtain piecewise linear functions relating G-CSF levels to their effect on those parameters. Obviously, more experimental data could be used to produce more accurate functions.

We define a number of points in the mitotic compartment (see main text) as being potential amplification points. At these points we use the linearly approximated multiplication operator (Eq 2.1) instead of the actual product defined in Eq. 1.3.

At points where no amplification occurs the quantity from one compartment is simply transferred to the next:

$$m_{n+1}^{t+1} = m_n^t$$

m_n^0 is set according to the steady state values of the mitotic compartment or is depleted according to the kill function of the chemotherapy.

The flow out of the post mitotic compartment (Eq. 1.6) is similarly defined as a linear approximation of a product.

3. Formulation of the Model as an Optimization Problem for Linear Programming

The simulation spans a finite number of discrete time steps denoted by T .

We define as control variable the vector that represents G-CSF administration at every given hour t : $G_{adm}^t, t \in \{1..T\}$

The objective function is defined as maximization of the following expression:

$$\sum_{t=1}^T (\beta^t \cdot p^t - G_{adm}^t) \quad (\text{Eq. 3.1})$$

where p^t is the number of cells in the post mitotic compartment at time t , and \cdot is a scalar weighting coefficient. The logic for formulating the objective function this way is that the ability to maintain the post mitotic compartment's steady state size for a prolonged period of time is sufficient for rehabilitation of the neutrophil lineage as a whole. Also, our goal is to minimize the total administered quantity of G-CSF. \cdot is introduced to allow us to factor in both these goals in one objective. Also, this would allow a different weight to be given for certain times, e.g. were it determined (by clinicians) that the later states of the post-mitotic compartment should be weighted more than the first ones. Obviously this is only one of the possible formulations of the objective function as defined in the previous section.

The pharmacokinetics and pharmacodynamics of G-CSF that were defined generally in the mathematical model are defined piecewise linearly. Some of the considerations that we put into formulating these functions were based directly on experimental evidence (elaborated in the main body of text). We note however, that actual experimental data regarding the direct effects of G-CSF on the kinetic parameters in which this model is interested is rather scant. Therefore, some formulations were conducted through partly analytic and partly trial-and-error methods.

Determination of Parameter Values

The Mitotic Compartment

The mitotic compartment is where any long-term effects of G-CSF administration take place. Obviously, the post mitotic compartment's shortening of transit time due to G-CSF administration is the major contributor to heightened blood neutrophil counts in the short term. However, this high level cannot be maintained at all over the longer term without increased production in the mitotic compartment.

The mitotic compartment was modeled with an intention to facilitate the specific cell-cycle cytotoxic effects of chemotherapy. Therefore, cohorts of one hour are modeled as undergoing a process of maturation and amplification (Eq. 1.3) culminating in their entry into the post-mitotic compartment (Eq. 1.5). Chemotherapy will be incorporated into the model by mapping the various cell-cycle phases (G1, S, G2, M) to the hourly cohorts modeled and formulating a function of the cytotoxic effects of chemotherapy on these phases.

The experimental literature shows wide agreement regarding the steady state normal sizes of the circulating neutrophils, post-mitotic compartment and the three morphologically distinct sub-compartments of the mitotic compartment as well as post-mitotic transit time and the amplification rates in the mitotic sub-compartments (Dancey 1976, Price 1996, Dresch 1986). To determine other kinetic parameters of importance to our model, which were either not available in the literature or were given a wide range by experimentalists, we assumed steady state kinetics and employed an iterative process. These parameters include: the inflow of stem cells to the myeloblast compartment and the transit times of the mitotic sub-compartments.

The half life of blood neutrophils and the steady state number of neutrophils was taken as 7.6h and 0.4×10^9 cells/kg body weight, respectively (Dancey, 1976). Similarly, the same calculation may be made for each patient that is to be modeled. This would allow the dynamics of every patient to be described by the simulation. We note, that the average size of the post-mitotic compartment (5.84×10^9 cells/kg body weight – Dancey, 1976) and the transit time of the compartment (160h – Dancey, 1976; Mary, 1986; Price, 1996) are compatible with the size and half-life of the circulating neutrophil compartment reported by Dancey. This supports our steady state analysis.

In order to determine the amount of cells in the hourly sub-compartments in the mitotic compartment we used a steady state assumption on all compartments in the lineage. The number of cells exiting the circulating neutrophil pool equals the number of cells exiting the post mitotic compartment (this was ascertained as explained above), which in turn equals the

hourly production of cells in the mitotic compartment. This means that the number of cells in the last hourly cohort of the mitotic compartment can be determined from the neutrophil decay rate, which is available in the literature. We note however, that this calculation is based on the assumption, that there is no apoptosis in the post-mitotic compartment. According to direct experimental data (Thiele 1997) it seems that apoptosis is not a significant phenomenon in the normal human bone marrow. If it is determined, that apoptosis occurs in the post mitotic compartment, our values for the production of cells in the mitotic compartment will obviously need to be modified upwards. We note however, that the size we calculate for the mitotic compartment is extremely close to that experimentally obtained by Dancey and Price, thus supporting the notion, that apoptosis is not a significant kinetic factor in the lineage.

Regarding the transit time of the mitotic compartment there is little agreement in the literature with a range of 90-160 hours given by most experimentalists (Dresch, 1986). In order to determine the transit times of the mitotic morphological (Eq. 1.4) sub-compartments we considered the following constraints: The sizes of the theoretically obtained morphological sub-compartments must fit those reported experimentally in normal human hematopoiesis (Dancey, 1976) and under the effects of G-CSF (Price, 1996); at least 24h –the typical cell cycle- must separate amplification points; the size of the last hourly sub-compartment must equal the hourly production of the mitotic compartment (calculated with the aforementioned iterative process assuming steady state kinetics); amplification inside the compartment is set at the levels determined by Mary 1984; and finally, the total transit time of the mitotic compartment must be within the 90-160h range. We obtained an excellent fit with all of these constraints by using the values given in Table 1.

Note, that when attempting other alternatives with shorter transit times we could not obtain results that agreed with the literature regarding the size of the mitotic pool or its production. Furthermore, a fit between our simulation model's results regarding PMN counts in peripheral blood with empirical data could not be achieved without speculating extensively on the nature of G-CSF effects on non-committed stem cells (data not provided).

The effects of G-CSF on this compartment are modeled as an increase in the rate of cells entering the myeloblasts from the uncommitted stem cell pool (Eq. 1.2), increases in the rates of mitosis and introduction of new points of amplification. Since little data is available regarding the increases in amplification due to G-CSF, we first assumed that amplification reaches full potential at points that under normal conditions undergo an amplification of below a factor of 2. Additionally we assume that the transit time in all mitotic sub-compartments and the typical cell cycle duration are not affected by G-CSF, since as far as we know, there are no statistically robust data in the literature. Lord's (1989) results in this connection are ambivalent.

These modifications yield increased neutrophil production in accordance with the neutrophil counts reported by Price et al (figs 4,5). In addition, these increases are in good accordance with Price's data about neutrophil bone marrow pool sizes.

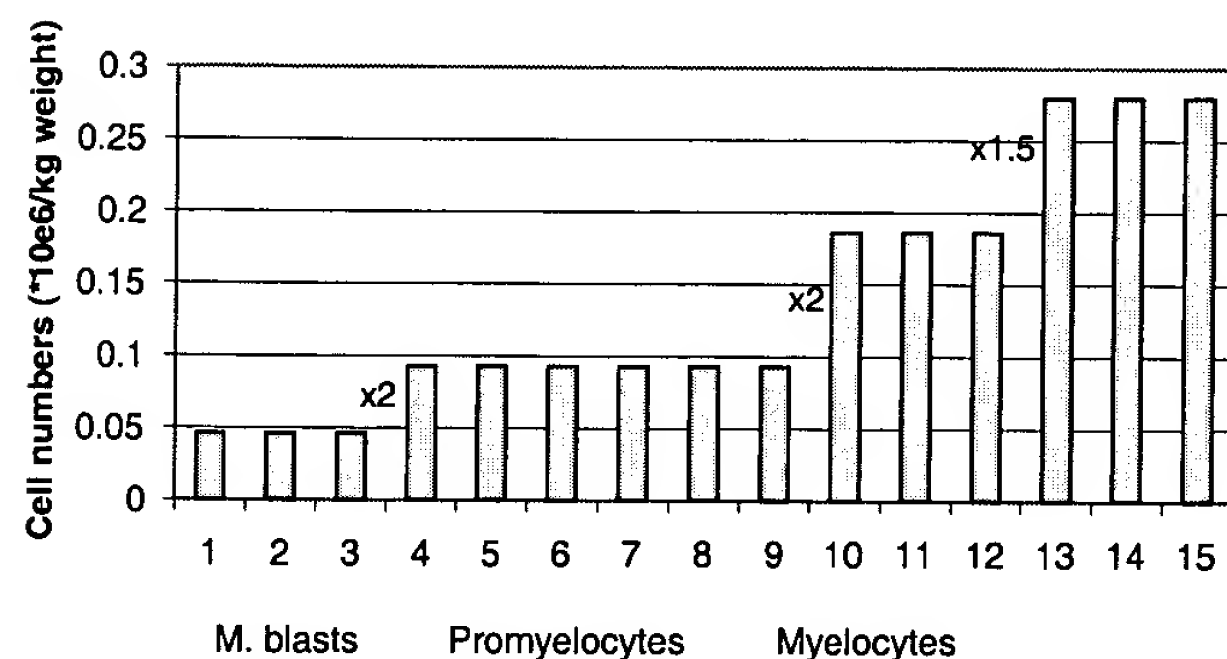
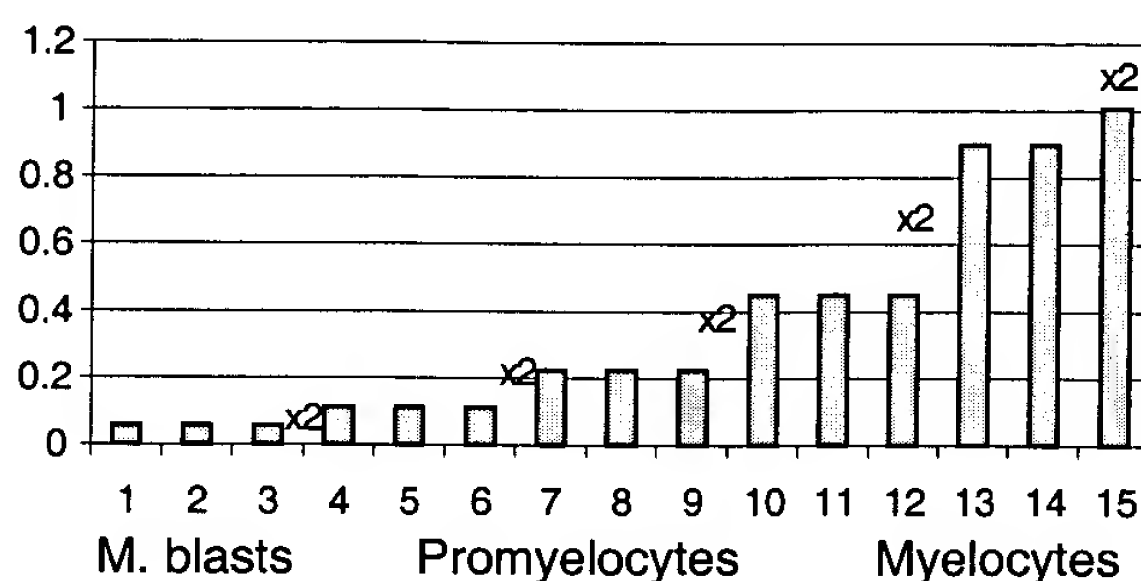


Fig 1. Simulated mitotic compartment age distribution and amplification values in untreated humans. Each bar represents a grouping of 8 cohorts of one hour. Amplification is noted at the place of occurrence.



amplification values in humans treated with 300µg of G-CSF after 15 days. Each bar represents a grouping of 8 cohorts of one hour. Amplification is noted at the place of occurrence. Note, that the last hourly cohort of the Metamyelocytes undergoes mitosis, but its effects are dampened in this graph due to the 8h grouping.

To the extent of our knowledge, there is no experimental data regarding the effects of G-CSF on the commitment of stem cells to the mitotic compartment. However, we were not able to reproduce the effect of G-CSF on neutrophil counts and the mitotic compartment sizes beyond day 5 of administration without assuming an increase (15% with the highest dose of G-CSF) in the rate of cells entering the myeloblast compartment. We note however, that alternatively, G-CSF may change the behaviour of the myeloblast compartment such that some of the cells there undergo self-renewal instead of moving on to the promyelocyte compartment. If more concrete experimental data emerges about G-CSF effects on stem-cells *in-vivo* that points otherwise the model can be modified.

Post Mitotic Compartment

The post mitotic compartment doesn't include mechanisms of amplification or apoptosis, and is apparently relatively insensitive to cytotoxic chemotherapy. Therefore, it is biologically acceptable and computationally sensible to model this compartment as a single pool of cells, such that the last hourly cohort of the mitotic compartment enters it, and a proportion of the cells in it enter the neutrophil pool every hour (Eq. 1.5).

The effects of G-CSF on the post-mitotic compartment are shortening its transit time (increasing l_3 in Eq. 1.5). Price notes, that the number of cells in the post mitotic compartment is not significantly changed following administration of G-CSF. This determination is based on counts made on day 5 after G-CSF administration. We can therefore safely assume that any increased production of the mitotic compartment flowing into the post mitotic compartment is translated over the long-term to an increase in the flow of cells from the post mitotic compartment to the neutrophil pool. This increased flow is compensated by increased production in the mitotic compartment only at a later stage. Therefore, we set an upper limit to the number of cells in the post mitotic compartment, which is at the values given as steady state counts (Π).

In brief, the effects of G-CSF on the neutrophil lineage are modeled during the first few days primarily as a decrease in the counts of the post-mitotic compartment, which is then compensated by an increased production in the mitotic pool. This compensation sustains the increase in neutrophil counts in peripheral blood. Though no empirical data is available on this point, simulations of our model predict (fig 3.) that the number of cells in the post-mitotic compartment decreases substantially during the first two days of G-CSF administration, and then replenishes, so that on the sixth day the counts return almost to their normal levels. This replenishment lags behind that of Price et al report by a few hours. We can thus formulate a **testable hypothesis**, i.e., whether using the same G-CSF protocol Price et al used, there is indeed a nadir on day 3 of the treatment.

Compartment	Day 0 (no G-CSF) ($\times 10^9$ cells/ kg. Body weight)	Day 15 of G-CSF treatment ($\times 10^9$ cells/ kg. body weight)	Relative increase in compartment size due to G-CSF
Myeloblasts	0.140	0.153	1.09
Promyelocytes	0.582	0.898	1.54
Myelocytes	1.373	3.564	2.60
Mitotic Total =	2.10	4.615	2.20
Circulating neutrophils	0.4	2.35	5.88

Table 1. Simulated kinetics after 15 days of subcutaneous administration of 300 μ g G-CSF/kg weight. Day 0 values are the mean values Dancey et al (1976) use.

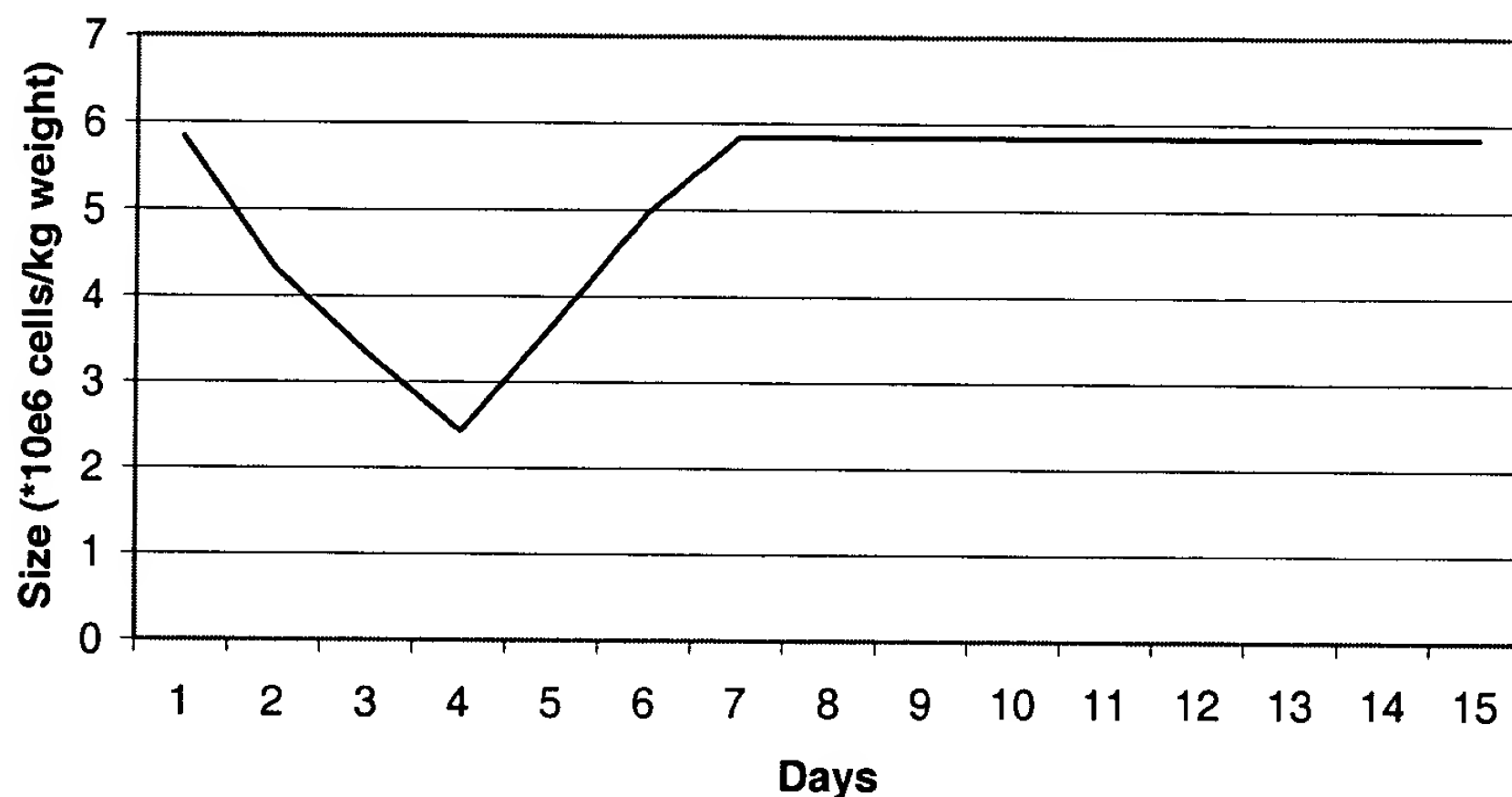


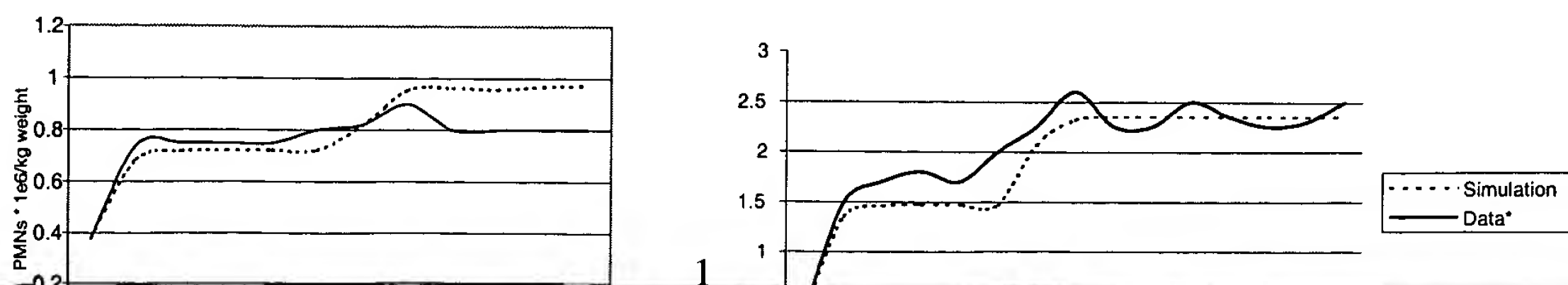
Fig 3. The simulated effects of daily administration of 300 μ g of G-CSF on the post mitotic compartment. Note the nadir on day 3 is almost entirely compensated by day 6.

Neutrophils and G-CSF in the Circulating Blood

The elimination of neutrophils from peripheral blood follows a Poisson distribution, and can therefore be described as an exponential function (Cartwright, 1964).

Therefore the rate of cells leaving this compartment is based on half-life determinations available in the literature (Eq. 1.7). Since no direct cytotoxic effects of chemotherapy have been described for this compartment it is also modeled as a single pool of cells.

The kinetics of G-CSF is also modeled as an exponential distribution with a half-life of 3.5 hours (Stute, 1992) (Eq. 1.1).



The effects of G-CSF on the kinetics of the neutrophil lineage appear not to be a linear function of G-CSF administration levels. Since data provided in the literature (Chatta 1994) only refers to two doses (30, 300 μ gram/kg. Body weight) we can only speculate on the effects of other levels of G-CSF. After trial and error analysis, we found that assuming that the effects of the 300- μ gram dose are the maximal, at the 30- μ gram its effects are about 30% of the maximum. The effects as a function of G-CSF level are connected piece-wise linearly. This way, we obtain the neutrophil levels observed clinically under both the 300 and the 30- μ gram protocols (fig. 4).

Discussion

Our model successfully predicts the kinetics of the neutrophil lineage of healthy humans following different protocols of G-CSF. This was determined based on actual experimental data.

The formulation of the model in piecewise linear terms will allow us to use this model as a clinical tool in three ways: Firstly, the model will determine the effectiveness of various protocols suggested by clinicians prior to their actual use on human patients. Secondly, the software will allow us to compute the optimal protocol in a given situation of neutrophil counts, so that the neutropenic period following chemotherapy is either shortened or completely avoided at a minimal cost and exposure to G-CSF. Thirdly, the model will serve as a constituent in a broader framework of clinical tools that will compute the most optimal treatment plan for chemotherapy and growth factors.

We expect all these to help clinicians administer more rational treatment to their patients minimizing both suffering and medical costs.

Amplification at the exit	Mean transit time (hours)	Size (10^6 cells/kg weight)	Compartment
2^+	24 ⁻	0.139 [*]	Myeloblasts
2^+	48 ⁻	0.558 [*]	Promyelocytes
1.5^+	48 ⁻	1.4 [*]	Myelocytes
1	160 [*]	5.84 [*]	Post mitotic
0	10.96 [*]	0.4 [*]	Neutrophils

Table 1. Kinetics under steady state conditions in healthy humans.

^{*}Dancey, 1976.

^{*}Dresch, 1986.

^{*}Calculated based on the steady state assumption as elaborated in the main text.

Bibliography

1. **Cartwright GE, Athens JW, Wintrobe MM.** 1964. The kinetics of granulopoiesis in normal man. *Blood*. **24**(6): 780-803.
2. **Chatta GS, Price TH, Allen RC, Dale DC.** 1994. Effects of *in vivo* Recombinant Methionyl Human Granulocyte Colony-Stimulating Factor on the Neutrophil Response and Peripheral Blood Colony-Forming Cells in Healthy Young and Elderly Adult Volunteers. *Blood*. **84**(9): 2923-9.
3. **Dancey JT, Deubelbeiss KA, Harker LA, Finch CA.** 1976. Neutrophil Kinetics in Man. *J Clin Invest*. **58**(3): 705-15.
4. **Dresch, Mary.** 1986. Growth Fraction of Myelocytes in Normal Human Granulopoiesis. *Cell Tissue Kin*. **19**: 11-22.
5. **Duhrsen, U., Villeval, J.L., Boyd, J., Kannourakis, G., Morstyn, G., Metcalf, D.** 1988. Effects of Recombinant Human Granulocyte Colony-Stimulating Factor on Hematopoietic Progenitor Cells in Cancer Patients. *Blood*. **72**(6): 2074-81.
6. **Gill, P.E., Murray, W., Wright, M.H.** 1991. *Numerical Linear Algebra and Optimization*. Redwood City CA: Addison-Wesley.
7. **Lord B.I, Bronchud, M.H., Owens, S., Chang, J., Howell, A., Souza, L., Dexter, T.M.** 1989. The Kinetics of Human Granulopoiesis Following Treatment with Granulocyte Colony-Stimulating Factor *in vivo*. *Proc. Natl. Sci. USA*. **86**: 9499-9503.
8. **Mary, J.Y.** 1984. Normal Human Granulopoiesis Revisited I. Blood data, II. Bone Marrow Data. *Biomedicine & Pharmacotherapy*. **38**: 33-43, 66-67.
9. **Price TH, Chatta GS, Dale DC.** 1996. Effect of Recombinant Granulocyte Colony-Stimulating Factor on Neutrophil Kinetics in Normal Young and Elderly Humans. *Blood*. **88**(1): 335-40.
10. **Schmitz, S., Franke, H., Brusis, J., Wichmann, H.E.** 1993. Quantification of the Cell Kinetic Effects of G-CSF Using a Model of Human Granulopoiesis. *Experimental Hematology*. **21**:755-760.
11. **Schmitz, S., Franke, H., Wichmann, H.E., Diehl, V.** 1995. The Effect of Continuous G-CSF Application in Human Cyclic Neutropenia: A Model Analysis. *British Journal of Haematology*. **90**:41-47.
12. **Stute N, Furman WL, Schell M, Evans WE.** 1995. Pharmacokinetics of recombinant human granulocyte-macrophage colony stimulating factor in children after intravenous and subcutaneous administration. *J Pharm Sci*. **84**(7): 824-8.
13. **Terashi, K., Oka, M., Ohdo, S., Furukubo, T., Ikeda, C., Fukuda, M., Soda, H., Higuchi, S., Kohno, S.** 1999. Close Association between Clearance of Recombinant Human Granulocyte Colony Stimulating Factor (G-CSF) and G-CSF Receptor on Neutrophils in Cancer Patients. *Antimicrob. Agents Chemother*. **43**(1): 21-24.
14. **Thiele J, Zirbes TK, Lorenzen J, Kvasnicka HM, Scholz S, Erdmann A, Flucke U, Diehl V, Fischer R.** 1997. Hematopoietic Turnover Index in Reactive and Neoplastic Bone Marrow Lesions: Quantification by Apoptosis and PCNA Labeling. *Ann Hematol*. **75**(1-2): 33-39.

APPENDIX C

Optimizing cytotoxic drug delivery (administration/efficacy) for cancer patients

Introduction

Cancer is the second leading cause of mortality in the US, resulting in approximately 550,000 deaths a year. There has been a significant overall rise in cancer cases in recent years, attributable to the aging of the population. Another contributing factor to the rise in the verifiable number of cases is the wider use of screening tests, such as mammography and elevated levels of prostate specific antigen (PSA) in the blood.

Neither better detection nor the natural phenomenon of aging, however, can entirely explain the increase in new cases of tumors. Meanwhile, other cancers, like brain tumors and non-Hodgkin's lymphoma, are becoming more common. Their increase could reflect changes in exposures to as yet unidentified carcinogens. Current trends suggest that cancer may overtake heart disease as the nation's no. 1 killer in the foreseeable future. As gene therapy still faces significant hurdles before it becomes an established therapeutic strategy, present control of cancer depends entirely on chemotherapeutic methods.

Chemotherapy is treatment with drugs to destroy cancer cells. There are more than 50 drugs that are now used to delay or stop the growth of cancer. More than a dozen cancers that formerly were fatal are now treatable, prolonging patients' lives with chemotherapy.

Treatment is performed using agents that are widely non-cancer-specific, killing cells that have a high proliferation rate. Therefore, in addition to the malignant cells, most chemotherapeutic agents also cause severe side-effects because of the damage inflicted on normal body cells. Many patients develop severe nausea and vomiting, become very tired, and lose their hair temporarily. Special drugs are given to alleviate some of these symptoms, particularly the nausea and vomiting. Chemotherapeutic drugs are usually given in combination with one another or in a particular sequence for a relatively short time.

Chemotherapy is a problem involving many interactive nonlinear processes which operate on different organizational levels of the biological system. It usually involves genomic dynamics, namely, point mutations, gene amplification or other changes on the genomic level, which may result in increasing virulence of the neoplasia, or in the emergence of drug resistance. Chemotherapy may affect many events on the cellular level, such as cell-cycle arrest at different checkpoints, cell transition in and out of the proliferation cycle, etc. Chemotherapy may also interfere with the function of entire organs, most notably, with bone marrow blood production. In recent years molecular biology and genetics has made an important step forward in documenting many of these processes. Yet, for assessing the contribution of specific molecular elements to the great variety of disease profiles, experimental biology must be provided with tools that allow a formal and systematic analysis of the intricate interaction between the genomic, cellular and cell population processes in the host and in the disease agent.

This system is so complex that there is no intuitive way to know how small changes in the drug protocol will affect prognosis. But in spite of this intricacy, attempts to improve chemotherapy have been carried out by "trial and error" alone, with no formal theory underlying the application of specific drug schedules. Such an approach "is apt to result in no improvement, only discouragement and little useful information for future planning" (Skipper, 1986).

1. General Description

The product is a method for identifying clinically feasible and efficacious optimal treatment protocols for anticancer drugs. We do this by using (1) optimization methods taken from Operation Research, and involving heuristic search algorithms. These are applied for (2) testing the performance of a very large number of drug protocols on (3) "virtual cancer patients," in the form of realistic computer simulations of detailed mathematical models of the involved dynamics. **Our method is the first which can identify optimal treatment protocols, without any constraint on the level of complexity of the mathematical models of the biological, clinical and pharmaceutical processes. This means that the description of the system can be as realistic as required.** Previous optimization methods imposed constraints on the level of complexity of the mathematical methods, so that the simulated systems were always too simplistic to retrieve the clinical situation.

The assumption that underlies this method is, that the effect of a certain drug on a certain cancer cells population depends on the overall population dynamics of the tumor. To describe these complicated dynamics we use a set of models that follow up the changes in cancer cell numbers, spatial distribution and other relevant phenotypic (epigenetic) factors, taking into consideration also the genetic profile of the patient, in cases where this one is available. To also allow for the use of cell-cycle-phase-specific drugs, we follow-up each drug susceptible body cell (normal and cancer) according to its cell-cycle status. Because any realistic description of such "virtual patient" is too complex to be attacked by analytical optimization method, then our introduction of the heuristic optimization methods approach is a highly significant novelty.

The project consists of 6 successive stages:

- 1) Developing the appropriate mathematical models to describe the cancer cell populations with respect to the cell-cycle as well as spatio-temporal dynamics. This model can be as complex as necessary for enabling an accurate computation of the number of cancer cells at any given moment.

- 2) Inputting individual parameters into the model and, hence, bridging between the model and accessible clinical data regarding profiles of the tumor and of the patient.

- 3) Introducing drug characteristics (mode of action, effect and on tumor cells etc.), the pharmacokinetics and the pharmacodynamics into the model, using experimental data about the relevant drugs.

- 4) Combining this model with additional models that consider toxic effects of the drug on the host (e.g., granulocytic and thrombocytic lineages).

5) Defining a general fitness function for given protocol, so that this system may serve as prediction tool for anticancer treatment (with an option of tuning by the user).

6) Using search algorithms and computer simulations to search through the possible protocols space in order to obtain the best/most suitable solution.

The search process may be performed on several levels, starting from the most general (for a given type of disease), to the most detailed and patient-specific level (which will require relevant clinical data about the patient). In the case of a more generalized search, the certain region of protocols may be proposed as most suitable for given type/profile of cancer; in the case of specified search, this region can be narrowed according to additional patient data.

2. Mathematical Model:

2.1. Basic Tumor Layer

The basic layer of the model incorporates a description of age distribution of cycling cells and number of resting (quiescent) cells. The term "age of the cell" here refers to chronological age starting from the conventional beginning point of mitotic cycle.

In what follows we give the definition of this basic model:

- The whole cycle is divided into 4 compartments, or *stages* (G_1 , S , G_2 and M). Each compartment is divided into equal *subcompartments*, where i^{th} *subcompartment* in each stage represents cells of age i in this stage (i.e. they have spent i time-steps in this stage).
 - Let $\{G_1, S, G_2, M\}$ denote the corresponding stages of the cell cycle, and G_0 – the quiescence.
 - Let T_k denote the maximum duration of k^{th} stage in the cycle.
 - We denote as $\bullet t$ the time resolution of the model – discrete time steps.
 - $x_k^i(t)$ is a function which represents the number of cells in stage k with age i into this stage, at time t to $t + \bullet t$. Both time and age are measured in same units (hours).
 - $Q(t)$ represents the number of resting cells at time t to $t + \bullet t$.
 - $Trans(k, i, t)$ represents the probability that a cell of age i in the stage k will move to the next $(k+1)$ compartment. Cells entering the new stage always start from the first subcompartment, i.e. from $i=1$. This probability may change with time.
- By definition: $\forall k : Trans(k, T_k) = 1$ That means that the cell cannot remain more than T_k in k compartment.
- Let T_0 and T_R denote the onset of G_1 and the age at which the cell passes through R-point (**restriction point**) in G_1 , respectively. The later is associated with commitment to complete the mitotic cycle.
 - The total number of proliferating cells $P(t)$ can be calculated as follows:

$$P(t) = \sum_{k=G_1, S, G_2, M} \left(\sum_{i=1}^{T_k} x_k^i(t) \right)$$

- In every time interval, quiescent cells may return to the proliferation pool. Alternatively proliferating cells may change their state to become quiescent if they are in G1 stage and at age i , where $T_R \cdot i > 0$. To describe this process we introduce the function $G_{1 \rightarrow 0}(i, t)$ which describes the number of G1 cells in age i which become quiescent, during time interval $[t, t + \Delta t]$. This function may receive negative values, accounting for cells that return from resting to proliferation.

As we assume that the exit to quiescence can occur only prior to the R-checkpoint (even in cancer cells), and that a resting cell which returns to proliferation enters the cycle at T_0 , it can be stated:

$$\forall i > T_R, \forall t : G_{1 \rightarrow 0}(i, t) = 0$$

It must be noted, that this function is not dependent on i and t solely. Its value is determined according to current cell distribution and all the general parameters that characterize the described cells group. The same should be said about the values of *Trans* vector that can change during the history of given population.

- The model traces the development of described group of cancer cells using given parameters, by calculating the number of cells in each and every subcompartment according to the following stepwise equations:

$$x_k^i(t) = \begin{cases} x_k^{i-1}(t-1) \cdot [1 - \text{Trans}(k, i-1, t-1)], & 1 < i \leq T_k \\ \sum_{j=1}^{T_{k-1}} [x_{k-1}^j(t-1) \cdot \text{Trans}(k-1, j, t-1)], & i = 1 \end{cases}$$

$$x_s^i(t) = \begin{cases} x_s^{i-1}(t-1) \cdot [1 - \text{Trans}(S, i-1, t-1)], & 1 < i \leq T_{G1} \\ \text{for } k=G_2, M, \text{ } k-1 \text{ returns the previous stage (e.g. } G_2-1=S\text{).} \\ \sum_{j=1}^{T_{G1}} [x_{G1}^j(t-1) \cdot \text{Trans}(G1, j, t-1)] \cdot [1 - G_{1 \rightarrow 0}(i-1, t-1)], & i = 1 \end{cases}$$

$$x_{G1}^i(t) = \begin{cases} x_{G1}^{i-1}(t-1) \cdot [1 - \text{Trans}(G1, i-1, t-1)] \cdot [1 - G_{1 \rightarrow 0}(i-1, t-1)], & 1 < i \leq T_{G1} \\ 2 \cdot \left\{ \sum_{j=1}^{T_M} [x_M^j(t-1) \cdot \text{Trans}(M, j, t-1)] \right\}, & i = 1 \end{cases}$$

- These equations make it possible to calculate the number of cells in each subcompartment at every time interval $[t, t + \Delta t]$ starting from initial distribution (e.g. at time $t=0$).

Remarks:

1) As stated above, cells ages are measured in absolute time units, and therefore refer to the chronological age of the cell (as opposed to biological age, which refers to maturity of the cell and its units are relative to maturation rate that is different from cell to cell). As a consequence, in this model no cell can remain in the same age subcompartment after every time step. On the other hand, a fraction of the cells that leaves any subcompartment may be transferred to the first subcompartment of the

next stage, according to probability vector $Trans(k,i,t)$. This fact enables us to account for variability of cycle lengths while retaining deterministic approach.

2) The behavior of the cell population in this model is wholly controlled by two components: *Trans* vector, and *G1toG0* function. These two functions determine uniquely the outcome of every single time step, and, consequently the result over the long periods. We name them here "*control functions*". As we have mentioned, the values of these functions may be dependent not only on time and age of cells, but also on the current population state (or, generally, on the whole history of the population) as well as on the environment associated with given cells group. On the other hand, those parameters are similar for all the cells in the group. This implies that the model presented here is suitable for describing highly homogenous group of cells. As it will be claimed later, control functions values are determined by the parameters that describe the local conditions for given population. Therefore, we expect the basic layer of the model to give realistic description of uniform group of cancer cells for which environmental conditions and relevant biological properties are defined, in a way that will allow the construction of the control functions for this group.

2.2. The General Tumor Model

In the general approach the whole model is viewed as constructed from similar components, each of them derived from the basic structure described in the previous paragraph. Each component represents cells that are situated in the same environmental conditions and, therefore behaves similarly. We call them *groups*. The whole tumor is modeled as union of heterogeneous groups of cells, where the development of every group can be accurately predicted (when local conditions are known).

This general model simulates progress of tumor in time by discrete steps. At each step the number of cells in each subcompartment of each group is calculated according to the previous state, parameters of tumor, drug concentration, etc. The parameters of the tumor must include all the information that is relevant to the prognosis. Some of these parameters are defined locally, e.g., those relating to the tumor's geometry. For this reason the representation of the spatial structure will be included.

The cells will be able to pass between the groups during the development of the tumor. This allows the representation of the changes in the local conditions, during the tumor evolution (e.g. forming of necrotic core, improvement in "living conditions" in vascularized regions, etc.). In addition, all the parameters of the tumor may change in accordance with the dynamics of the cancer.

The calculation of the tumor development over time will be done by stepwise execution of the described simulation and can be used to predict the outcome of the treatment or in fitness function for search algorithms.

2.3. From General to Individual Tumor Model

When the general theoretical description of the model is accomplished, the model is fitted to represent the actual tumors. We render it patient-specific by adjusting all the parameters that determine the behavior of the modeled tumor to those of the real cancer in the patient's body. In order to accomplish this task we will establish the

connections between mathematical parameters (most of them will have direct biological implication) and every kind of data that is practically obtainable in the clinic. This individualization procedure includes three aspects:

- 1) individual parameters of tumor dynamics
- 2) individual parameters of specific drug pharmacokinetics for a specific patient.
- 3) individual parameters of the dynamics of dose-limiting normal host tissues.

These connections may be defined through research on statistic correlation between different parameters (including genotype-phenotype correlation), or using advanced biochemical research (which may establish quantitative relations).

In the general model important dynamic parameters are estimated from experimental studies that are conducted in certain patient populations. Any of these parameters, when available on the per patient basis, can be individualized, while others left as population-based means. This approach allows continuous increase in the degree of individualization of the treatment protocols with progress in the technology.

Defined so, the model will be able to give realistic predictions for treatment outcome either for specific patient or for a broad range profiles of patients and diseases. This tool can serve to perform the prognosis of an untreated cancer patient, or as a basis for treatment modeling.

3. Introducing Pharmacology

In order to simulate cancer treatment we add to this model the pharmacologic component. We model pharmacokinetics as well as pharmacodynamics for specific anticancer drugs. We begin by representing cell-cycle specific drugs, however the model implies no restriction on the type of drugs to be employed.

We model the distribution of the drug in and around the tumor as well as in the blood (the drug kinetics). For this purpose, we use the suitable model, defining it precisely for every certain type of the drug. The concentrations of drug in the body are calculated at every time step in accordance with the drug administration specified by the protocol.

The dynamics of the drug are represented through the direct influence of the drug on tumor cells. The effects on the proliferating cells are mostly blocking the cycle in different stages (which can be modeled as cell arrest) and cell death (immediate or after being in the block). Cell-cycle specific drugs have no direct influence on quiescent cells, but can affect them indirectly by killing proliferative cells and therefor changing local conditions. Where additional types of drugs added to the model, their effect on any kind of cells may be too modeled as killing certain fraction of cells (which is dose-dependent) or changing the behavior of the cells.

Additional phenomena that may come out to be significant in drug kinetics and dynamics (e.g. rate of absorption by the cells, development of tumour resistance to specific drug, etc.) can be introduced into the model to make it as realistic as needed.

The description of the drug in the model is done in terms of quantitative functions, which enable to calculate the drug amounts at certain locations and the tumor response to it at every time step. In the general case, these functions include parameters that depend on the specific data (drug type, body parameters, characteristic of the tumor, etc.) and can be determined in given situation. The relation between clinical data and these parameters can be established in the ways similar to those described for the cancer model.

The combination of cancer model with the drug model described above makes it possible to predict the outcome of the treatment, given the relevant parameters for the

drug, the cancer and the patient. Again, the prognosis may be made for specified cases as well as for broad profiles of patients or disease. This simulation also serves to build the fitness function used in search algorithms in optimization system.

4. Combining with minimizing host toxicity.

Although being accurate predictive tool, the model that represents chemotherapy of tumor alone cannot be used in optimization, for it posts no constraint on the choosing of the treatment. Actually, this model implies using as much drug as it is possible until the final elimination of the tumor; while in the live system the toxicity of the drug is the most important constraint limiting the treatment. In most cases of anticancer chemotherapy the dose-limiting toxicity is bone marrow suppression, the two most sensitive bone marrow lineages being granulopoiesis and thrombopoiesis. Accordingly, those two were chosen as an example and are modeled separately and in the similar way to predict the negative effect of the chemotherapy on them. These models reconstruct the damage caused by the chemotherapy to the bone marrow cells and the recovery of these lineages (also treated by specific growth factors).

Thus, the whole system is able to predict the result of chemotherapy treatment for the tumor as well as for bone marrow cells, allowing the use of the protocols that combine anticancer drugs and growth factors for healthy cells.

Chemotherapy toxicity to any other normal host cell population can be similarly taken into account, if it is proven to be relevant for dose and schedule optimization.

5. Defining the Fitness Function

Fitness function is an important tool in operation research. In the method developed by us it allows the comparison between a number of different protocols each one of them scoring differently with respect to various objectives that can be set by the developers or by the users and identifying the protocol for which we predict the best weighted score. Fitness function calculates for any given protocol its relative efficacy, thus enabling a definite decision of the best protocol from a given set of protocols.

In different cases, different objectives can be formulated. There are 3 main settings in which such a model can be used:

- One) clinical practice- where objectives can change depending on type of disease, condition of the patient, purpose of treatment, etc;
- Two) pharmaceutical company- where objectives can be aimed at finding the therapeutic window and an optimal schedule;
- Three) scientific setting- where different and sometimes esoteric objectives can be aimed at.

For any such case, certain fitness function can be formulated, reflecting all given requirements. Thus, in any particular case one can compare between different protocols and obtain the most suitable to his/her special purposes and needs.

Using the fitness function we can: a) estimate the efficacy of a given protocol, b) search for the solution of an optimization problem, that is predict which protocol will be best of many potential protocols considered for curing/relieving the patient.

6. Solving the Optimization Problem

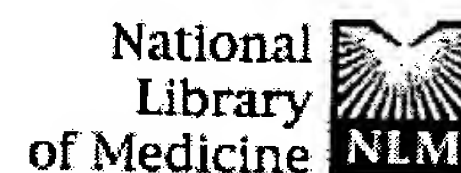
The optimization problem is stated using the described models: to find the protocol for drug administration (with option to growth factor administration) which maximizes the given fitness function.

As explained above, we define the fitness function according to the user requirements. For example, the goal of the treatment may be defined as minimizing the number of cancer cells at the end of the treatment, minimizing the damage to the BM cells throughout the treatment or at its end, and curing the patient (where cure is defined precisely) as quickly as possible. Note that the fitness function may also include goals such as maximizing life expectancy, minimizing cost of treatment, etc.

Generally, the aim of optimization is to find the best protocol, i.e. the protocol that generates the best value of fitness. Customarily, this is achieved by mathematical analysis. However, mathematical analysis is restricted to relatively simple models, whereas our models are very complex and, therefore, cannot be solved analytically. On the other hand, the practical purpose of the treatment is not to find *the best possible protocol* (i.e., the global optimum) but "only" one that will suit the user's objectives, even if its fitness is not absolutely the best (i.e., the local optimum). For this reason we can be satisfied with the solution that can be shown to promise that the patient will be cured.

Hence, the optimization problem may be reformulated as follows: for given starting conditions, find the treatment protocol that will fulfill the user's requirements (e.g. curing a patient according to given definitions of cure) and subjected to given limitations (e.g. treatment duration, drug amounts, etc.). To this end it is unnecessary to find **the** global solution. It is enough to perform search, using search algorithms, in certain regions of the protocols' space, and find the local maxima of the fitness function. After determining these locally best protocols, we can verify that they serve one's objectives and check them numerically for stability.

Such a strategy can be used for identifying patient-specific treatment, as well as in the general case, where only the profile of the disease and the drug specified. If more patient-specific data are supplied, the solution will be tailored more specifically. On the other hand, the optimization program could propose general recommendations for the protocol types for certain kinds of tumor.



PubMed Nucleotide Protein Genome Structure PMC Taxonomy OMIM Bc

Search PubMed for [] Go Clear

Limits Preview/Index History Clipboard Details

About Entrez

Display Abstract Show: 20 Sort Send to Text

Text Version

Entrez PubMed
Overview
Help | FAQ
Tutorial
New/Noteworthy
E-Utilities

PubMed Services
Journals Database
MeSH Browser
Single Citation Matcher
Batch Citation Matcher
Clinical Queries
LinkOut
Cubby

Related Resources
Order Documents
NLM Gateway
TOXNET
Consumer Health
Clinical Alerts
ClinicalTrials.gov
PubMed Central

Privacy Policy

☐ 1: Comput Biomed Res 2000 Jun;33(3):211-26

Related Articles, Links



Optimizing drug regimens in cancer chemotherapy by an efficacy-toxicity mathematical model.

Iliadis A, Barbolosi D.

Department of Pharmacokinetics, Faculty of Pharmacy, University of Marseilles, 27, boulevard Jean Moulin, Marseille Cedex 5, 13385, France.

In cancer chemotherapy, it is important to design treatment strategies that ensure a desired rate of tumor cell kill without unacceptable toxicity. To optimize treatment, we used a mathematical model describing the pharmacokinetics of anticancer drugs, antitumor efficacy, and drug toxicity. This model was associated with constraints on the allowed plasma concentrations, drug exposure, and leukopenia. Given a schedule of drug administrations, the mathematical model optimized the drug doses that can minimize the tumor burden while limiting toxicity at the level of the white blood cells. The main result is that the optimal drug administration is an initial high-dose chemotherapy up to saturation of constraints associated with normal cell toxicity and a maintenance continuous infusion at a moderate rate. Data related to etoposide investigations were used in a feasibility study. Simulations with the optimized protocol showed better performances than usual clinical protocols. Model-based optimal drug doses provide for greater cytoreduction, while limiting the risk of unacceptable toxicity. Copyright 2000 Academic Press.

PMID: 10860586 [PubMed - indexed for MEDLINE]

Display Abstract Show: 20 Sort Send to Text

Write to the Help Desk
NCBI | NLM | NIH
Department of Health & Human Services